CONTRACTOR REPORT

SAND83—7462
Unlimited Release
UC—92a

Offshore In-Situ Testing Techniques: 1983

Robert L. McNeill, ScD
3936 Garcia NE
Albuquerque, NM 87111

Iraj Noorany, PhD
San Diego State University
San Diego, CA 92182

This study sponsored by the Technology Assessment and Research Program, Minerals Management Service, United States Department of Interior

Prepared by Sandia National Laboratories Albuquerque, New Mexico 87185 and Livermore, California 94550 for the United States Department of Energy under Contract DE-AC04-76DP00789

Printed December 1983

Issued by Sandia National Laboratories, operated for the United States Department of Energy by Sandia Corporation.

Printed in the United States of America
Available from
National Technical Information Service
U.S. Department of Commerce
5285 Port Royal Road
Springfield, VA 22161

NTIS price codes
Printed copy: A05
Microfiche copy: A01

Category UC-92a

SAND83-7462
Unlimited Distribution
Printed December 1983

OFFSHORE IN-SITU TESTING TECHNIQUES: 1983

Prepared by

Robert L. McNeill, ScD
Consulting Engineer
Albuquerque, NM

Iraj Noorany, PhD
Professor
San Diego State U

for

Sandia National Laboratories
Albuquerque, NM 87185
Contract No. 68-3596

Sponsored by
The Technology Assessment and Research Program
Minerals Management Service
United States Department of Interior

ABSTRACT

This report is a summary of current offshore geotechnical in-situ testing techniques as of mid-1983. It is an update and expansion of an earlier effort (Noorany, 1981) and was accomplished by a comprehensive literature survey, interviews with prominent geotechnical engineers in the U.S. and Europe, and site visits to North Sea countries involved in oil and gas development.

TABLE OF CONTENTS

OFFSHORE IN-SITU TESTING TECHNIQUES: 1983

1. INTRODUCTION

Some of the most innovative and pioneering work in offshore construction during the past decade has taken place in the North Sea. In a particularly difficult marine environment and a complex geological setting, collaboration of European and U.S. engineers has produced spectacular engineering achievements in the form of large offshore platforms and oil storage reservoirs. New design concepts, such as gravity structures not pinned down to the sea floor, and highly sophisticated methods of analyses were used for offshore structures. Foundation investigations of these structures in the North Sea and elsewhere posed many challenging problems for the geotechnical engineers. New tools and techniques had to be developed for improved subsea explorations. As construction sites gradually moved into deeper waters and obtaining undisturbed soil samples became more difficult, in-situ testing played an increasingly crucial role in geotechnical explorations. Consequently, some new in-situ testing techniques were developed that were more sophisticated than the standard procedures commonly used on land.

The objective of this report is to review, synthesize and summarize the state-of-the-art of offshore in-situ testing practice in 1983. This was accomplished by a comprehensive survey of the published literature, interviews with prominent geotechnical engineers involved in offshore explorations in the U. S. and Europe, and site visits in the North Sea countries. The report is presented as a summary of current in-situ testing practice. Additional details are provided in the Appendix which contains copies of a number of significant reference papers.

2. SUPPORT SHIPS, DRILLING AND SAMPLING

Soil sampling and in-situ testing in the ocean is usually done from a drill vessel, an anchored barge, or a mobile jackup platform (Andersen et al, 1979; deRuiter, 1975 and 1976; deRuiter and Richards, 1983; Doyle et al, 1971; George, 1976; George and Wood, 1976; Hoeg, 1976; LeTirant, 1979; Noorany, 1972 and 1981; Perkins, 1957; Schjetne and Brylawski, 1979; Sullivan, 1980; Tirey, 1972; Vermeiden, 1978). A typical operation requires the use of a drill ship equipped with a drill rig and a central moon pool, usually 4 x 4 m, for lowering the drill string and the in situ testing instruments.

In the past, most of the drill ships have used anchors for maintaining fixed position in waters as deep as 300 m. More recently, dynamically positioned ships have been used. This method of positioning is often necessary for drilling and in situ testing in waters deeper than 300 m.

The standard drilling method for offshore explorations is rotary drilling with a hollow-stem auger. A schematic diagram of the drilling setup is shown in Figure 1. To prevent the sides of the hole from collapsing, drilling mud is continuously pumped into the drill pipe and flows upward through the annular space around the drill pipe. Since normally no casing is used, the mud carrying the drilled soil is disposed of on the sea floor.

The power swivel for the rotation of the drill pipe is located at the top of the drill string, as shown in Figure 2. The downward pressure at the tip of the drill bit is supplied by the weight of the drill string. Also, in order to prevent the buckling of the drill string, it is normally equipped with a motion compensator to keep it in constant tension while the ship heaves up and down. In addition to the heave compensator on the ship deck, downhole heave compensators (called bumper subs) can be used to facilitate telescopic movement of the drill string and to compensate for the up and down motions of the vessel.

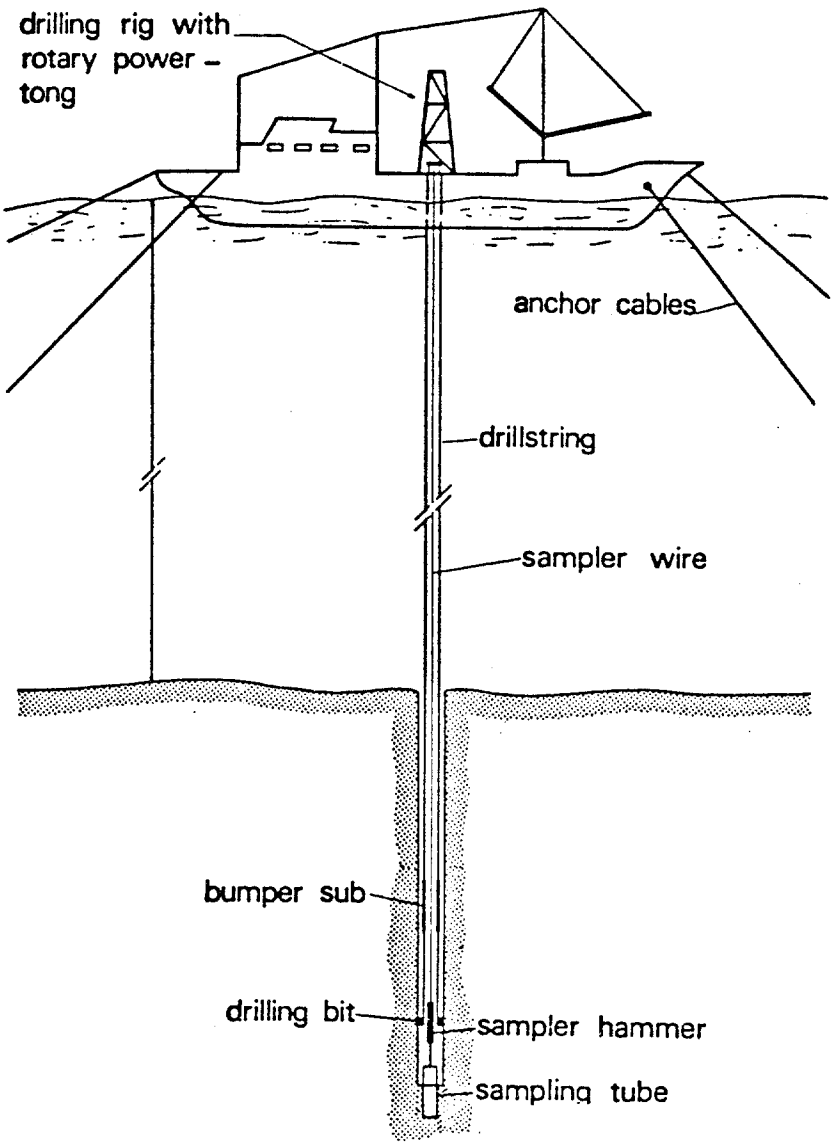

Fig. 1 - Wireline Sampling

(From Vermeiden, 1978)

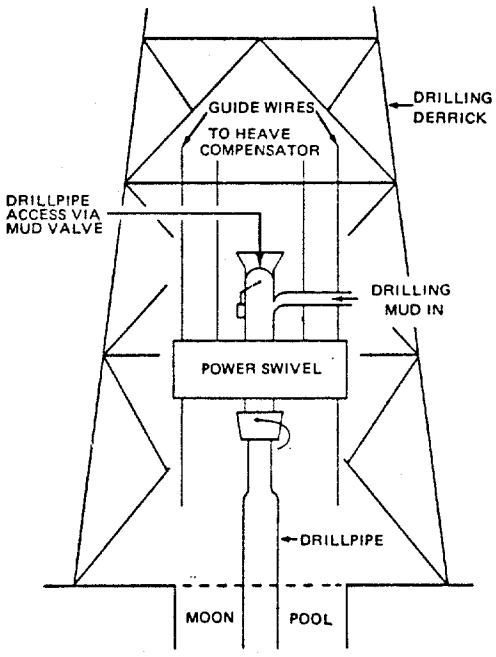

Fig. 2 - Schematic Diagram of the Upper Portion of Drill String

(From deRuiter and Richards, 1983)

Soil sampling and in-situ testing are done from inside the drill pipe. As shown in Figure 1, soil samples are taken by suspending a sampler on wireline through the center of the drill string and driving it by percussion method with a hammer inside the drill pipe. The downhole hammer, suspended from another cable, typically weighs from 77 to 132 Kg and has a stroke of 1.5 to 3 m. The weight of the hammer and the height of drop in underwater sampling practice have evolved based on experience. At present there is no standard procedure for monitoring the driving energy and correlating it with soil type. It would be desirable to standardize the driving procedure in the future.

As an alternative to drive sampling, the weight of the drill string can be mobilized to push the samplers into the soil. The drill string is first lifted approximately 60 cm above the bottom of the hole and the sampler is lowered until it latches onto the bottom of the drill pipe. The drill string is then lowered to push the sampling tube into the soil. In soft to firm clays this procedure results in better quality samples (Sullivan, 1980).

In order to increase the reaction force for push sampling as well as minimize the effects of heave of the vessel on sampling, V. B. Fugro in the Netherlands has developed the Drill String Anchor (deRuiter, 1975; Windle, 1981). A schematic diagram of the drill string anchor is shown in Figure 3. The anchor consists of a rubber packer that can be inflated to press against the side of the borehole, and can provide a reaction force of about 20 metric tons for push sampling or in-situ testing.

One of the problems associated with underwater drilling and wireline sampling described above is that no soil cuttings return to the surface vessel. Therefore, at the intervals between samples, variations in soil type can only be estimated from close observation of the drilling action.

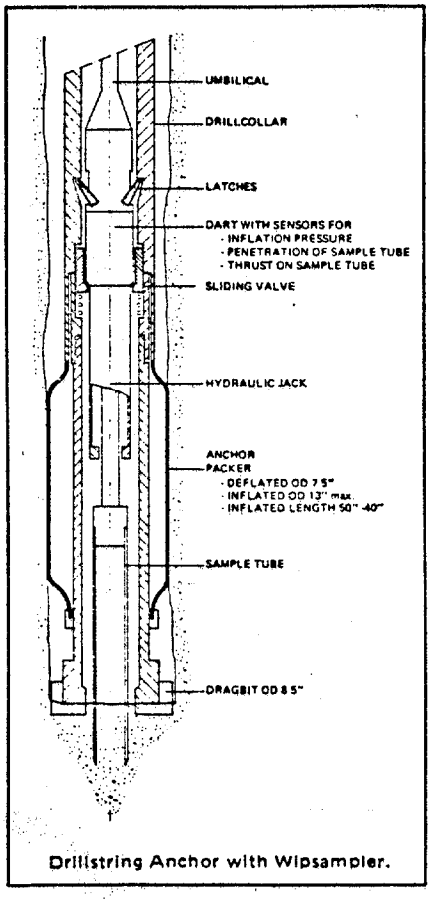

Fig. 3 - Drill String Anchor With Wireline Push Sampler

(From Fugro, B. V.)

3. METHODS OF OFFSHORE IN-SITU TESTING

Underwater in-situ tests for geotechnical explorations can be divided into the following four categories:

1. Wireline tests by means of instruments that are suspended on a wireline inside the drill string.
2. In-situ tests from seabed platforms which are placed on the sea floor to serve as a support and provide additional reaction for pushing the test instruments into the soil.
3. In-situ tests from a diving bell.
4. In-situ tests by means of ballistic penetrators.

The salient features of the current techniques in each category are described in the following sections.

4. WIRELINE IN-SITU TESTS

In the early days of offshore explorations in shallow waters, in-situ tests were made from a barge or a temporary platform using the standard land drilling and testing procedures. As underwater explorations gradually moved into deeper waters, new methods had to be developed. It was soon realized that an efficient way of testing would be to use the drill string as casing and run in-situ tests from inside the drill pipe. In the same manner that soil samples were taken by suspending a sampler on wireline, in-situ test devices were developed for use on wireline.

Using the wireline technique, in-situ tests can be carried out at any depth as the borehole is advanced. The drilling operation is stopped and the test instrument is lowered on cable inside the drill string until it reaches the bottom of the hole. An instrument suitable for in-situ tests in soft to firm clays is the wireline vane. Another instrument, the wireline cone penetrometer, can be used both in sands and in clays.

4.1 - Wireline Vane Shear Test

One of the oldest tests used for measuring the in-situ undrained shear strength of saturated clays is vane shear. A vane blade is pushed into the clay and twisted to shear the soil. The in-situ shear strength is computed from the torque required to shear the soil.

A remotely operated wireline vane shear device developed by McClelland Engineers has been used for offshore investigations since 1970. The latest model can measure in-situ undrained shear strengths up to 3 kg/cm^2 and has a combined water and penetration depth capability of approximately 1500 m (Doyle et al, 1971). It has been used in depths greater than 210 m below the sea floor in water depths in excess of 420 m (Doyle et al, 1971; Ehlers and Babb, 1980).

A schematic diagram of the remote vane equipment is shown in Figure 4. The instrument is suspended from a wireline and inserted in the drill pipe. The assembly consists of two parts: the vane tool and the motion compensating section. The motion compensating section allows a telescopic up and down movement up to 3 m. This permits the test to be run in moderately rough seas without disturbance. The vane tool consists of the main vane and a reaction vane. They are both pushed into the soil. The reaction blades maintain the tool in a fixed position while the main vane is rotated at a speed of 18 degrees per minute to shear the soil. The torque is applied by a small motor inside the tool. The torque is measured and continuously recorded on the ship deck.

The operational details of the remote vane are described by Ehlers and Babb, 1980). The hole is drilled to a depth approximately 1 m above the desired test depth. The drill string is then lifted about 1 m above the bottom of the borehole. The wireline vane tool package is lowered through the drill pipe until it reaches the bottom of the hole. The weight of the drill pipe is then used to push the vane assembly into the soil. The pipe is again lifted off the bottom and the

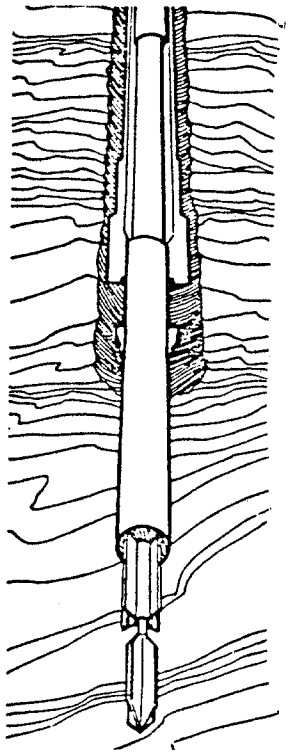

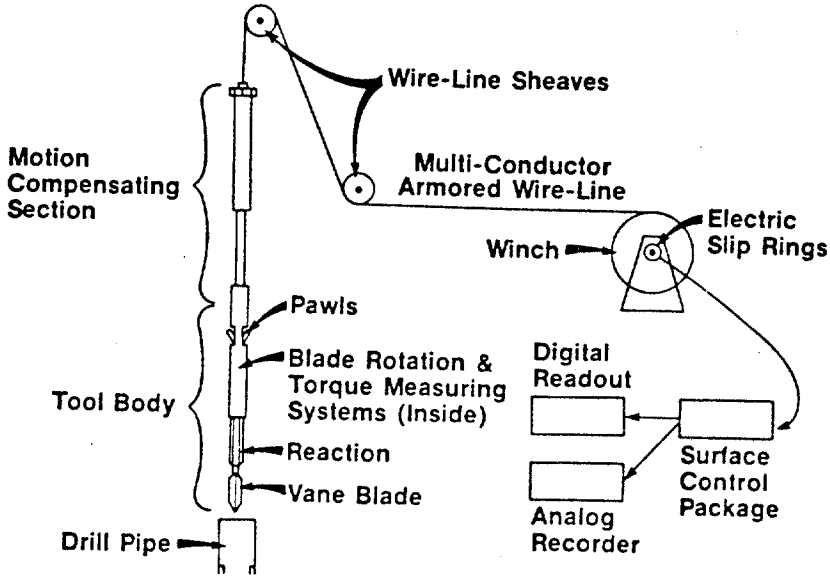

Fig. 4 - Remote Wireline Vane
(From Doyle et al, 1971,
and Ehlers and Babb, 1980)

test is performed by activating the controls on the ship deck. After completion of the test, the tool assembly is retrieved and drilling resumed.

The remote vane test as described above cannot be used until the borehole has advanced at least 5 m to provide sufficient lateral stability for the drill bit while the vane test is being run. For this reason, when an in-situ vane test is desired in shallower depths, a different procedure must be used. Instead of wireline technique, the vane testing tool is attached to a small seabed platform called the HALIBUT (Figure 5) at the desired distance below the platform. The platform is then lowered in the water until it rests on the sea floor and the vane penetrates the soil to the desired depth. The vane is then activated to measure the in-situ strength.

According to the test results presented by Doyle et al (1971) and Ehlers and Babb (1980), the remote vane is capable of obtaining reliable data for the in-situ undrained shear strength of underwater clays. A typical set of test data obtained by this instrument is shown in Figure 6. In this figure, the remote vane data are compared with the results of laboratory miniature vane shear tests on 5.7 cm driven samples. The adjustment factors indicated on the figure were selected based on an evaluation of a large number of test results (Ehlers and Babb, 1980).

4.2 - Wireline Cone Penetrometer

Another in-situ test adapted for offshore investigations is the cone penetrometer test. This test can be used both in sands and clays. The in-situ strength can be estimated from the cone tip resistance data. In addition, the soil-steel frictional resistance can be measured on the cylindrical surface of the cone penetrometer shaft.

A wireline cone penetrometer called WISON was developed by B. V. Fugro, Netherlands, and has been used in Europe and elsewhere since 1973 (deRuiter, 1975 and 1976; LeTirant, 1979;

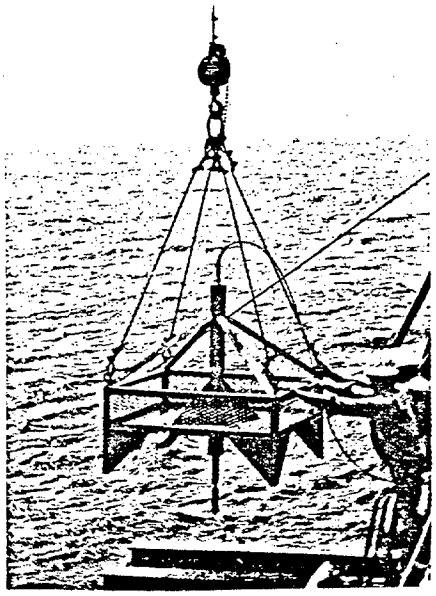

Fig. 5 - HALIBUT Frame for Remote Vane Shear Test

(From Ehlers and Babb, 1980)

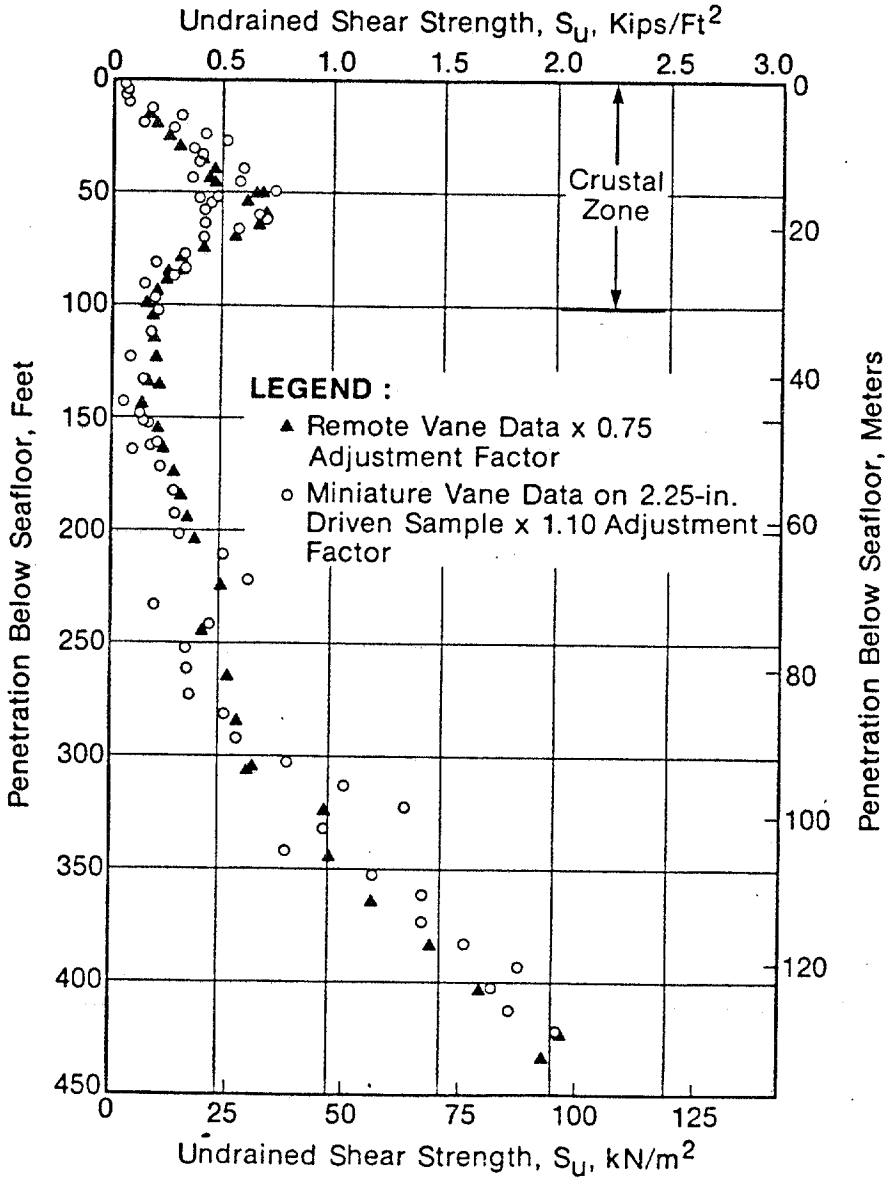

Fig. 6 - Comparison of Remote Vane Data and Miniature Vane Data

(From Ehlers and Babb, 1980)

Windle, 1981; Noorany, 1981; deRuiter and Richards, 1983). This was a particularly useful instrument for geotechnical investigations in the North Sea where subsea soils in many sites consisted of dense sands and stiff clays where the wireline vane could not be used.

Figure 7 shows a schematic diagram of the WISON. The device is only 9 cm in diameter and consists of a hydraulic jacking system and a cone penetrometer. The assembly can be suspended from the wireline inside the drill string and lowered to the bottom of the hole until it latches onto the bottom of the drill pipe. The weight of the drill string provides the reaction for cone penetration test. The cone is activated by hydraulic pressure and pushed into the soil.

The WISON cone has a cross-sectional area of 5 cm^2 and a stroke of 1.5 m. The cone tip resistance can be measured and recorded continuously. Also, simultaneously, the side friction on the cone shaft can be measured and plotted.

In very dense sands or hard clays the depth of penetration of the WISON cone may be limited by the maximum capacity of the hydraulic jack which is approximately 3 metric tons. However, an advanced design, WISON Mark III (Figure 8) has been developed for use with the Drillstring Anchor. The anchor provides sufficient reaction force for pushing a larger cone, the standard Dutch cone with a cross-sectional area of 10 cm^2, into the soil. Two sizes of WISON Mark III are available for 1.5 m and 3 m stroke, respectively.

The B. V. Fugro wireline cone penetrometer has been used extensively in the North Sea as well as other parts of the ocean. To stabilize the drill string in waters deeper than 30 m, heave compensators are necessary. In addition, a seabed platform called SEACLAM can be used to add to the stability of the drill string. A schematic diagram of the use of WISON in conjunction with SEACLAM is shown in Figure 9.

The depth of operation of WISON at present is 450 m combined water and penetration depth. There do not seem to be any major technical difficulties in extending these capabilities for use in deeper waters.

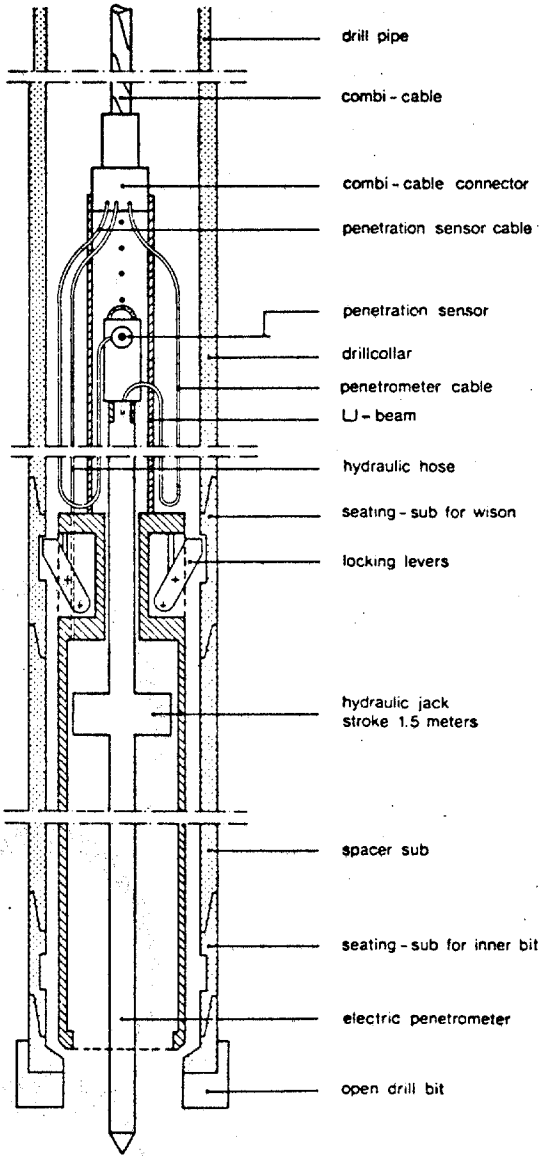

Fig. 7 - WISON Wireline Cone Penetrometer
(From Fugro, B. V.)

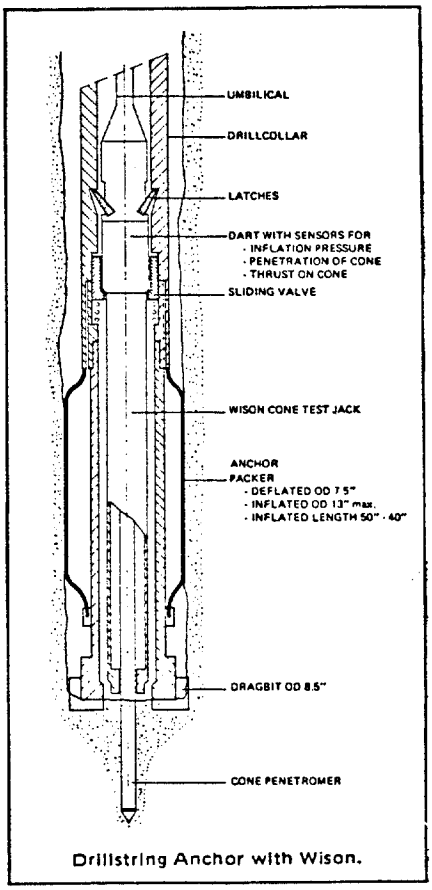

Fig. 8 - WISON Mark III with Drillstring Anchor

(From B. V. Fugro)

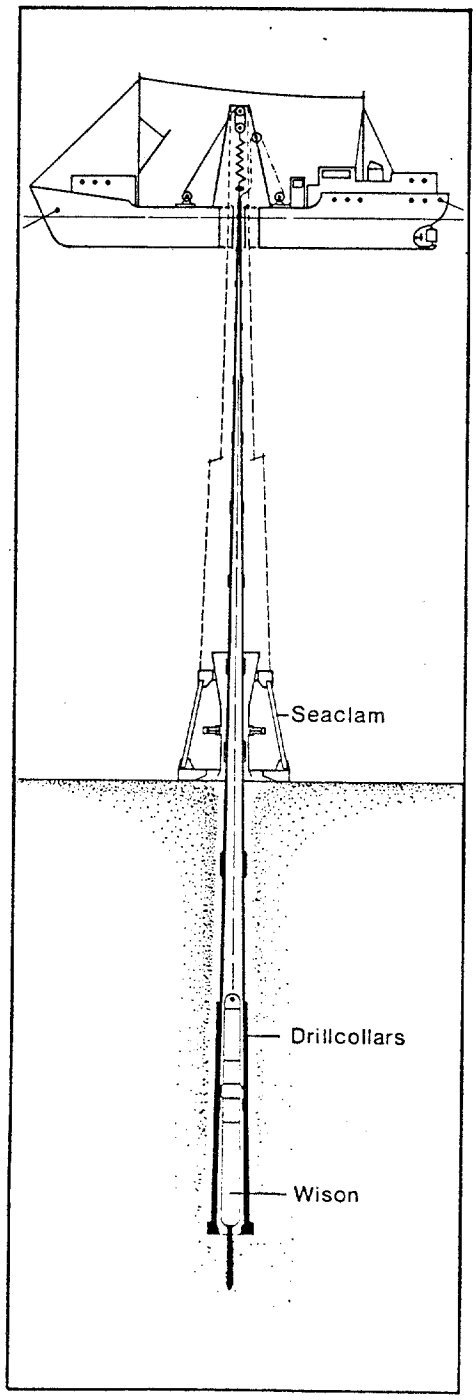

Offshore borings made for the purpose of geotechnical investigations are generally drilled without the use of a riser. The unsupported drillstring provides only limited reaction for downhole soil testing such as push-sampling and cone testing.
Better horizontal and vertical control can be obtained using the Fugro SEACLAM.

The 'SEACLAM' consists of a frame resting on the seabed which serves as a re entry base. It can be clamped on to the drillstring to stabilize the string vertically and to increase the reaction during downhole tests.
With its clamping feature, which provides the necessary horizontal and vertical control, the 'SEACLAM' enables soil testing with the present sophisticated 'WISON' and 'WIPSAMPLER' systems to be performed from mudline.

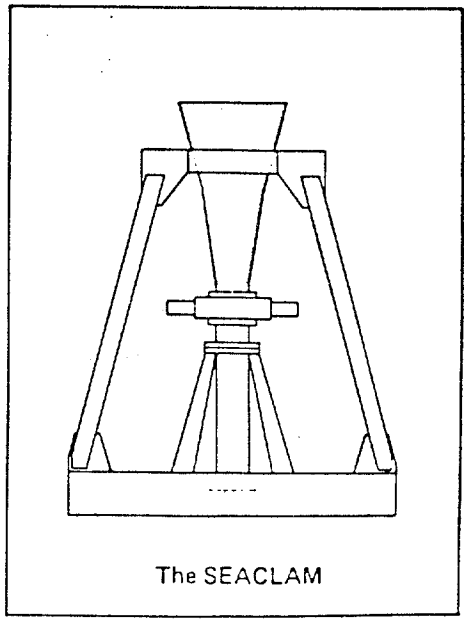
The SEACLAM

Fig. 9 - The Seaclam
(From B. V. Fugro)

4.3 - Wireline Piezometer

The seabed pore water pressure in clays may be different from the hydrostatic pressure because of sediment under consolidation, or as a result of wave action. To measure in situ pore pressure in boreholes, a downhole wireline pore pressure piezometer was developed by McClelland Engineers (Preslan and Babb, 1979) and used in 198 m of water in a borehole drilled to 61 m below the sea floor.

5. IN-SITU TESTS FROM SEABED PLATFORMS

The wireline and cone penetrometer tests described above are very useful for making in-situ strength and penetration resistance measurements in boreholes. For near surface measurements, however, to depths of tens of feet or tens of meters, more accurate cone penetration tests can be performed from a stable platform placed on the sea floor. Such a tethered platform can serve as a stable support and reaction for cone penetration or vane shear tests as well as a support and re-entry hole for the drill string.

At present, there are several seabed platforms for cone penetration testing. They were primarily developed for site explorations in the North Sea and are all for the purpose of cone penetration tests on the sea floor. However, these seabed platforms can presumably be modified for conducting other types of in-situ tests including the vane shear test. The main features of these types of underwater in-situ testing instruments are described in the following sections.

5.1 - The Seacalf

The first underwater cone penetrometer rig was developed by B. V. Fugro, Netherlands (deRuiter, 1975 and 1976; Zuidberg, 1975; Sullivan, 1980; Noorany, 1981). A schematic diagram of this system called the Seacalf is shown in Figure 10. It

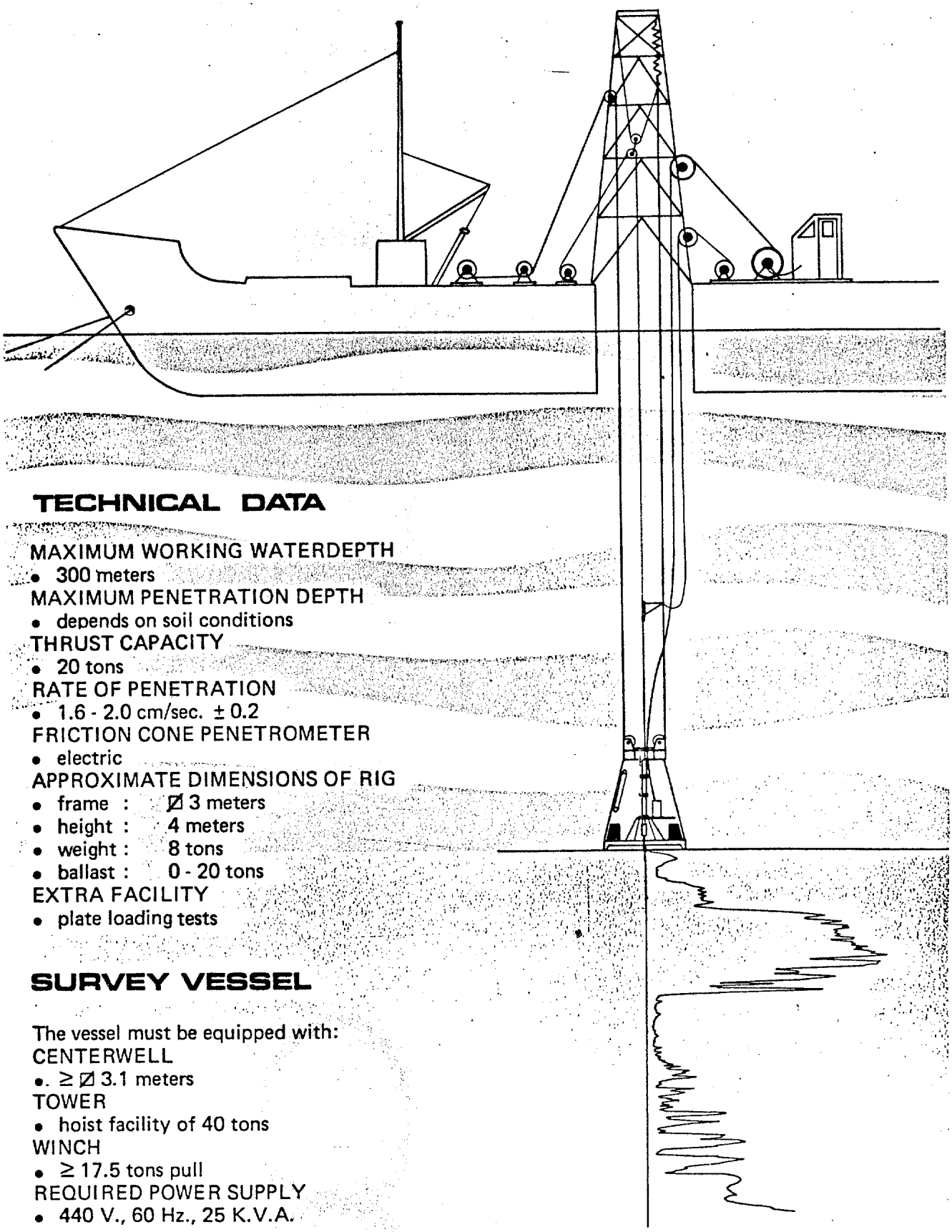

TECHNICAL DATA

MAXIMUM WORKING WATERDEPTH
- 300 meters

MAXIMUM PENETRATION DEPTH
- depends on soil conditions

THRUST CAPACITY
- 20 tons

RATE OF PENETRATION
- 1.6 - 2.0 cm/sec. ± 0.2

FRICTION CONE PENETROMETER
- electric

APPROXIMATE DIMENSIONS OF RIG
- frame : Ø 3 meters
- height : 4 meters
- weight : 8 tons
- ballast : 0 - 20 tons

EXTRA FACILITY
- plate loading tests

SURVEY VESSEL

The vessel must be equipped with:

CENTERWELL
- ≥ Ø 3.1 meters

TOWER
- hoist facility of 40 tons

WINCH
- ≥ 17.5 tons pull

REQUIRED POWER SUPPLY
- 440 V., 60 Hz., 25 K.V.A.

Fig. 10 - The Seacalf
(From B. V. Fugro)

consists of a 3 m x 3 m base and 4 m high tethered platform for performing cone penetration tests from the seabed. Its maximum water depth capability varies from 300 to 650 m depending on the type of rigging. The rig can be deployed from any drill vessel having a moon pool larger than 3.1 m x 3.1 m. The hydraulic jacking system is mounted in a ballasted frame that can provide reactions ranging from 6 to 26 metric tons.

Various sizes of cones with cross-sectional areas from 10 to 15 cm^2 can be used with Seacalf. The tip resistance and skin friction can be measured independently, and the data can be recorded continuously on the ship deck. Typical penetration depths of Seacalf's penetrometer vary from 10 to 60 m depending on the soil conditions.

5.2 - The Stingray

Another underwater cone penetrometer rig is the Stingray (Figure 11) which was developed by McClelland Engineers (Ferguson et al, 1977; Sullivan, 1980; Noorany, 1981). Like Seacalf, Stingray can provide a stable sea floor base for cone penetration tests. The jacking system of Stingray consists of two horizontal rams and two vertical rams; the horizontal rams clamp onto the drill string and the vertical rams raise it approximately 1 m off the bottom. The cone penetrometer is then lowered on wireline through the center of the drill string, and the vertical rams of the Stingray push it 1 m into the soil. The jacking process is repeated until the 5 m cone rod has fully penetrated the soil or until refusal is reached. The cone and rod are then retrieved by wireline and drilling is continued to a new depth for another cone penetration test.

Three different sizes of cone can be used with Stingray: 5 cm^2, 10 cm^2, and 20 cm^2. This rig has been utilized in the North Sea since 1977 and has made cone penetration tests in hard clays to a depth of 24 m below the sea floor.

Another seabed platform of this type, with operational details very similar to the Stingray, is the Seabed Jack,

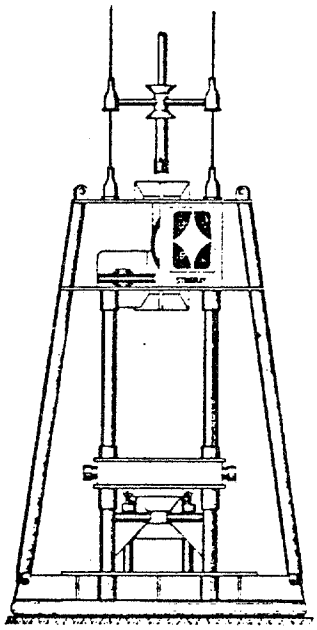

(a) Jacking unit on bottom, drill pipe being lowered.

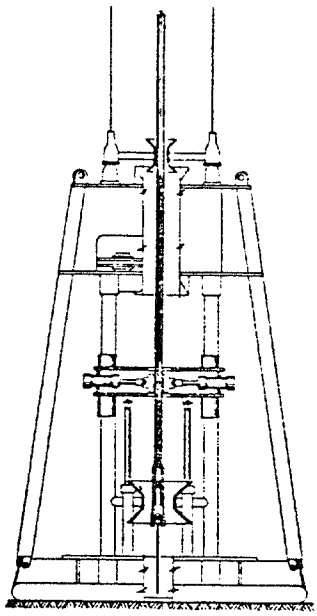

(b) Drill pipe clamped and held 3 ft. off bottom, and wire-line cone penetrometer locked into drill bit 20-ft. cone rod attached.

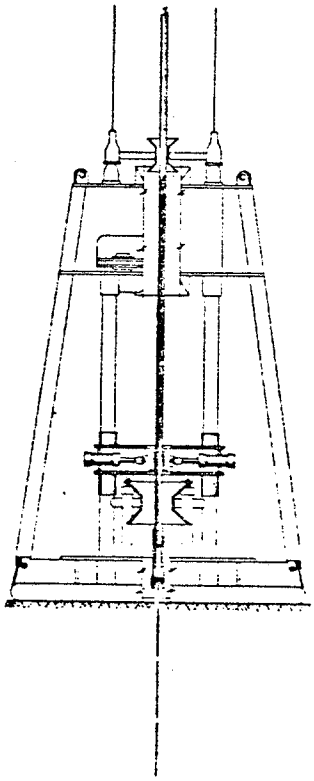

(c) Cone forced to 15-ft. penetration by repeated jack strokes.

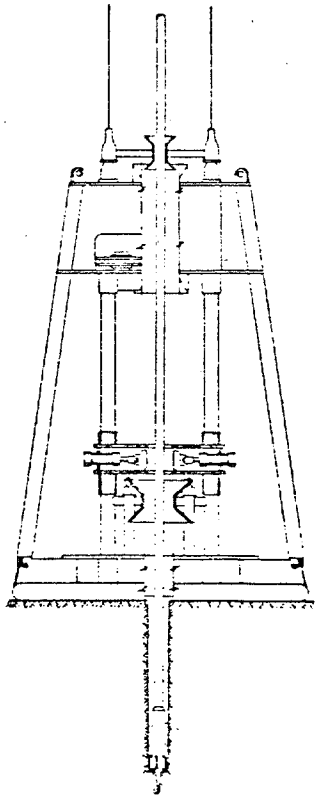

(d) Cone and rod removed, hole drilled to 14-ft. depth, ready for repeat of cone test cycle.

Fig. 11 - The Stingray

(from McClelland Engineers)

developed through the joint efforts of the Norwegian Geotechnical Institute and Norsk Teknisk Byggekontroll Company in Norway (Hoeg, 1976; Andersen et al, 1979).

5.3 - Other Seabed Penetrometers

In addition to the Seacalf, the Stingray, and the Seabed Jack, there are two other seabed platforms for conducting static cone penetrometer tests. These are the Hyson penetrometer, and the NGI penetrometer. The Hyson penetrometer weighs about 1500 kg and can be ballasted or anchored down on the sea floor and operated by divers. It has a 13 metric ton jacking capacity and a cone penetrometer. The Norwegian Geotechnical Institute (NGI) penetrometer is a seabed penetrometer deployed from a jackup platform. Additional details regarding these seabed cone penetrometers are described by LeTirant (1979).

5.4 - Piezocones

The piezocone is a cone penetrometer which is equipped with a pore water pressure piezometer at the tip (Figure 12). This device was first used offshore of B. V. Fugro, Netherlands, in 1981 (deRuiter and Richards, 1983). The pressure transducer built into the cone tip gives a continuous reading of the pore pressure as the cone is being pushed into the soil. The measured pore pressure is generally different from the hydrostatic ambient water pressure because of the shearing caused by the cone insertion. When the cone penetration is stopped, dissipation of the excess pore pressure can be recorded with time.

In the B. V. Fugro piezocone the pore pressure transducer is installed on the cone tip. In some other piezocones, including the Oxford University Differential Piezometer, the porous annulus for the pore pressure piezometer is installed on the sleeve just above the cone tip. The simultaneous recording

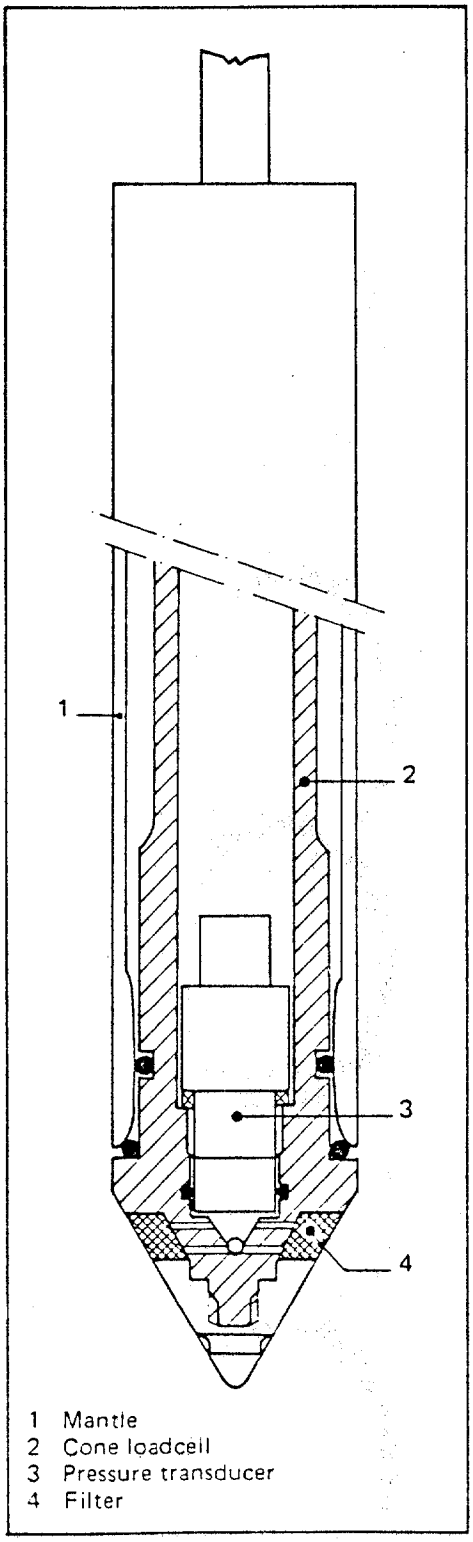

Piezocone description type F5CW

The Fugro pore pressure cone gives a continuous recording of the pore pressure and cone resistance during penetration. The standard FC type penetrometer cone has been modified to incorporate a pressure transducer to measure the pore pressure. A porous ceramic filter is built directly into the cone. Figure 1 shows the basic lay-out.

The pressure transducer's sensing element is placed at the same level as the porous stone and is therefore in direct contact with water which enters through the filter. There are no cavities or small water ports which may effect the pressure response of the pressure transducer. The pressure transducer is of the piezoresistive type with a minimum water displacement and high output signal. Only 0.2 mm^3 water displacement is needed for its full range. The range of the pressure transducers can be chosen depending on expected excess pore pressures. In stiff clays these may be as high as 4 MN/m^2.

To obtain a correct response of the pore pressure, the whole system has to be de-aired. This can be done by boiling the tip in water or by means of a vacuum pump. The filter and cone are covered by a plastic bag or cap which also contains deaired water. Mounting is done under water.

Before making the cone penetration test a hole must be predrilled to about 0.2 m below the water table. This has to be done to avoid air entry into the porous stone. When the CPT is started the plastic bag will be damaged by the cone and is left above the soil.
The dynamic pore pressures during penetration are recorded continuously and simultaneously with the cone resistance. When the test is stopped, dissipation of the excess pore pressure can be recorded on a time scale.

Fig. 12 - The Piezocone
(from Fugro, B. V.)

of the cone penetration resistance and the excess pore pressure at the cone tip can be useful in identification of soil stratigraphy as illustrated by the sample data shown in Figure 13. In sands, the excess pore pressure dissipates very quickly, but in clays high pore pressure builds up instantaneously and dissipates very slowly depending on the soil permeability. The present trend indicates that all future cone penetrometers will be equipped with pore pressure transducers. This would help in the interpretation of the test results in terms of effective stresses.

5.5 - Pressuremeters

Pressuremeter (Figure 14) has been in use in Europe for many years (Menard, 1957; Gambin, 1971; LeTirant, 1979). The pressuremeter has been adapted for use in offshore boreholes in waters up to 792 m deep.

The principle of operation of the pressuremeter is illustrated in Figure 14. An expandable cylinder is placed inside a borehole and pressurized to expand against the sides of the borehole. Pressures and the corresponding volume changes are measured to interpret the stress-strain behavior of the soil in situ.

A self-boring pressuremeter developed at Cambridge University and referred to a Camkometer (Wroth and Hughes, 1973; Windle and Wroth, 1977) is shown in Figure 15. The apparatus is jacked into the soil and the soil entering it is brought to the surface with a cutter and water flushing. The self-boring pressuremeter is superior to the normal pressuremeter in that there is complete contact between the soil and the walls of the pressuremeter at all times and K_o stress conditions are satisfied. Various techniques of deployment of pressuremeters for offshore in situ measurements are described by LeTirant, 1979.

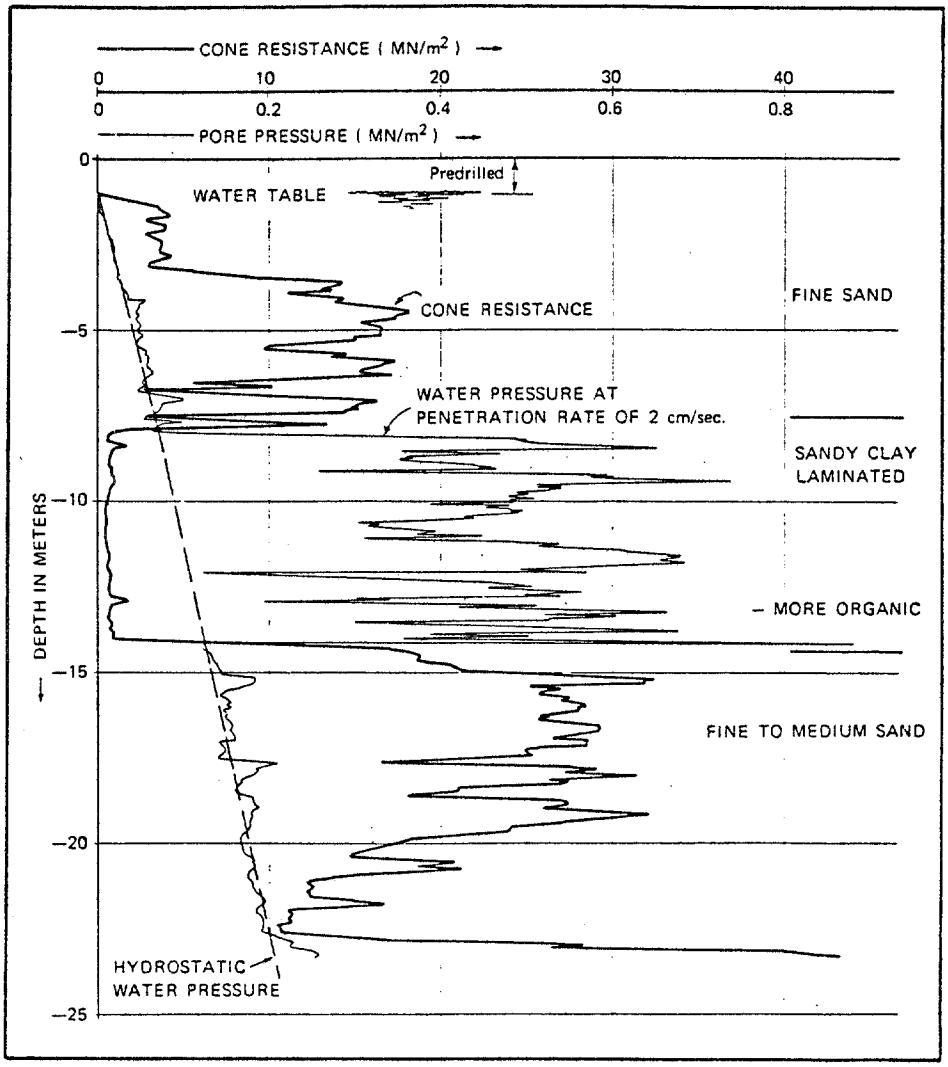

Fig. 13 - Typical Results of Piezocone
(from deRuiter and Richards, 1983)

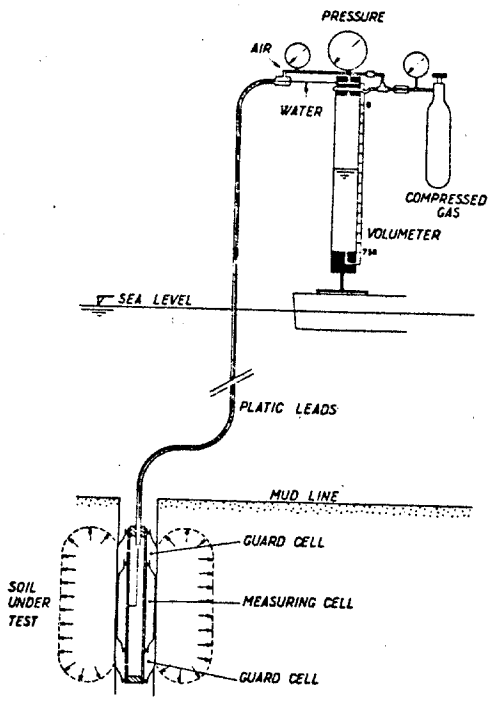

Fig. 14 - Pressuremeter
(from Gambin, 1971)

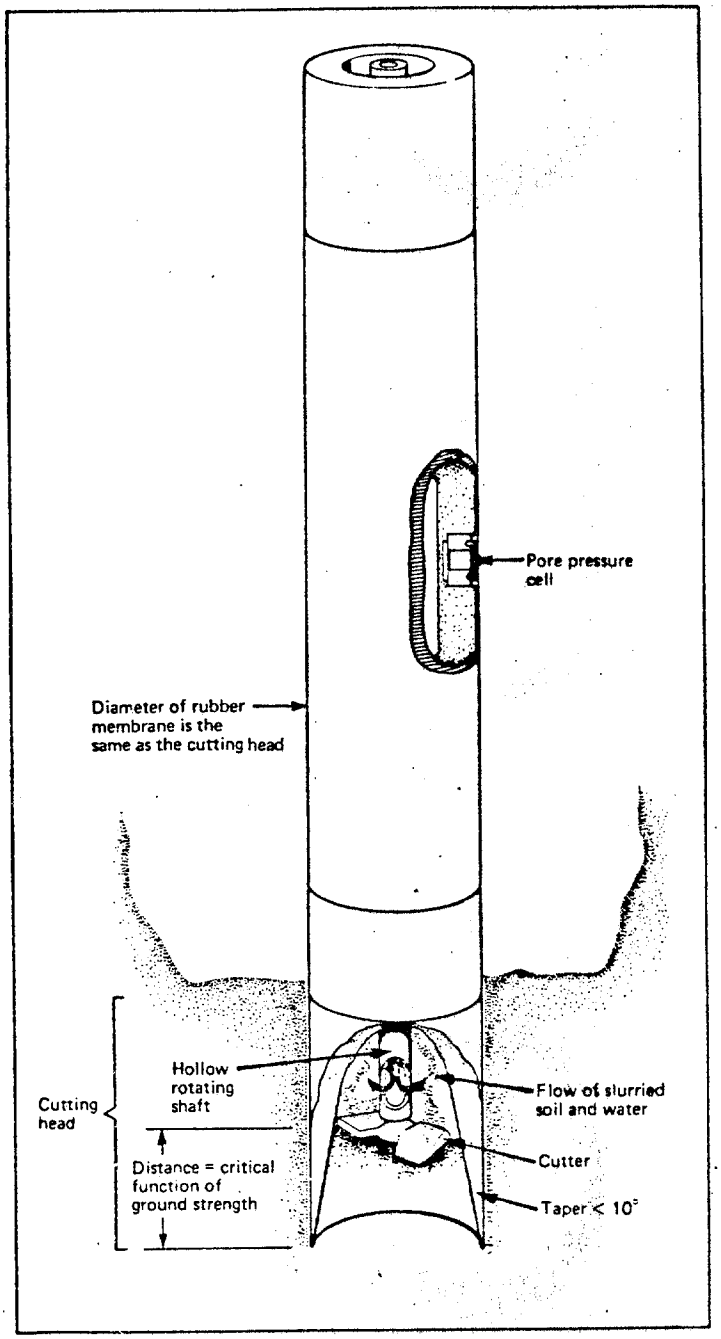

Schematic diagram of the self-boring pressuremeter before insertion

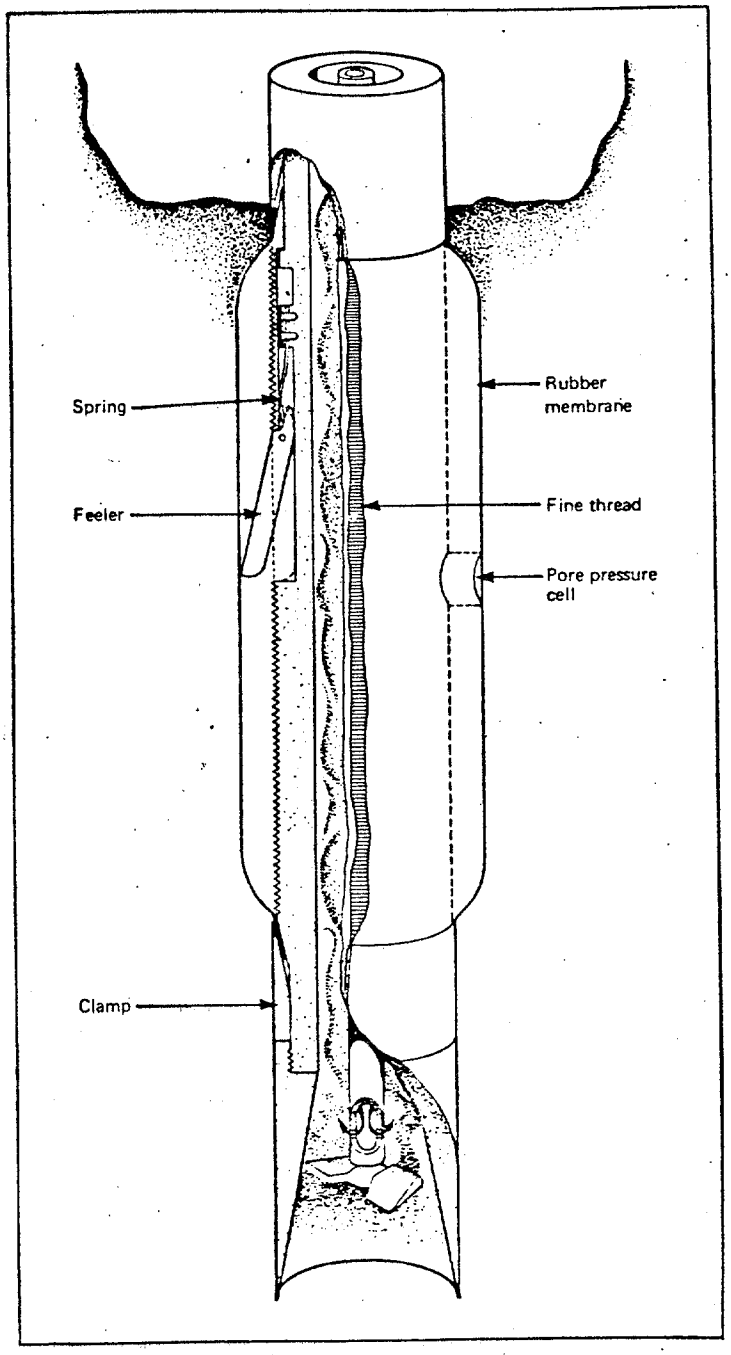

Schematic diagram of the self-boring pressuremeter during an expansion test

Fig. 15 - Self-Boring Pressuremeter
(from Windle and Wroth, 1977)

5.6 - Pressiopenetrometer

An in situ probe consisting of a cone penetrometer, piezometer, and pressuremeter has been developed at the Laboratoire Cetral des Ponts et Chaussees in France (Baguelin and Jezequal, 1983). A schematic diagram of this device, called LPC pressiopenetrometer, is shown in Figure 16. The instrument is deployed from a sea floor support frame. A hammer or a vibrating drive head can be used to drive the probe into the soil. The cone penetrometer has a diameter of 89 mm. The piezometer cell element is installed above the cone penetrometer friction sleeve, and the pressuremeter cell is above the piezometer cell. The maximum depth of penetration is 12 m. Because vibration is used for driving, it is not necessary for the seabed support frame to be very heavy.

5.7 - Soil-Steel Friction Test

B. V. Fugro, Netherlands, has developed a test unit for in-situ measurement of soil-steel friction on a model pile installed in the bottom of a borehole. A schematic diagram of this test facility is shown in Figure 17. The model pile is deployed in the same manner that the WISON cone is deployed inside the drill string. After the test unit latches onto the drillstring, the model pile is jacked into the soil. It is then slowly pulled out, and the force and displacement are measured by lifting the entire drill string. The vertical lifting force applied to the drill-string is provided by a seabed jack which is a ballasted underwater frame with clamps and hydraulic jacks as illustrated in Figure 17.

6. IN-SITU TESTS FROM DIVING BELL

A diving bell for geotechnical investigations has been developed jointly by the Delft Soil Mechanics Laboratory (LGM) and the Dutch diving company Duikbedrijf Vriens (Vermeiden,

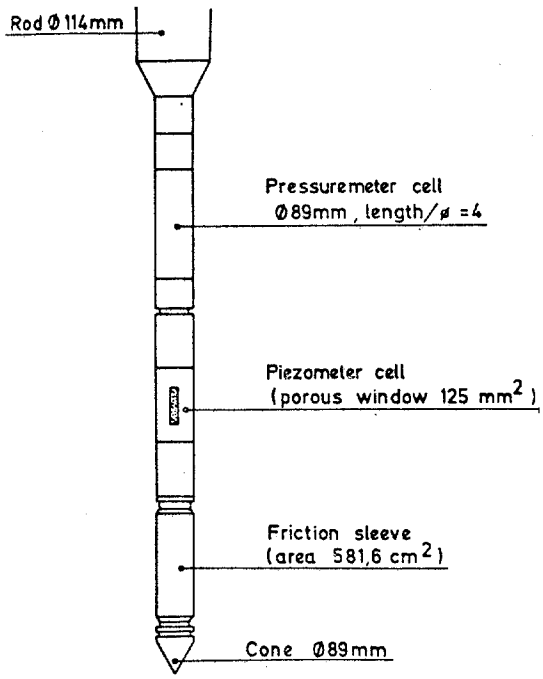

Fig. 16 - Pressiopenetrometer
(from Baguelin and Jezequal, 1983)

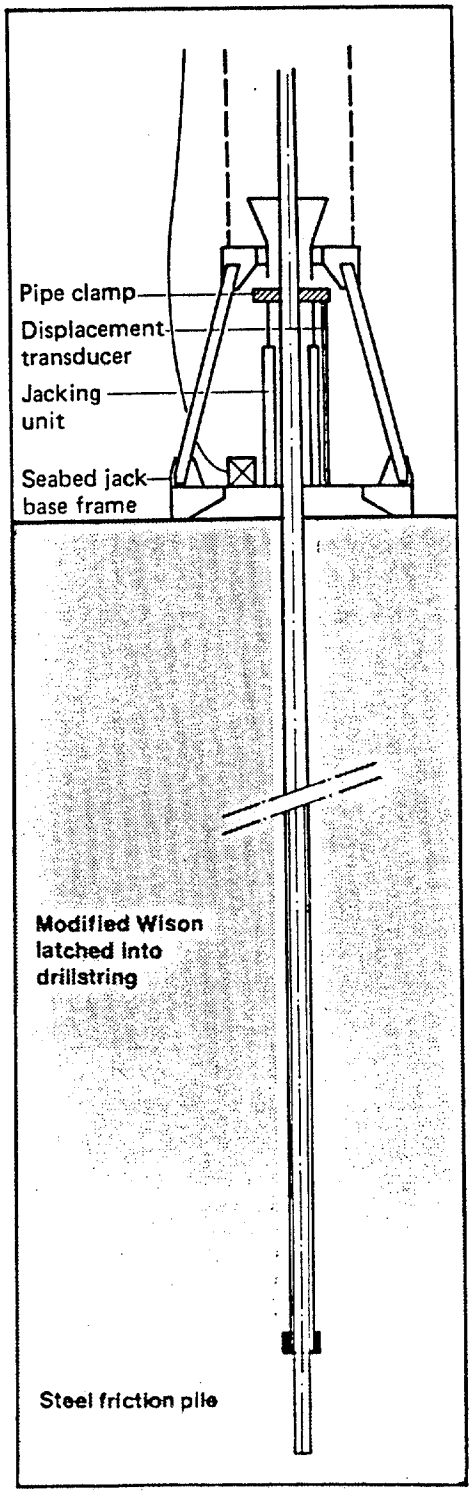

The Steel Friction Test equipment has been developed to perform axial load tests on a model pile installed in the bottom of a borehole.
The test provides reliable in-situ data on the friction developed upon the model pile during tension.
Tests can be performed in either static or cyclic mode and to a maximum depth of 650 m below waterlevel.
Testing time is typically one hour per static test.

The complete testing system consists of two major components: the Seabed Jack and the Steel Friction Test unit.
The Seabed Jack is a ballasted underwater test device, which when in position on the seabed, is used to provide the vertical lifting force to the model pile during testing. In addition, it can be used as a re-entry base and to clamp the drillstring to stabilise its vertical movement and to increase the available reaction during additional in-situ downhole tests.
The Steel Friction Test unit consists of a model instrument pile attached to a modified Wison testing unit. This unit is used to push the model pile into the soil and to measure tensile forces and displacements during extraction.

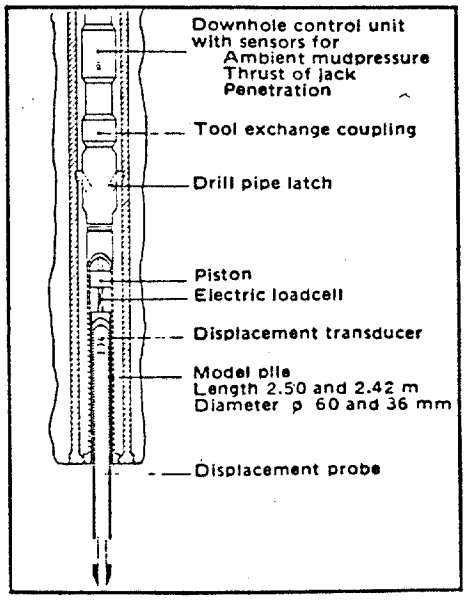

Fig. 17 - Steel Friction Test
(from B. V. Fugro)

1978; Noorany, 1981). A schematic diagram of the diving bell is shown in Figure 18. It consists of a work chamber, a sampling and cone penetration tower, and a ballasted base plate. The base plate has a diameter of 6 m and can be ballasted to provide a reaction force as high as 67 metric tons. The work chamber has sufficient space for two drillers and the test rods and tools required for drilling, sampling or in-situ testing.

The water depth capability of the diving bell is 200 m. Cone penetration tests can be run while the work chamber is at atmospheric pressure. However, during drilling and sampling operations, the chamber must be pressurized.

The deployment of the diving bell requires a barge with a special decompression chamber for the decompression of the driller-divers. The diving bell has been used in the coastal waters of Holland, and in the Beaufort Sea for sampling and in-situ cone penetration tests.

7. IN-SITU TESTS BY MEANS OF PENETRATORS

A penetrator is a long, thin pointed metal billet which impacts the earth and penetrates. The deployment of a seabed penetrator is shown in Figure 19. Impact velocity is usually achieved by free-fall, but an underwater launcher and data retrieval system have been developed (James, 1983). The accelerations developed by the penetrator as it is slowed by the soils are sensed, and these are used to calculate the strengths of the soils penetrated (McNeill, 1981). The accelerations are sensed directly (Dayal et al, 1980; McNeill, 1981) or are being calculated by differentiating Doppler velocity records (Beard, 1977). The former has been used in by far the majority of applications, but the latter has been applied to very deep waters, e.g., 18,000 ft.

The soil shear strength, S, at a given depth is calculated approximately from the simple relationship

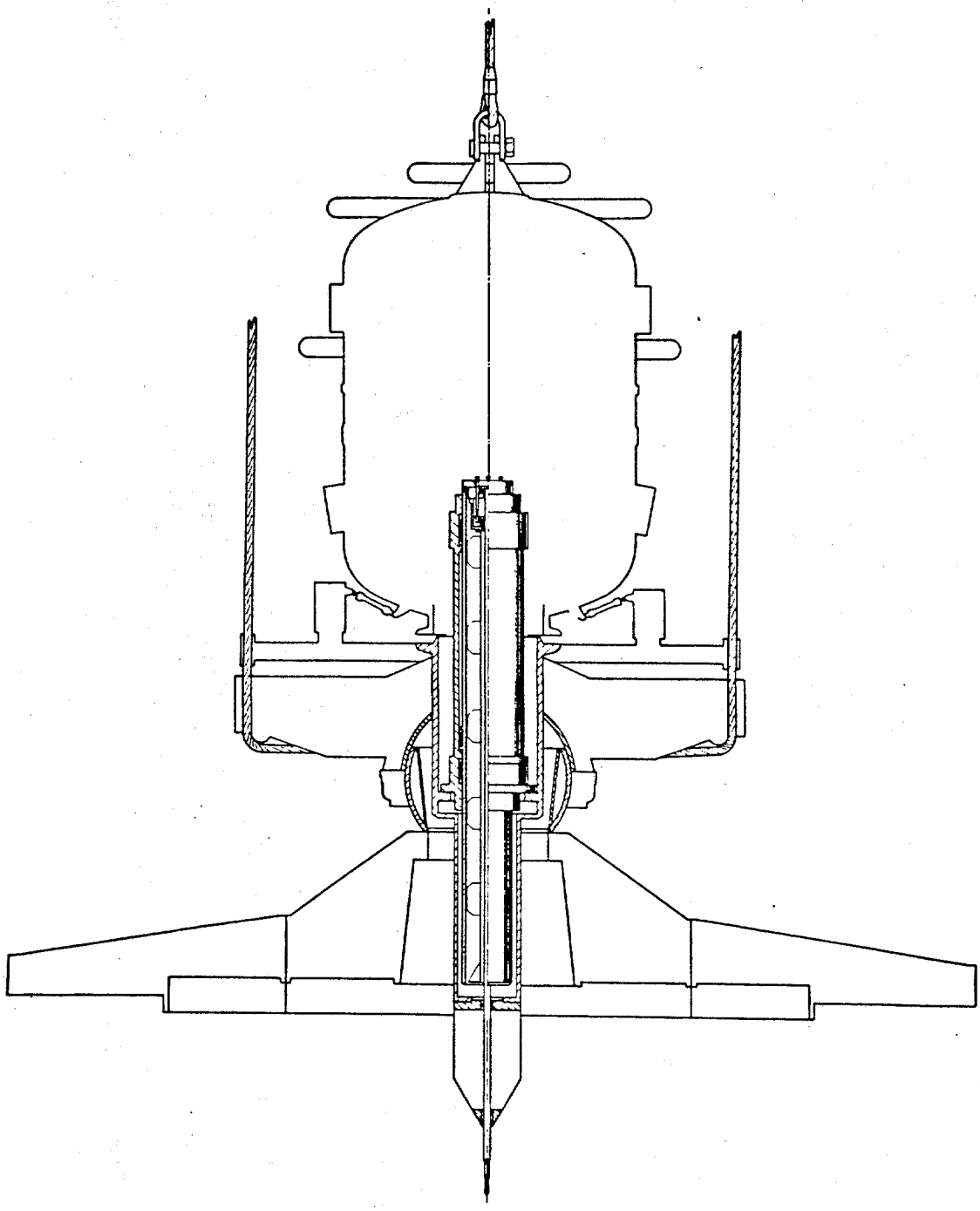

Fig. 18 - The Diving Bell
(from the Delft Soil Mechanics Laboratory)

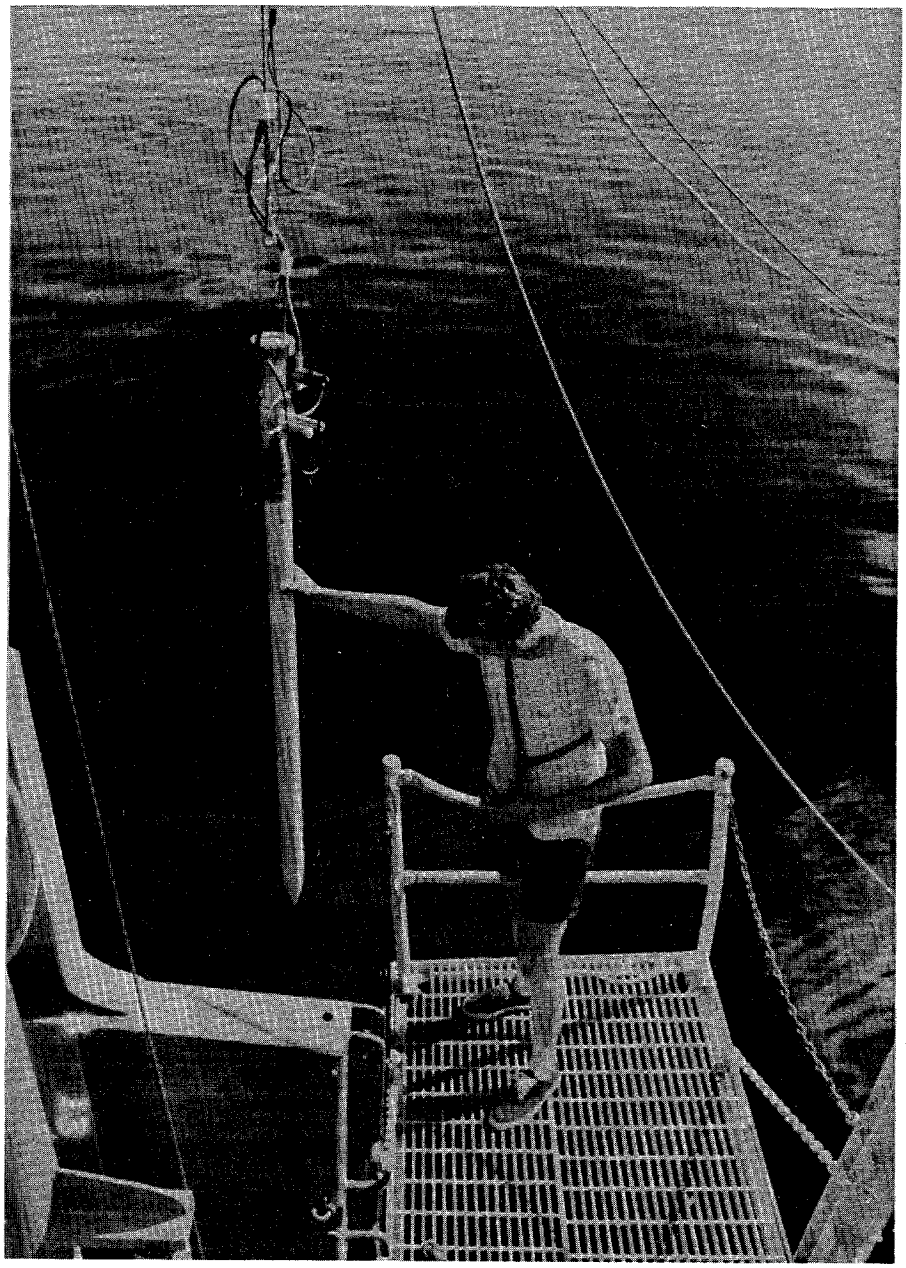

Fig. 19 - Deployment of a Sandia National Laboratories Seabed Penetrator (MSP) in the Gulf of Mexico

$$S = KD$$

where

$$D = \text{measured acceleration at that depth}$$

and

$$K = (QR)/(2gH) \quad .$$

In that formulation (McNeill, 1981), g is the local acceleration of gravity, H is the length of the penetrator, R is the radius of the penetrator, and Q is the sectional pressure (weight divided by frontal area). The calculated shear strengths are only good below a depth equal to one or perhaps one and one-half penetrator body lengths. Below those depths, however, strengths calculated from penetrator accelerations seem to be more sensitive to minor variations in soil properties than do conventional samples or in-situ tests; and if the soil is gassy, the penetrator values are probably better than those obtained from conventional drill sample test procedures (where expansion of the depressurized gasses destroys the structure of the soil).

Penetrators have been shown to give accurate strengths for soils ranging in shear strength from as low as 200 or so psf to as high as 100,000 psf. The strength values are very good in cohesive soils, but the values in cohesionless soils have not yet been assessed.

Penetrators appear to have their greatest potential in enhancing the knowledge derived from offshore geophysical profiling (McNeill, 1979). In that application, an expendable penetrator is thrown off the geophysics boat from time to time as the profiling is being done. The profiling furnishes travel time layering on a continuous two dimensional basis, while the penetrator furnishes the layer thicknesses and soil shear strengths at the selected points. The layer thicknesses allow

estimation of the velocities (in conjunction with the seismic travel times), and the shear strengths allow enhanced interpretation of the geophysical profile between the penetrator drop points. By executing a series of crossing geophysical lines, a three dimensional lithological picture can be developed to include the shear strengths of the layers. In situations where geotechnical conditions might influence the location of an offshore structure (e.g., submarine slide potential, driveability of piles, etc.) such a model is invaluable.

No off-the-shelf penetrator operating system is presently on the market. Most of the work has, however, been performed by Sandia National Laboratories so that the data and information on the hardware are readily available for the asking.

8. SUMMARY

At present (1983), offshore in-situ tests for geotechnical explorations can be made by means of wireline technique, from seabed platforms, from a diving bell, or by means of ballistic penetrators. The support vessel for wireline operations as well as in-situ tests from seabed platforms requires a central moon pool and preferably dynamic positioning gear. The wireline in situ tests include remote vane, WISON cone penetrometer and wireline piezometer. The tests performed from seabed platforms include the Seacalf, the Stingray, the Hyson and the NGI penetrometers. Other in-situ tests are pressuremeter, piezocone, and a new penetrometer which combines cone penetrometer, piezometer, and pressuremeter in one probe. The Dutch diving bell is the only underwater pressurized vessel for performing deep penetration sampling and in-situ testing on the sea floor.

At present, the available in-situ testing tools are suitable for tests in waters as deep as 300 to 400 m. The technology is available to extend the operational depth of these tools to deeper waters.

9. REFERENCES

Anderson, A., T. Berre, A. Kleven, and T. Lunne, "Procedures Used to Obtain Soil Parameters for Foundation Engineering in the North Sea," Marine Geotechnology Journal, Vol. 3, No. 3, 1979, pp. 201-266.

Baguelin, F. J., and J. F. Jezequal, "The LPC Pressiopenetrometer," Proceedings of the ASCE Conference on Geotechnical Practice in Offshore Engineering, Austin, Texas, 1983, pp. 203-219.

Beard, R. M., "Expendable Doppler Penetrometer: A Performance Evaluation," TR-R 855, NCEL, Port Hueneme, CA, July 1977.

Dayal, U., J. H. Allen, and D. V. Reddy, "Low Velocity Projectile Penetration of Clay," J., Geotech. Div., Vol. 106, Paper 1556S7, GT8, ASCE, NY, August 1980.

deRuiter, J., "The Use of In-Situ Testing for North Sea Soil Studies," Offshore Europe Conference, Aberdeen, 1975, 219.1.

deRuiter, J., and D. A. Fox, "Site Investigations for North Sea Forties Field," Proceedings of the Offshore Technology Conference, OTC paper No. 2246, 1975, pp. 21-36.

deRuiter, J., "North Sea Site Investigations - the Role of the Geotechnical Consultant," Offshore Soil Mechanics published by Cambridge University Engineering Dept. and Lloyd's Register of Shipping, England, 1976, pp. 61-78.

deRuiter, J., and A. F. Richards, "Marine Geotechnical Investigations, a Mature Technology," Proceedings of the ASCE Conference on Geotechnical Practice in Offshore Engineering, Austin, Texas, 1983, pp. 1-24.

Doyle, D. H., B. McClelland, and G. H. Ferguson, "Wireline Vane Probe for Deep Penetration Measurements of Ocean Sediment Strength," Ocean Technology Conference, 1971.

Ehlers, C. J., and L. V. Babb, "In Situ Soil Testing: Remote Vane," in Soundings, published by McClelland Engineers, Spring 1980.

Ferguson, G. H., B. McClelland, and W. D. Bett, "Seafloor Cone Penetrometer for Deep Penetration Measurements of Ocean Sediment Strength," Proceedings, Offshore Technology Conference, OTC Paper No. 2787, 1977.

Gambin, M. P., Discussion, Journal of Soil Mechanics and Foundation Engineering Division, ASCE, Vol. 97, No. SM6, June 1971, pp. 937-939.

George, P. J., "Notes on Site Investigation with Respect to the Design of Offshore Structures," Offshore Soil Mechanics published by Cambridge University Engineering Dept. and Lloyd's Register of Shipping, England, 1976, pp. 101-116.

George, P., and D. Wood, "Offshore Soil Mechanics," Cambridge University Engineering Dept. and Lloyd's Register of Shipping, England, 1976.

Hoeg, K., "Foundation Engineering for Fixed Offshore Structures," Norwegian Geotechnical Institute Publication No. 114, 1976.

James, L. T., "Gun-Launched Instrumented Seabed Penetrators: Initial Field Tests of the ISP-1 and ISP-2 Systems," SAND83-0095, Sandia National Laboratories, June 1983.

LeTirant, P., "Seabed Reconnaissance and Offshore Soil Mechanics for the Installation of Petroleum Structures," English translation of J. Chilton-Ward, Gulf Publishing Co., Houston, Texas, 1979.

McNeill, R. L., "Enhancement of Geophysical Soil Profiles Using Instrumented Marine Sediment Penetrators," Proc., No. 3526, OTC, Houston, TX, April 1979.

McNeill, R. L., "Approximate Method for Estimating the Strengths of Cohesive Materials from Penetrator Decelerations," Vol. 2, IEEE Pub. No. 81CH1685-7, The Conf. Rec., Oceans 81, IEEE, NY, Sept. 1981, pp. 688-693.

Menard, L., "Mesures in situ des Propertes Physiques de Sols," Annales des Ponts et Chaussees, Vol. 127, 1957, pp. 357-377.

Noorany, I., "Underwater Soil Sampling and Testing: A State-of-the-Art Review," in Underwater Soil Sampling, Testing and Construction Control, published by the American Society of Testing and Materials, Special Technical Pub. STP501, 1972, pp. 3-41.

Noorany, I., "Offshore Sampling and In Situ Testing: 1981 Update," Proceedings of Conf. on Updating Subsurface Sampling of Soils & Rocks & Their In Situ Testing, Engineering Foundation, NY, in press.

Perkins, R. L., "Floating Rig Takes Core Samples in Deep, Swift Water," Engineering New Record, September 1957.

Presland, W. L., and L. Babb, "Piezometer Measurement for Deep Penetration Marine Applications," Proceedings, Offshore Technology Conference, OTC 3461, 1979, pp. 901-907.

Schjetne, K., and E. D. Brylawski, "Offshore Soil Sampling in the North Sea," State of the Art on Current Practice of Soil Sampling, Singapore, pp. 139-156, published by the Japanese Society of Soil Mechanics and Foundation Engineering, 1979.

Sullivan, R. A., "North Sea Foundation Investigation Techniques," Marine Geotechnology Journal, Vol. 4, No. 1, 1980, pp. 1-30.

Tirey, G. B., "Recent Trends in Underwater Sampling Methods," in Underwater Soil Sampling, Testing and Construction Control, published by the American Society of Testing and Materials, Special Tech. Publication STP 501, 1972.

Vermeiden, J., "Site Investigation Underwater and From a Floating Pontoon," published by the Delft Soil Mechanics Laboratory, 1978.

Windle, D., and C. P. Wroth, "The Use of Self-boring Pressuremeter to Determine Undrained Properties of Clays," Ground Engineering, Sept. 1977.

Windle, D., "Discussion: North Sea Foundation Investigation Techniques," Marine Geotechnology Journal, Vol. 4, No. 5, 1981, pp. 269-278.

Wroth, C. P., and J. M. O. Hughes, "An Instrument for In-Situ Measurements of the Properties of Soft Clays," Proceedings, 8th International Conf. on Soil Mechanics & Foundation Engineering, Moscow, 1973, Vol. 1.2, pp. 487-494.

Zuidberg, H. M., "Seacalf: A Submersible Cone-Penetrometer Rig," Marine Geotechnology, Vol. 1, No. 1, 1975, pp. 15-32.

OCEANS 81 conference record volume two

The Ocean . . . An International Workplace

Boston, Massachusetts

September 16-18, 1981

IEEE Publication Number **81CH1685-7**

APPROXIMATE METHOD FOR ESTIMATING THE STRENGTHS OF COHESIVE MATERIALS FROM PENETRATOR DECELERATIONS

Robert L. McNeill

Sandia National Laboratories
Geotechnical Engineering Division 4752
Albuquerque, NM 87185

ABSTRACT

Using the approximate relationship between shear strength, S, and penetrator deceleration, D,

$$S \sim KD$$

the shear strength of cohesive soils may be closely estimated (an explicit form of K is given in the paper). The calculated values of S lie between the peak undisturbed and the remolded values, and closely approximate the values obtained in conventional boring/sampling/testing procedures. For gassy soils at depth offshore, penetrator-calculated values of shear strength may be more representative of in-situ strengths than conventionally measured strengths. The use of penetrators to augment offshore geophysical surveys greatly increases the value of those surveys.

1. INTRODUCTION

A penetrator is a long, thin, pointed metal billet which impacts the earth and penetrates. Impact velocity is usually achieved by free-fall. Penetrators instrumented with accelerometers have demonstrated that the decelerations are a strong function of the strength of the soil being penetrated. Thus, in principle, it should be possible to estimate soil strengths utilizing the measured decelerations of a given penetrator impacting at a given velocity. This paper presents an approximate approach to making such soil-strength calculations. This approximate approach is guided strongly by the observed behavior of several hundred instrumented penetrators, ranging in diameter from a few inches to 1-1/2 feet; weighing from a few tens to several hundreds of pounds; impacting at velocities from a few tens to a few thousands of feet per second into soils, rocks, ice, and permafrost ranging in shear strength from a few tens to a many tens of thousands of pounds per square foot; and penetrating from a few inches to several hundred feet.

2. PREVIOUS WORK

A number of investigators are studying the mechanisms of penetration. A state-of-the-art review up to 1972 has been presented by McNeill (Ref. 1) and up to 1975 by Triandafilidis (Ref. 2). Young (Refs. 3,4,5) has derived empirical equations to calculate penetration depths into various soils and rocks, each being characterized by a single penetrability constant. The value of the penetrability constant has not been related to soil strength, so that Young's method has not been applied to calculate soil strength.
True (Ref 6) and Beard (Ref. 7) have developed closed-form solutions to calculate soil strengths from penetrator decelerations. The method requires estimates of four soil properties (strain-rate factor, side adhesion factor, sensitivity, and drag coefficient) which are not generally familiar to geotechnical engineers, so that the method has not been widely applied.

McNeill (Ref. 8) developed a simple closed-form solution to estimate soil strengths from penetrator decelerations. Although those derivations did not rigorously account for all of the mechanics of the situation, the method has been shown to yield good estimates of soil strengths over a wide range of practical conditions (Ref. 9). Deyal et al (Ref 10) applied similar mechanics to estimate the entry conditions of a penetrator at low velocities. McNeill and Foster (Ref. 11) improved upon the mechanics of Ref. 8, and demonstrated that the method possibly gives better results for gassy marine clays than do conventional methods of boring, sampling, and testing. The method does, however, require seven coefficients, and will therefore require more verification before it can be recommended for general use. Finally, Forrestal, et. al. (Ref. 12) have applied the theory of an expanding cavity to estimate decelerations at high velocities in rock. The theory constrains the soil/rock particles to move only horizontally, and requires intimate frictional contact of the soil/rock on the penetrator nose and body.

CH1685-7/81/0000-0688 $00.75 © 1981 IEEE

3. PHILOSOPHY OF THE APPROXIMATE SOLUTION

It may be worthwhile to determine what levels of accuracy are required for problems dealing with soil strength.

It is taken as axiomatic, at this stage in penetrator technology, that penetrator-calculated soil strengths will not be used for final design. Instead, penetrators are used in remote areas, principally offshore, to provide areal measures of soil profiles, in conjunction with seismic surveys. The approximate methods of this paper can be used to estimate the strengths for site selection and preliminary designs, and for planning detailed investigative programs for final designs.

To put the philosophy in context, Fig. 1 presents the results of a very carefully conducted study of the shear strengths of a reasonably uniform soft silty clay, deposited in a saline lacrustine environment. The strengths were measured by: in-situ vane, peak undisturbed value; in-situ vane, remolded; and by boring/sampling, and laboratory unconfined and triaxial compression and Torvane. The results show the effects of disturbance on the conventionally measured strengths.

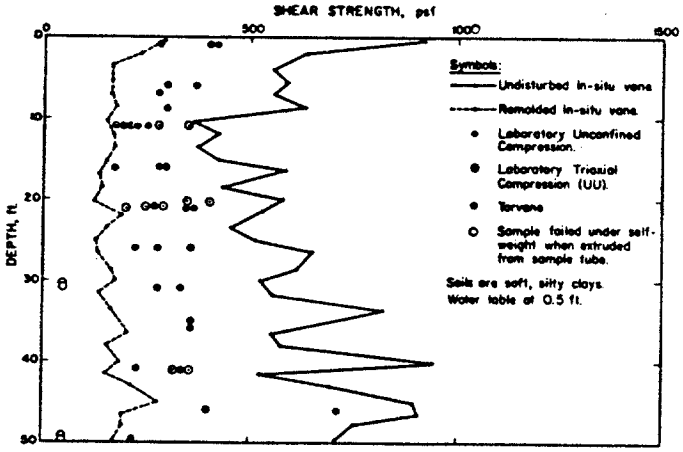

Figure 1: Results of Conventional Shear-Strength Determination

Dealing with situations such as Fig. 1, which is not unusual, has led geotechnical engineers to think in terms of soil-strength classifications, rather than to represent a soil strength as if it were an unique and accurate number. Terzaghi and Peck (Ref. 13) in 1948 proposed such a classification for clays, which is still used today:

Strength Classification	Shear Strength, psf
Very Soft	250
Soft	250-500
Medium	500-1000
Stiff	1000-2000
Very Stiff	2000-4000
Hard	>4000

In the same way, if a penetrator-estimated strength would reliably place a soil in its proper classification, that would be adequately accurate for many geotechnical problems.

Thus the approximate approach to be developed in this paper is motivated by the attitude that extreme accuracy is not necessary, and in fact may be unrealistic. This approximate approach is also motivated by the empirical observation that, for a given penetrator, there seems to be a constant which, when multiplied by the measured deceleration at a given depth, yields a close estimate of the soil's shear strength at that depth, when the penetrator is deeper than its own body length (or so) in a cohesive soil. That is, it appears that a cohesive soil's shear strength, S, can be estimated by,

$$S \sim KD \quad \ldots\ldots\ldots\ldots (1)$$

where: D = measured deceleration of the penetrator
K = apparent constant for that penetrator

Clearly, Eqn. (1) is a substantial approximation because it does not contain velocity or other dynamic terms. Nevertheless, if a means were available to calculate the value of K in Eqn. (1), for a given penetrator, to yield consistent approximate estimates of shear strength between the undisturbed and remolded values, for a wide variety of soils, the use of penetrators in remote areas could provide useful data. Recognizing the approximate nature of Eqn. (1), and acknowledging that Eqn. (1) ignores some aspects of the dynamics of the process, this paper will present an approximate method for calculating K for a given penetrator.

4. PROPOSED MECHANISM

Observations of recovered penetrators which impacted at moderate velocities (up to a few hundred feet per second) in most cases show the following: the hole made by the penetrator is straight; the paint on the nose, and sometimes the nose metal itself, are eroded; the paint on the body is intact, except occasionally for crescent-shaped areas near the tail; and the hole left by the penetrator is usually slightly smaller than the diameter of the penetrator. These observations seem to indicate that, at least under a wide range of conditions, the soil is not strongly in contact with the body of the penetrator throughout most of the penetration event, except at places on the tail, where such contact apparently maintains a stable trajectory.

Figure 2 presents a proposed mechanism of the penetration event which includes features which seem to match the observed phenomena. That mechanism postulates three phases to the penetration event: (1) the entry phase, Fig. 3(a), where the penetrator is forming its hole and a small

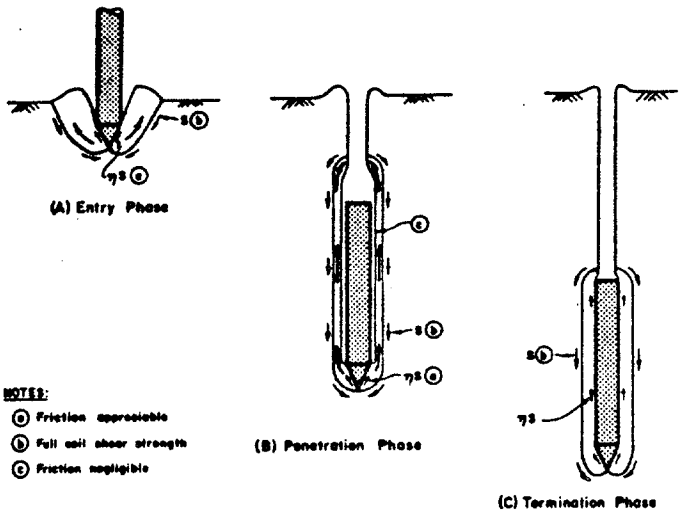

Figure 2: Proposed Mechanism of the Penetration Event

crater by shearing and pushing outward and upward an annular volume of adjacent soil; (2) the penetration phase, Figure 3(b), where the penetrator is forming its hole by pushing outward but principally upward an annular volume of adjacent soil; and (3) the termination phase, Figure 3(c). The mechanism assumes that the splitting action of the nose imparts a horizontal velocity to the soil, which therefore cannot be in strong contact with the body of the penetrator. Thus it is postulated that friction between the soil and the body is small, even negligible. During the penetration phase, the volume of the penetrator can be accommodated by the continuous transport of an annulus of sheared soil up the sides of the penetrator, if the soil is saturated; and/or by densification of the soil, if the soil is partially saturated.

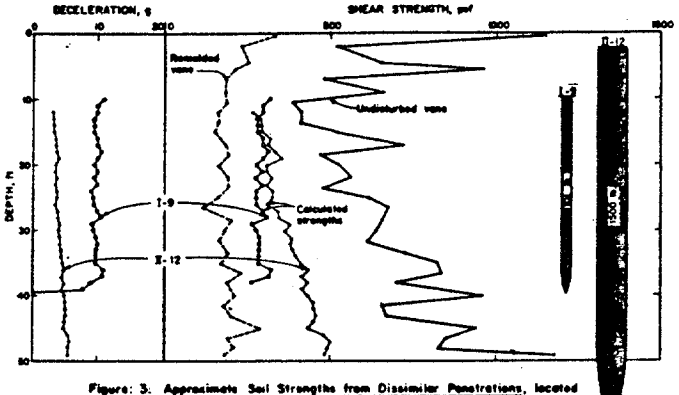

Figure: 3. Approximate Soil Strengths from Dissimilar Penetrations, located 40 ft. apart.

Penetrator	V_o, fps	Q_{max} psi	Diam. in	L/d, in
• I-9	163	143	3	60
• I-12	183	249	9	112

As a practical matter, most penetration events are designed to achieve depth, so that the trajectory is at least several body lengths. Thus the most important part of the event is the penetration phase, Figure 3(b), which is the only phase which will be analyzed by the approximate method of this paper.

The basic derivation of this approximate method has been given by McNeill (Ref. 14). The results are,

$$K \sim \frac{QR}{2gH} \quad \cdots\cdots \quad (2)$$

where: g = local acceleration of gravity
H = penetrator body length
Q = penetrator sectional pressure (W/A, weight divided by frontal area)
R = penetrator radius

The next section will present some examples of soil-strength estimates by this approximation.

5. COMPARISONS TO MEASURED STRENGTHS

The site represented by the strength data of Figure 1 has been used extensively for penetrator experiments. An example shown in Figure 3 is for very dissimilar penetrators which impacted only 40 ft apart. The deceleration curves are quite different, but the resulting calculated strengths using Eqns. (1) and (2) agree quite closely, and lie in the midrange of the nearby measured values. It appears from this example, as well as from many others, that strengths calculated by this approximate method are about the same as those obtained from conventional boring/sampling/testing procedures (cf., Figs. 1, 3); except for deep gassy soils offshore, where the penetrator-calculated values usually exceed the conventionally measured values. Thus, penetrators appear to provide fairly reliable measures of soil strengths.

Penetrators are also apparently very good indicators of small differences in the strengths of the soils which they penetrate. For example, Fig. 4 shows the decelerations of two similar penetrators which impacted about 400 ft from each other: their geometries and impact velocities were the same, but one was slightly heavier than the other. Inspection of the deceleration values shows little convincing evidence of difference. When, however, the shear strengths are calculated, the small differences in decelerations become appreciable differences in shear strength: the soil at I-16 appears to be 20 or so percent weaker than the soil at I-10. Figure 5 presents the results of in-situ vane tests at both locations: the soil at I-16 is indeed weaker, by about 10 to 30 percent. These small differences were detected by both the vane and the penetrator. Figure 6 shows conventional boring/sampling/laboratory-testing data from adjacent borings. It is clear that, without performing a detailed statistical analysis, the conventional data would not reveal the differences in soil strengths detected by the penetrators and the in-situ vane.

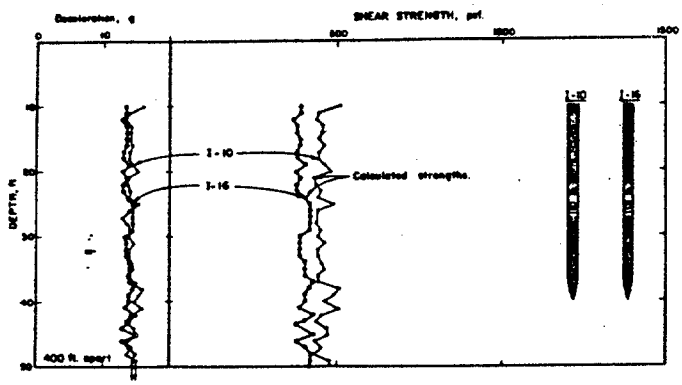

Figure 4: Approximate Soil Strengths From Apparently Similar Penetrations, located 400 ft. apart.

Penetrator	V_m, fps	Q, psi	Down, in.	LOA, in.
• 1-10	243	8.6	3	60
• 1-16	242	14.2	3	60

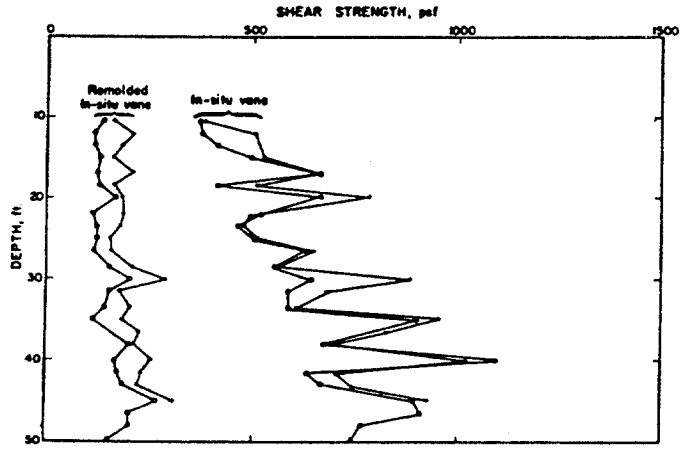

Figure 5: Vane Strengths Near Apparently Similar Penetrations

• Hole near 1-10
• Hole near 1-16

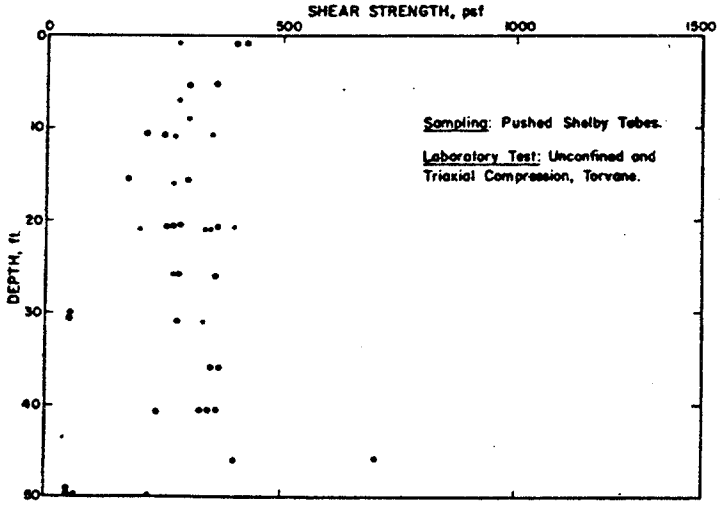

Figure 6: Conventional Strengths Near Apparently Similar Penetrations

• Hole near 1-10
• Hole near 1-16

The above examples indicate that penetrator decelerations seem to correctly sense a soft soil's strength classification. Examples with harder materials are rare, but some will be presented here for comparison. Figure 7 shows the results of a penetrator impacting into a deposit classified by the geotechnical engineer as 9 ft of hard to very hard silty clay, overlying a very dense clayey sand above, ("hard clay" means a shear strength of 4,000 psf or greater). One unconfined compression test was performed, as plotted on Figure 7. The engineer performed standard penetration tests (SPT, right side of figure), determining that the deposit increased in hardness with depth. The calculated strengths also show the soil to be hard, increasing in hardness with depth.

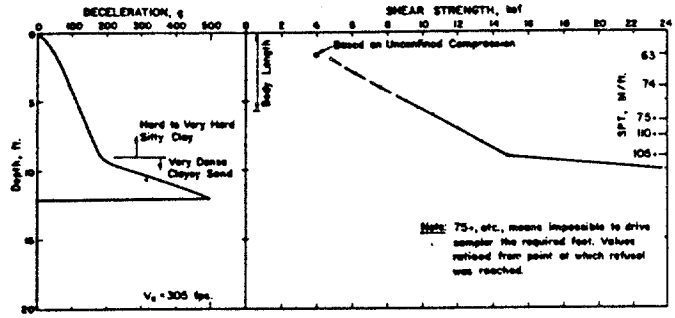

Figure 7: Approximate Soil Strengths For Penetrator in Hard Soil

The example of Fig. 7 was for a moderately high velocity (305 fps). The next example is for very high velocities and for harder materials.
In the example of Figure 8, the area around the selected impact point was excavated to a depth of 16 ft, then backfilled with 8 ft of lean-mix concrete grout, covered by a compacted soil fill. The underlying materials were semi-indurated desert playa deposits, as shown on the engineer's log to the left of the figure. The penetrator yielded the decelerations shown in the center of the figure. The strength of the grout was measured by crushing 30-day cured cylinders, measuring only the peak strength, with the results shown on the right of the figure. The residual or high-strain strength of the grout was not measured. The soil fill was excavated after the penetration event, to reveal that the 10-ft diameter block of grout had substantial cracks radially from the penetrator holes. Therefore, the apparent strength of the grout to a penetrator would be expected to be less than the strength of a small intact sample because of the cracking which occurred. This expectation is borne out by the calculated strengths of the grout from 8 to 16 ft: the calculated strengths are about 700 psi, whereas the laboratory strengths were 750-1,000 psi. Additionally, the penetrator clearly communicated that it was passing through something extremely hard, and certainly not a soil. In the two clay layers, 16 to 25 ft, and 28 to 38 ft, the calculated strengths all indicate the "hard" classification of greater than 28 psi. The calculated strengths of the upper backfill indicate

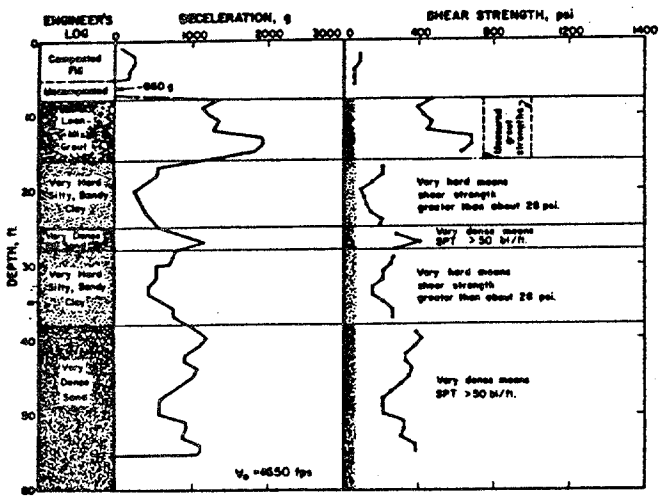

Figure 8: Penetration Through Concrete Target over natural soil

that it was compacted to be very stiff to hard, which is a reasonable result for well compacted backfill. Thus, even for the rather bizarre conditions of this example, it appears that this approximate method yields a reasonably accurate picture of the situation.

6. SOME LIMITATIONS OF THIS APPROXIMATE METHOD

The most apparent limitation of this approximate method is the neglecting of velocity and inertial effects. The examples given above tend to indicate that those effects may be second-order: if velocity and inertial deceleration components are used as part of the total deceleration to calculate strength, then the calculated strengths are expected to be consistently high, but that is not observed, even at the high velocities of Fig. 8. This is perhaps so because of the practical bias on the data set: penetrators are launched at low velocities in soft soils and at high velocities in hard soils and rocks. Thus, the relative effects of soil strength and velocity may be proportionally similar for the available-data set, so that even the gross approximations presented in this paper give adequate results. Clearly, this approximate method should not be applied to cases of high-velocity/soft-soil or low-velocity/hard-soil until some test cases have been performed.

The shear strength, S, mobilized at the periphery of the annulus of sheared soil is not the static strength. For cohesive soils, the dynamic strength is often taken as 1.5 to 2 or so of the static strength, and sometimes even more. It is recognized, however, that the shear strains are very large in the sheared annulus, and that the soil is therefore probably thoroughly remolded. For cohesive soils, the remolded strength is often taken as 1/2 to 2/3 or so of the static strength, and sometimes even less. Thus, it is to be expected that in soils with a very high strain-rate sensitivity, the proposed approximation would probably tend to over-predict the static strength.

Similarly, it is to be expected that in soils with a structure very sensitive to remolding, the proposed approximation would probably tend to underpredict the maximum static strength. Fortuitously, these two effects, the strain-rate and the remolding sensitivity, have opposite trends so that their effects are not additive. In many soils, these effects could be essentially counter-balancing, so that the resulting calculated strengths could be within the expected scatter of a measured soil-strength profile, using conventional boring-sampling-testing methods. The data comparisons presented in this paper seem to indicate that this expectation may be fulfilled for many soils and penetrators, under a wide range of practical conditions.

7. SOME APPLICATIONS OF THIS APPROXIMATE METHOD

This approximate method appears to be adequate to estimate the shear strengths of cohesive materials, about as well as conventional boring/sampling/testing, but not as well as in-situ vane testing. The estimated shear-strength values are useful for soil-profile assessment, comparing relative strengths at various locations, detecting harder or softer zones, and for evaluating pile driveability. For estimating strengths of deep, gassy soils offshore, the penetrator-derived strengths may be more representative of the in-situ conditions than strengths obtained by conventional boring/sampling/testing.

It is not intended that this approximate method be used to derive strength values for final designs; but it is of great assistance in planning appropriate investigations to obtain final-design data.

This approximate method is very useful as an adjunct to offshore geophysical profiling. The penetrator decelerations give layer thicknesses which, when properly correlated with seismic reflection-time profiles, allow estimates of wave velocities. At the same time, the method yields estimates of shear strengths, which greatly enhance the value and use of the geophysical profile.

8. CONCLUSIONS

The examples in this paper indicate that, over a wide range of soil conditions and for a wide range of penetrator geometries, use of the approximate formula,

$$S \sim \left[\frac{QR}{2gH}\right] D$$

yields adequate estimates of shear strengths of cohesive materials. The penetrator decelerations, and the resulting calculated shear strengths, seem to be very sensitive to soil strengths, perhaps more so than conventional procedures. The use of penetrators as a part of a geophysical survey greatly enhances the value of that survey.

ACKNOWLEDGEMENTS

The figures were drafted by I. McNeill.
The text was prepared by N. Gatchell.

REFERENCES

1. McNeill, R. L., "Rapid Penetration of Terrestrial Materials," Proc., Conf. on Rapid Penetration of Terrestrial Materials, Texas A&M Univ., College Station, TX, 1972.

2. Triandafilidis, G. E., "State-of-the-Art of Earth Penetration Technology", DNA4080E, Univ. NM, Albuquerque, 1976.

3. Young, C. W., "Depth Prediction for Earth-Penetrating Vehicles," J. SM&FE Div., Vol. 95, SM3, ASCE, NY, May, 1969.

4. Young, C. W., "Empirical Equations for Predicting Penetration Performance in Layered Earth Materials for Complex Penetrator Configurations," SC-DR-72-0523, Sandia National Laboratories, Albuquerque, NM, Dec., 1972.

5. Young, C. W., "Wendover Soil Penetration Test Results," Letter to E. C. Pightley-1324, Sandia National Laboratories, Albuquerque, NM, 3 Nov. 1977 (formal report in progress, 1981).

6. True, D. G., "Penetration of Projectiles into Seafloor Soils," TR-R-822, NCEL, Port Hueneme, CA, May, 1975.

7. Beard, R. M., "Expendable Doppler Penetrometer: A Performance Evaluation," TR-R-855, NCEL Port Hueneme, CA, July, 1977.

8. McNeill, R. L., "Preliminary Analysis of MSP-1, MSP-2, and MSP-2A Penetration Events in Ocean-Bottom Soft, Saturated Clays," letter report to Morgan Kramm, Sandia National Laboratories, Albuquerque, NM, April, 1977.

9. McNeill, R. L., "Enhancement of Geophysical Soil Profiles Using Instrumented Marine Sediment Penetrators," Proc., No. 3526, OTC, Houston, TX, April, 1979.

10. Dayal, U., J. H. Allen, and D. V. Reddy, "Low Velocity Projectile Penetration of Clay," J. Geotechnical Division, Paper 15657, Vol. 106, GT8, ASCE, Aug., 1980.

11. McNeill, R. L., and A. D. Foster, "Estimation of In-Situ Clay Strengths Using Marine Sediment Penetrators," Proc., International Conference on Recent Advances in Geotechnical Earthquake Engineering and Soil Dynamics, St. Louis, 1981.

12. Forrestal, M. J., D. B. Longcope, and F. P. Norwood, "A Model to Estimate Forces on Conical Penetrators into Dry Porous Rock" J. Appl. Mech., Paper 81-APM-5, ASME, NY, 1981.

13. Terzaghi, K., and R. B. Peck, Soil Mechanics in Engineering Practice, Wiley, NY, 1948.

14. McNeill, R. L., "Derivation of an Approximate Equation for Estimating Shear Strength of Cohesive Materials from Penetrator Decelerations," SAND81-1364 Sandia National Laboratories, Albuquerque, NM, 1981.

Ice strength, f_c, varies with temperature, salt content, load rate, etc. However, values in the range between 200 and 500 psi (1.38 and 3.45 MPa) may be expected. The coefficient, C, depends on shape, speed of application, etc., and will range between 0.3 and 0.7. The values used for design should be determined by appropriate means and should be consistent with the intended use of the structure.

2.3.6 Earthquake

2.3.6a. General. This section presents guidelines for the design of a platform for earthquake ground motion. Strength requirements are intended to provide a platform which is adequately sized for strength and stiffness to insure no significant structural damage for the level of earthquake shaking which has a reasonable likelihood of not being exceeded during the life of the structure. The ductility requirements are intended to insure that the platform has sufficient energy absorption capacity to prevent its collapse during rare intense earthquake motions, although structural damage may occur.

It should be recognized that these provisions represent the state-of-the-art, and that a structure adequately sized and proportioned for overall stiffness, ductility, and adequate strength at the joints, and which incorporates good detailing and welding practices, is the best insurance of good performance during earthquake shaking.

The guidelines in the following paragraphs of this section are intended to apply to the design of new major steel framed structures. Only vibratory ground motion is addressed in this section. Other major concerns such as those identified in Par. 1.3.8 and 1.4.5, (e.g., large soil deformations or instability) should be resolved by special studies.

2.3.6b. Preliminary Considerations

1. Evaluation of Seismic Activity. For seismically active areas it is intended that the intensity and characteristics of seismic ground motion used for the strength design be determined by a site specific study. Evaluation of the intensity and characteristics of ground motion should consider the active faults within the region, the type of faulting, the maximum magnitude of earthquake which can be generated by each fault, the regional seismic activity rate, the proximity of the site to the potential source faults, the attenuation of the ground motion between these faults and the platform site, and the soil conditions at the site.

   To satisfy the strength requirements a platform should be designed for ground motions having average recurrence intervals determined in accordance with Par. 1.5. In the absence of detailed seismic data and studies the seismicity of a platform site may be determined from Fig. 2.3.6-1.

2. Evaluation for Zones of Low Seismic Activity. In areas of low seismic activity, (Zones 0, 1, or 2 in Fig. 2.3.6-1) platform design would normally be controlled by storm or other environmental loading rather than earthquake. For Zone 0, no earthquake analysis is required, since the design for environmental loading other than earthquake will provide sufficient resistance against potential effects from seismically active zones. For Zones 1 and 2 all of the earthquake requirements except those for deck appurtenances may be considered satisfied if the horizontal shear at each level in the structure resulting from the strength requirements (Par. 2.3.6c) is less than one-half of that induced by other design environmental conditions. Deck appurtenances should be designed for earthquake in accordance with Par. 2.3.6e2. All other earthquake requirements including ductility requirements (Par. 2.3.6d) and the requirements for tubular joints are waived if the shear condition stated above is met.

3. Seismic Analysis Methods. Response analysis of an offshore platform to earthquake induced motion may be accomplished using any recognized method. For example:

   (a) Response Spectrum: This method uses a response spectrum representation for each component of ground motion to develop the response of the platform.

   (b) Time History: This method uses recorded or constructed earthquake time histories for each component of ground motion to develop the response of the platform.

2.3.6c. Strength Requirements

1. Environmental Description. In the absence of seismic data and site specific studies, the platform should be designed by either the response spectrum or the time history method using the following effective horizontal ground accelerations:

Z =	0	1	2	3	4	5
G =	0	0.05	0.10	0.20	0.25	0.40

   Where Z = Zone or relative seismicity factor given in Fig. 2.3.6-1.

   G = Ratio of effective horizontal ground acceleration to gravitational acceleration.

   Using the response spectrum approach, the ordinates of the spectrum taken from Fig. 2.3.6-2 should be multiplied by the factor G for the zone in which the platform is to be located. The resulting spectrum should be applied along a principal horizontal axis of the structure. An acceleration spectrum of two-thirds that for the given zone should be

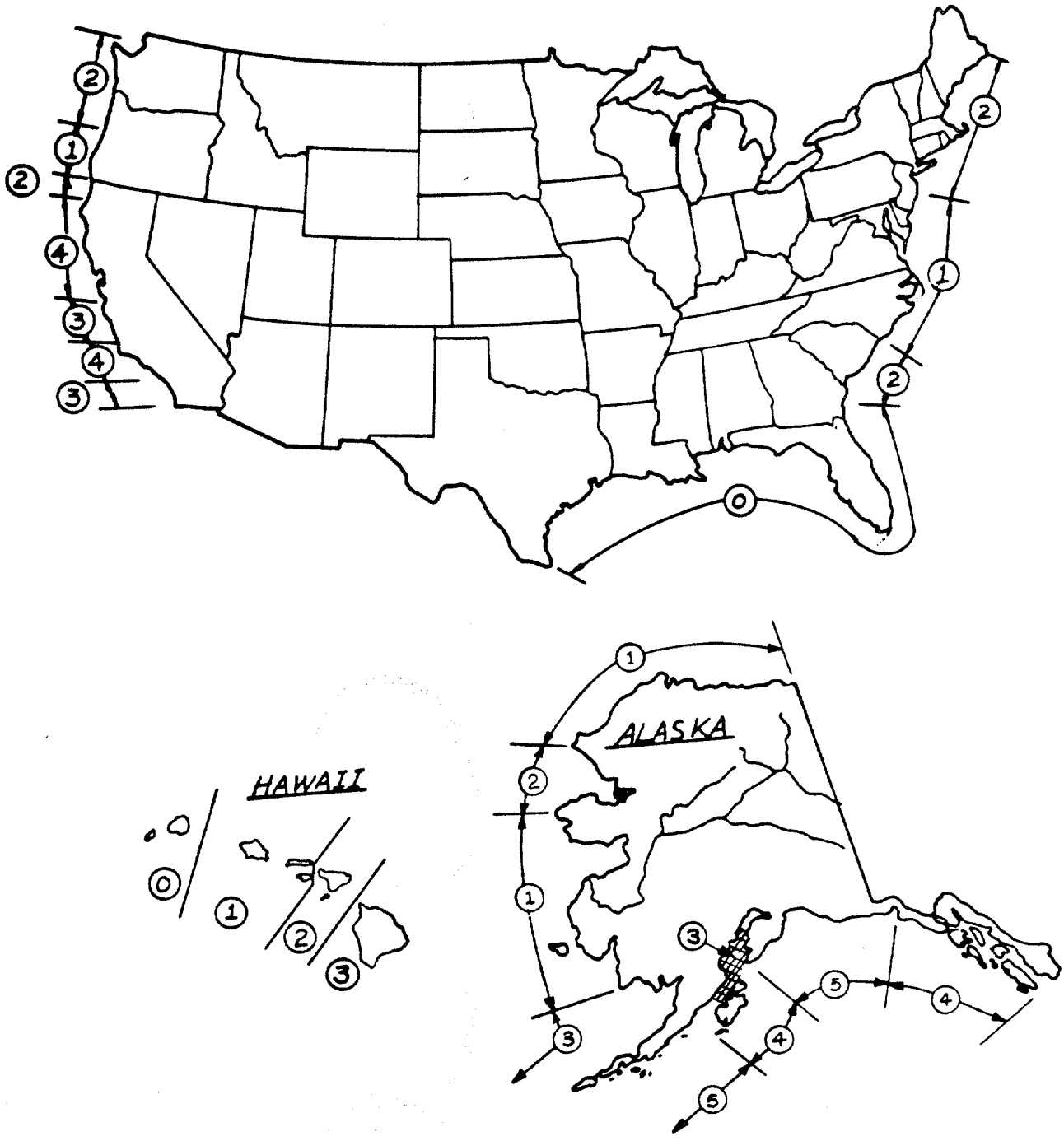

FIG. 2.3.6-1
SEISMIC RISK MAP OF
UNITED STATES COASTAL WATERS

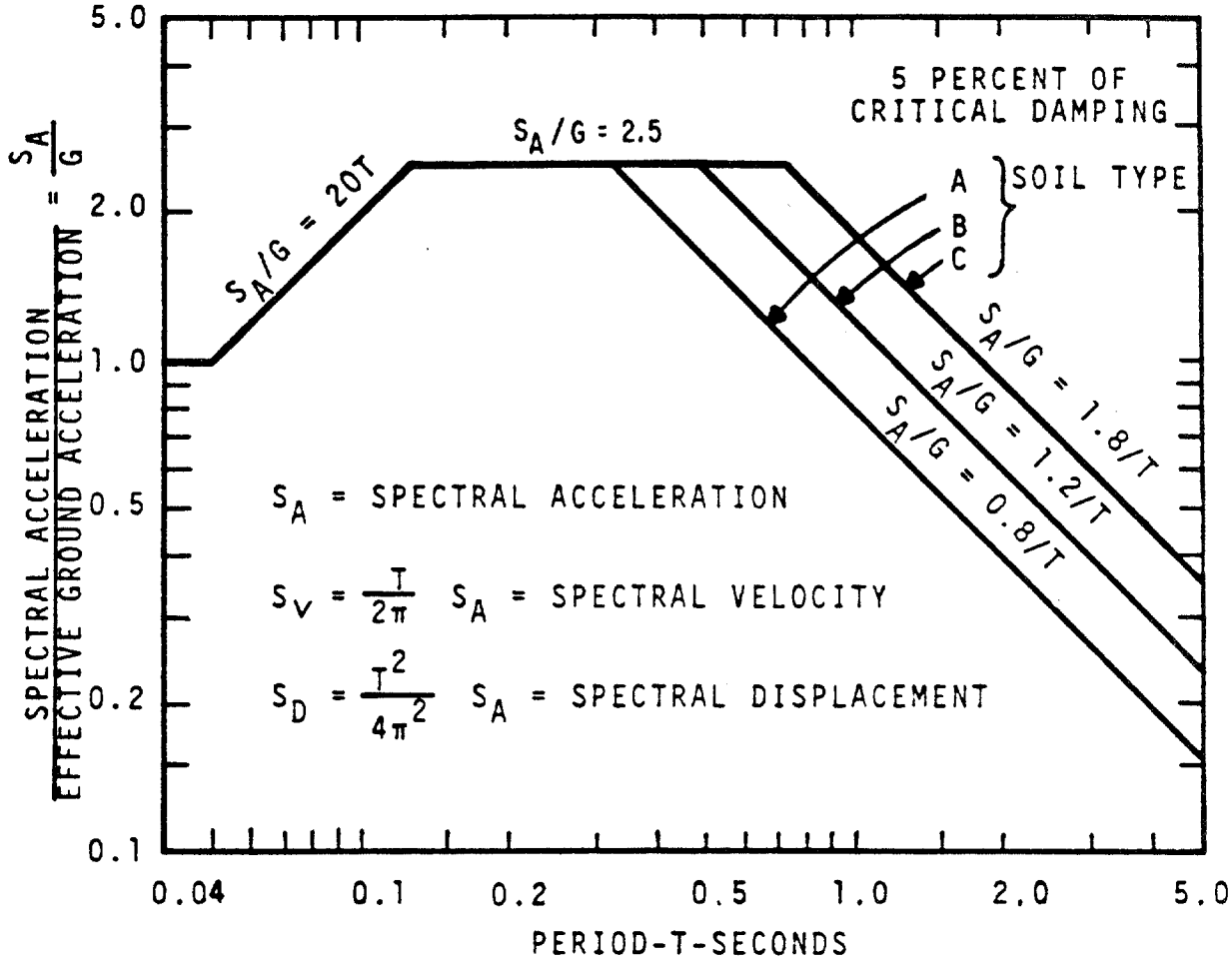

SOIL TYPE

A. ROCK — CRYSTALLINE, CONGLOMERATE, OR SHALE-LIKE MATERIAL GENERALLY HAVING SHEAR WAVE VELOCITIES IN EXCESS OF 3000 FT/SEC (914 M/SEC).

B. SHALLOW STRONG ALLUVIUM — COMPETENT SANDS, SILTS AND STIFF CLAYS WITH SHEAR STRENGTHS IN EXCESS OF ABOUT 1500 PSF (72 kPa), LIMITED TO DEPTHS OF LESS THAN ABOUT 200 FEET (61 M), AND OVERLYING ROCK-LIKE MATERIALS.

C DEEP STRONG ALLUVIUM — COMPETENT SANDS, SILTS AND STIFF CLAYS WITH THICKNESSES IN EXCESS OF ABOUT 200 FEET (61 M) AND OVERLYING ROCK-LIKE MATERIALS

FIG. 2.3.6-2
RESPONSE SPECTRA
SPECTRA NORMALIZED TO 1.0 GRAVITY

applied in an orthogonal horizontal direction, and an acceleration spectrum of one-half that for the given zone should be applied in the vertical direction. All three spectra should be applied simultaneously and the responses combined as given in Par. 2.3.6c3. The design should consider each of the two principal axes as possible directions of the larger horizontal ground acceleration.

If the design is accomplished by the time history method of analysis, the time histories used in each orthogonal direction should be scaled as stated in the above paragraph and generated or modified so that their normalized response spectra for five percent critical damping reasonably match the design spectrum shown in Fig. 2.3.6-2 in the period range of interest. The phasing of each of the three time history components may be different. Because of the potential sensitivity of the platform response to variations in the input motion the design should consider at least three sets of time histories.

The design spectra shown on Fig. 2.3.6-2 are referenced to three principal types of local soil-geological conditions. Platforms to be located in soil conditions which are characterized by significant accumulations of soft clays, loose sands and silts overlying alluvium or rock should have special investigations performed to determine the appropriate design ground motion. Such investigations may indicate significant amplifications of both horizontal and vertical ground motions in the range of the natural periods of the soft soil column.

The lateral and axial soil resistances of a pile foundation system are normally developed at different locations along the pile length. Therefore, the horizontal ground motion spectrum or time history for the soil near the surface is associated with the lateral pile motion and may be different than the vertical ground motion spectrum or time history associated with the axial pile motion.

2. Structural Modeling. The mass used in the dynamic analysis should consist of the mass of the platform associated with gravity loading defined in Par. 2.3.6c3, the mass of the fluids enclosed in the structure and the appurtenances, and the added mass. The added mass may be estimated as the mass of the displaced water for motion transverse to the longitudinal axis of the individual structural framing and appurtenances. For motions along the longitudinal axis of the structural framing and appurtenances, the added mass may be neglected.

The analytical model should include the three dimensional distribution of platform stiffness and mass. Asymmetry in platform stiffness or mass distribution may lead to significant torsional response which should be considered.

In computing the dynamic characteristics of braced, pile supported steel structures, uniform modal damping ratios of five percent of critical should be used for an elastic analysis. Where substantiating data exists, other damping ratios may be used.

The ground motion implicit in the Environmental Description of Par. 2.3.6c1 represents that "free field" motion which would exist in the vicinity of the platform if the platform were not there. To be consistent, the mathematical model used in evaluating platform response should incorporate all important elements of the mass, stiffness and energy dissipation properties of both the structure and foundation components of the platform, as well as significant aspects of interaction between the foundation elements and the surrounding soil.

3. Response Analysis. It is intended that the design response should be comparable for any analysis method used. When the response spectrum method is used, the square root of the sum of the squares of the individual modal responses may be used for the calculation of the design response. Other methods of combining modal response may be more appropriate in some instances, such as the axial pile response for a structure which has nearly equal fundamental mode periods in each of the two principal bending directions. For the response spectrum method, as many modes should be considered as required for an adequate representation of the response. At least two modes having the highest overall response should be included for each of the three principal directions plus significant torsional modes.

Where the time history method is used, the design response should be calculated as the average of the maximum values for each of the time histories considered.

Earthquake loading should be combined with other simultaneous loadings such as gravity, buoyancy, and hydrostatic pressure. Gravity loading should include the platform dead weight (comprised of the weight of the structure, equipment, appurtenances), actual live loads and 75 percent of the maximum supply and storage loads.

4. Response Assessment. In the calculation of member stresses, the stresses due to earthquake induced loading should be combined

with those due to gravity, hydrostatic pressure, and buoyancy. For the strength requirement, the basic AISC allowable stresses and those presented in Par. 2.5.2 may be increased by 70 percent. Pile-soil performance and pile design requirements should be determined on the basis of special studies. These studies should consider the design loadings of Par. 2.3.6c3, installation procedures, earthquake effects on soil properties and characteristics of the soils as appropriate to the axial or lateral capacity algorithm being used. Both the stiffness and capacity of axial and lateral pile response should be addressed in a compatible manner.

2.3.6d. Ductility Requirements. The intent of these requirements is to ensure that structures in seismically active areas have adequate energy absorption capacity to prevent collapse under a rare intense earthquake, normally through inelastic deformation.

1. Performance Goal. Adequate ductility may be demonstrated by showing that the structure-foundation system can absorb at least 4 times the amount of energy absorbed at the strength design requirement with the structure remaining stable. In addition, all highly stressed panels should be detailed to permit ductile performance.

   Account should be taken of the limited strength of framing that has either buckled or yielded. The P-Δ effects of loads acting through elastic and inelastic deflections of the structure and foundation should be considered.

2. Inelastic Deformation. Tubular members and piling at locations which are required to maintain their capacity through substantial concentrated inelastic deformation should be designed to meet the compact section requirements of $D/t \leq 1300/F_y$ given in Par. 2.5.2a3. For tubular members with $1300/F_y \leq D/t \leq 1900/F_y$ development of full plastic load and moment capacity plus some limited plastic rotation capacity, may be presumed. Portions of tubular members and piling which may be only slightly deformed beyond yield or column buckling may be sized only to preclude premature local buckling ($D/t \leq 60$), provided their limited deformation capacity and degrading post-buckling characteristics are recognized.
3. Pile Performance. If individual pile loads exceed the design capacity, then redistribution of pile loads may be permitted.

2.3.6e. Additional Guidelines

1. Tubular Joints. For Zones 3, 4, and 5 and for Zones 1 and 2 where the design of the structure is governed by earthquake loading, joints for primary structural members should be sized for either the tensile yield load or the compressive buckling load of the members framing into the joint, as appropriate for the ultimate behavior of the structure.

   The maximum punching shear stress for joints should not exceed AISC requirements for plastic design or the following:

   $$V_p = Q_q Q_p Q_f \frac{F_y}{0.6\gamma^{0.7}} \quad \text{(2.3.6-1)}$$

   where the terms are as defined in Par. 2.5.5c (one third increase not applicable) except that A should be computed as follows:

   $$A = \frac{|f_a| + |f_b|}{F_y} \quad \text{(2.3.6-2)}$$

2. Deck Appurtenances and Equipment. Deck equipment, piping and other appurtenances should be designed to minimize the possibility of resonance with the structure. Equivalent horizontal and vertical motion of the supports of the appurtenances should be that induced by the design earthquake for the strength requirements. The appurtenances and their supports should be designed to normal allowable stresses plus one-third. Ductile connections should be used.

2.4. INSTALLATION FORCES

2.4.1 General. Installation forces are those forces imposed upon the component parts of the structure during the operations of moving the components from their fabrication site to the offshore location, and installing the component parts to form the completed platform. Since installation forces involve the motion of heavy weights, the dynamic loading involved should be considered and the static forces increased by appropriate impact factors to arrive at adequate equivalent loads for design of the members affected.

2.4.2 Lifting Forces

2.4.2a. General. Lifting forces are imposed on the structure by erection lifts during the fabrication and installation stages of platform construction. The magnitude of such forces should be determined through the consideration of static and dynamic forces applied to the structure during lifting and from the action of the structure itself. Lifting forces on padeyes and on other members of the structure should include both vertical and horizontal components, the latter occurring when lift slings are other than vertical. Vertical forces on the lift should include buoyancy as well as forces imposed by the lifting equipment.

To compensate for any side loading on lifting eyes which may occur, in addition to the calculated horizontal and vertical components of the static load for the equilibrium lifting condition, lifting eyes and

FINAL REPORT

ACCELERATION TIME HISTORIES FOR EARTHQUAKE ANALYSIS STUDIES OF OFFSHORE STRUCTURES API PRAC PROJECT 80-26A

INTRODUCTION

The American Petroleum Institute (API) has initiated a research project for the analysis of the response of offshore structures under earthquake loading conditions (API PRAC project 80-26A). The scope of the investigation entails three dimensional time history dynamic analyses of a typical offshore platform under design conditions comparable to American Petroleum Institute recommended practice (API RP 2A) earthquake design provisions for Southern California offshore environment.

The API RP 2A earthquake design provision provides for strength and ductility requirements. The strength requirements are intended to provide a platform, which is adequately sized for strength and stiffness to insure no significant structural damage for the level of earthquake shaking that has a reasonable likelihood of not being exceeded during the life of the structure. The ductility requirements are intended to insure that the platform has sufficient energy absorption capacity to prevent its collapse during rare intense earthquake motion, although structural damage may occur.

In the absence of a detailed site-specific seismic exposure study, the strength level earthquake is described through a normalized major horizontal component response spectra (soil dependent), an effective ground acceleration design coefficient (G-scaling factor) as a function of zone relative seismicity, and provisions for the orthogonal weaker horizontal and vertical components as a fraction of the specified major component. The major horizontal component (applied along a major axis of the platform) consists of the response spectrum (appropriate to the specific soil condition) shown in

Figure 1 and scaled by a design coefficient appropriate to the various seismic zones presented in Figure 2. The minor horizontal component (acting in an orthogonal direction to the major axis of the structure) is taken as two-thirds of that assigned to the major horizontal component. A response spectrum of one-half the major component is assigned to the vertical component.

The ductility requirements are defined in terms of performance goals to insure that the platform has adequate energy absorption capacity to prevent collapse under a rare intense earthquake. However, for the present study, the ductility requirements will be defined in terms of response spectra having ordinates twice those defined for the strength requirement.

This report summarizes Woodward-Clyde Consultants' effort conducted for the API on this project to evaluate earthquake time histories appropriate to characterize design earthquake provisions of the API RP 2A strength and ductility requirements for offshore Southern California environment.

APPROACH

The objective of this study was to develop ground motion time histories appropriate to API RP 2A provisions for a deep site (type C) in Southern California environment (zone 4). The approach used to achieve this objective was that of examining empirical data consisting of strong motion recordings obtained during historical earthquakes, coupled with some analytical procedures as a means of supplementing and extending the emperical data base. This approach involved the following sequence of operations:

1. A thorough search of Woodward-Clyde Consultants' recorded ground motions data base was conducted. A preliminary candidate data set of 117 recorded time histories (39 recording stations) was selected for further study. This preliminary data set was limited to earthquake ground motions recorded in Southern California at recording stations having subsurface geological conditions which may be classified as deep sites.

2. An examination of the characteristics of recorded ground motions, comprising the preliminary data set, was performed. Studied characteristics included magnitude of recorded earthquakes, distance from the causative fault to the recording station, peak recorded acceleration, velocity and displacement of the three components of each record and their relative values, and frequency contents of each time history comprising the preliminary data set. Based on this study, the preliminary data set was reduced to 27 time histories (9 recording stations). The criteria used to select this intermediate candidate data set included:

   a) Magnitude: The intermediate data set included time histories recorded from earthquakes ranging in magnitudes between 6.3 and 7.2 on the Richter scale. Magnitudes on the lower end of this range incorporate what was considered to have reasonable likelihood of occurring during the life of an offshore platform in Southern California environment. Additionally, it was considered that recordings from earthquakes, having a magnitude on the higher end of this range, incorporate some of the ground motion characteristics that may be expected from rare intense earthquakes associated with the ductility requirements.

   b) Distance: Considerations were given to select time histories from recording stations having distance to causative faults ranging between a very close (nearby) to a large (distant) distances. Selected time histories for the intermediate data set were recorded at distances as small as 0.3 km. and as large as 121 km.

3. A detailed study of the characteristics of the time histories, comprising the intermediate data set, was performed. In addition to the criteria considered in the previous step, the response spectrum of each of these time histories was computed and their frequency contents were examined in relation to the API RP 2A earthquake provision normalized response spectra. A final data set was selected based on

this consideration. This final data set consisted of 12 time histories (4 recording stations) which provided the closest fit to the API RP 2A response spectra. The final data set was reduced to 9 time histories (3 recording stations) after consultation with the project technical Advisory Committee based on project requirements considerations.

4. The final evaluation of the time histories, appropriate to the API RP 2A provisions for Southern California environment, was achieved by scaling the frequency contents of each of the time histories comprising the final data set to provide a "best fit" to that of the API RP 2A provisions. The scaling was performed by varying both the time step and the peak acceleration of the recorded time histories of the final data set. A single time step scaling factor was used on time histories comprising the three components of each record, so that natural phasing between the components is preserved.

RESULTS

Table 1 presents pertinent information associated with the 27 time histories comprising the intermediate data set. The acceleration response spectra of each of these time histories normalized to their respective zero period acceleration, along with the API RP 2A normalized response spectrum (soil type C) corresponding to critical damping of 5 percent, are shown in Figures 3 through 29. The system of identification, adopted in the title of these figures, consisted of the recording station name designated by the California Institute of Technology (CIT) and the component direction. For example, the major horizontal component of the Kern County (7/21/52) earthquake would be "component A006-S00W." Exception to this identification system was made for the Imperial Valley earthquake (10/15/1979) for which there is no CIT designation yet. Consequently, the earthquake date, name and recording station was used, instead of the CIT designation for time histories recorded from this earthquake. In this manner, information associated with these time histories may be easily correlated between Table 1 and Figures 3 through 29.

Table 2 summarizes pertinent information associated with the three earthquake records (9 time histories) comprising the final data set. This table also presents the time step and acceleration scaling factors used to evaluate the components of the final recommended time histories. It should be noted that the peak acceleration of the evaluated time histories is not exactly equal to the product of the peak acceleration of the original time histories and the corresponding scaling factors. This is caused by a small variation in the peak acceleration of the original time histories due to the induced time step change and following interpolation process. The evaluated three earthquake records were designated as Earthquake I, II, and III, and their time history components were designated as Major and Minor for the two horizontal orthogonal components and Vertical for the third orthogonal component. Figures 30 through 38 present the computed acceleration response spectra of the modified time histories and the corresponding API RP 2A design response spectra appropriate to the strength requirements in offshore Southern California environment. These response spectra were computed using a critical damping of 5 percent.

Table 3 presents a summary of the computed spectral response values of the evaluated time histories corresponding to critical damping of 5 percent in the period range of .5 to 3 seconds.

The acceleration response spectra of the Major, Minor and Vertical components of the three designated earthquakes are presented together with the corresponding API RP 2A spectra in Figures 39 through 41. As shown in these figures, the evaluated time histories appear to well represent the API RP 2A provision in the frequency range of interest for offshore platform design.

Appropriate time histories for the ductility requirements may be obtained by doubling the amplitudes of the evaluated time histories for the strength requirements provided herein.

TABLE 1. INTERMEDIATE DATA SET

Earthquake Name and Date	Magnitude M_L	Station Name (CIT) [USGS]	Distance (km)	Site* Conditions WCC Data Bank	Component	Acceleration (g)	Peak Values Velocity (cm/sec)	Displacment (cm)
Imperial Valley 5/18/40	6.4	El Centro, IVID (A001) [117]	10.8	BDD	S00E S90W VERT	.348 .214 .210	33.4 36.9 10.8	10.9 19.8 5.6
Kern County 7/21/52	7.2	Hollywood Storage Bldg. (A006) [133]	121.0	EBD	S00W N90E VERT	.055 .044 .023	6.1 9.4 4.2	5.1 5.9 2.2
Eureka 12/21/54	6.5	Eureka Federal Bldg. (A008) [1022]	18.9	EBD	N11W N79E VERT	.168 .258 .083	31.6 29.4 8.2	12.4 14.1 4.7
		Ferndale City Hall (A009) [1023]	40.2	BBD	N44E N46W VERT	.159 .201 .043	35.6 26.0 7.6	14.2 9.6 3.9
Borrego Mountain 4/8/68	6.4	El Centro, IVID (A019) [117]	46.0	BDD	S00W S90W VERT	.130 .057 .030	25.8 14.7 3.4	12.2 11.0 3.9

TABLE 1. INTERMEDIATE DATA SET (cont'd)

Earthquake Name and Date	Magnitude M_L	Station Name (CIT) [USGS]	Distance (km)	Site* Conditions WCC Data Bank	Component	Acceleration (g)	Peak Values Velocity (cm/sec)	Displacment (cm)
San Fernando 2/9/71	6.4	Hollywood Storage Bldg. (D057) [133]	34.0	EBD	S00W N90E UP	.106 .151 .051	17.0 19.4 6.0	8.6 13.1 3.8
		15250 Ventura Blvd., LA (H115) [466]	26.5	EBD	N11E N79W DOWN	.225 .149 .096	28.2 23.5 9.3	13.4 10.3 4.3
Long Beach 3/10/33	6.3	Public Utility Bldg. (V315) [131]	8.7	ECD	SOUTH WEST UP	.196 .158 .285	29.4 16.5 30.1	22.7 11.8 26.3
Imperial Valley 10/15/79	6.6	Imperial Valley College, El Centro Array 7 [5028]	0.3	ADD	230 140 VERT	.462 .333 .514	107.83 44.96 25.86	41.36 19.52 10.17

TABLE 1. INTERMEDIATE DATA SET (cont'd)

Site Condition Designations	
BDD -	Instrument located at the lowest level of a two to four-story structure on deep broad recent alluvium.
EDB -	Instrument located at the lowest level of a structure of heavy construction on shallow recent alluvium.
BBD -	Instrument located at the lowest level of a two to four-story structure on deep broad soft rock.
ECD -	Instrument located at the lowest level of a structure of heavy construction on deep broad old alluvium.
ADD -	Instrument located at the lowest level of a one-story structure or free field on deep braod recent alluvium.

TABLE 2. FINAL DATA SET AND EVALUATED TIME HISTORIES

Final Data Set			Scaling Factors		Evaluated Time Histories		
Earthquake Record CIT Designation	Component	Peak Acceleration (g)	Time Step	Acceleration	Earthquake Designation	Component	Peak Acceleration (g)
A001	S00W S90W VERT	.348 .214 .210	1.37 1.37 1.37	.74 .78 2.00	EQ 1	MAJOR MINOR VERT	.250 .167 .375
A006	S00W N90E VERT	.055 .044 .023	1.20 1.20 1.20	4.53 2.95 5.45	EQ II	MAJOR MINOR VERT	.250 .130 .125
Imperial Valley (1979)	230 140 VERT	.462 .333 .514	1.00 1.00 1.00	.53 .49 1.00	EQ III	MAJOR MINOR VERT	.250 .167 .514

TABLE 3. SUMMARY OF SPECIAL RESPONSE VALUES OF EVALUATED TIME HISTORIES CORRESPONDING TO CRITICAL DAMPING OF 5 PERCENT

Spectral Period	SPECTRAL RESPONSE VALUES - EARTHQUAKE I								
	MAJOR COMPONENT			MINOR COMPONENT			VERTICAL COMPONENT		
	Relative Displacement (cm)	Relative Velocity (cm/sec)	Absolute Acceleration (G's)	Relative Displacement (cm)	Relative Velocity (cm/sec)	Absolute Acceleration (G's)	Relative Displacement (cm)	Relative Velocity (cm/sec)	Absolute Acceleration (G's)
.50	3.1	38.8	.497	2.2	23.7	.351	2.5	32.2	.399
.60	4.6	45.1	.515	3.8	34.7	.421	2.9	30.2	.332
.70	7.7	74.3	.632	6.0	54.5	.498	4.0	36.1	.333
.80	10.3	79.8	.654	7.2	60.8	.455	5.4	40.2	.345
.90	10.7	69.2	.532	6.9	45.3	.342	6.0	45.9	.298
1.00	10.9	69.4	.439	8.5	45.4	.343	4.5	30.4	.181
1.10	12.1	66.9	.402	10.1	55.5	.338	5.3	30.5	.177
1.20	14.7	79.1	.413	9.1	19.2	.255	6.0	33.9	.168
1.30	16.7	90.7	.400	9.3	46.6	.223	6.7	33.7	.160
1.40	17.9	86.6	.369	11.1	50.4	.228	5.5	36.0	.114
1.50	16.2	67.0	.291	11.9	47.5	.214	6.7	32.9	.120
1.60	16.1	67.7	.254	14.7	54.9	.233	6.6	27.0	.105
1.80	13.2	52.4	.164	17.0	61.4	.211	8.7	32.1	.109
2.00	13.3	46.8	.135	15.0	56.3	.151	8.8	25.3	.090
2.20	17.0	52.3	.142	14.7	53.4	.122	8.7	27.0	.073
2.40	19.4	52.6	.136	15.8	48.1	.111	12.5	32.7	.088
2.50	19.7	52.9	.128	19.3	48.8	.125	13.4	34.5	.087
2.60	21.2	54.7	.127	24.4	61.9	.146	12.9	33.8	.077
2.80	25.9	64.9	.134	34.3	82.3	.177	15.6	34.9	.081
3.00	30.8	67.7	.138	33.4	78.9	.150	17.7	39.1	.080

TABLE 3. SUMMARY OF SPECTRAL RESPONSE VALUES OF EVALUATED TIME HISTORIES CORRESPONDING TO CRITICAL DAMPING OF 5 PERCENT (cont'd)

Spectral Period	SPECTRAL RESPONSE VALUES - EARTHQUAKE II								
	MAJOR COMPONENT			MINOR COMPONENT			VERTICAL COMPONENT		
	Relative Displacement (cm)	Relative Velocity (cm/sec)	Absolute Acceleration (G's)	Relative Displacement (cm)	Relative Velocity (cm/sec)	Absolute Acceleration (G's)	Relative Displacement (cm)	Relative Velocity (cm/sec)	Absolute Acceleration (G's)
.50	4.2	47.5	.673	1.9	22.0	.298	1.8	17.8	.290
.60	7.1	72.8	.800	2.7	26.2	.309	2.7	26.5	.307
.70	6.1	54.6	.508	2.9	24.1	.242	3.9	34.5	.323
.80	6.4	47.2	.406	5.3	37.7	.334	4.9	36.1	.309
.90	10.6	69.3	.528	6.6	43.9	.332	4.8	34.3	.237
1.00	13.3	78.3	.540	9.7	56.5	.390	5.3	32.8	.216
1.10	17.1	106.2	.572	11.2	62.0	.373	8.9	46.4	.297
1.20	18.9	106.1	.530	10.8	57.1	.303	9.3	49.0	.261
1.30	22.8	110.2	.545	9.1	41.6	.216	7.1	34.6	.169
1.40	22.2	114.6	.459	12.1	50.6	.249	7.9	36.6	.164
1.50	18.7	91.0	.338	15.5	59.3	.278	10.9	45.7	.197
1.60	21.3	82.6	.337	19.3	72.3	.304	10.0	40.1	.158
1.80	24.0	84.8	.300	24.4	81.5	.305	9.8	36.8	.122
2.00	23.0	78.9	.233	21.6	68.8	.218	11.7	40.5	.118
2.20	18.3	60.1	.153	17.4	58.5	.146	12.6	36.3	.105
2.40	25.8	64.4	.181	18.3	62.7	.128	15.5	42.7	.109
2.50	27.9	70.0	.181	22.6	68.7	.146	20.5	48.0	.133
2.60	23.8	64.3	.143	27.7	73.4	.166	21.5	60.1	.128
2.80	23.6	60.5	.122	36.7	80.5	.190	22.1	60.8	.114
3.00	32.2	71.5	.145	38.8	86.7	.175	26.1	52.4	.117

TABLE 3. SUMMARY OF SPECTRAL RESPONSE VALUES OF EVALUATED TIME HISTORIES CORRESPONDING TO CRITICAL DAMPING OF 5 PERCENT (cont'd)

Spectral Period	SPECTRAL RESPONSE VALUES - EARTHQUAKE III								
	MAJOR COMPONENT			MINOR COMPONENT			VERTICAL COMPONENT		
	Relative Displacement (cm)	Relative Velocity (cm/sec)	Absolute Acceleration (G's)	Relative Displacement (cm)	Relative Velocity (cm/sec)	Absolute Acceleration (G's)	Relative Displacement (cm)	Relative Velocity (cm/sec)	Absolute Acceleration (G's)
.50	2.8	30.3	.450	1.7	18.4	.267	1.9	21.2	.312
.60	4.1	39.7	.463	2.8	27.0	.312	3.0	27.9	.336
.70	8.6	68.6	.710	4.8	43.4	.399	2.7	22.9	.221
.80	11.3	80.9	.712	5.6	43.3	.352	3.4	26.9	.213
.90	11.0	74.3	.548	6.7	43.7	.335	5.3	34.5	.263
1.00	9.0	54.3	.363	8.2	47.7	.331	7.2	43.8	.292
1.10	9.9	52.2	.331	9.1	50.5	.304	8.8	46.1	.294
1.20	10.7	49.2	.300	9.3	49.7	.261	9.7	52.1	.272
1.30	11.3	48.9	.270	9.3	48.9	.223	10.8	53.9	.259
1.40	13.0	52.1	.269	9.6	51.3	.198	12.8	53.8	.263
1.50	13.9	57.0	.251	9.7	51.7	.175	15.3	59.2	.275
1.60	15.0	50.7	.237	9.5	49.8	.149	17.7	65.5	.279
1.80	20.0	60.0	.250	9.8	40.9	.123	19.3	69.6	.241
2.00	24.4	71.8	.246	10.5	37.9	.106	18.3	56.5	.184
2.20	28.2	79.8	.236	14.2	37.2	.119	16.3	43.4	.136
2.40	31.8	83.7	.223	17.8	43.9	.125	13.4	37.1	.094
2.50	34.1	84.4	.221	19.1	47.0	.123	12.3	37.1	.080
2.60	38.4	84.4	.230	19.9	48.9	.119	11.7	37.1	.070
2.80	45.3	97.9	.234	21.0	48.6	.108	12.0	37.0	.062
3.00	51.2	109.0	.230	20.9	45.6	.094	13.7	36.7	.061

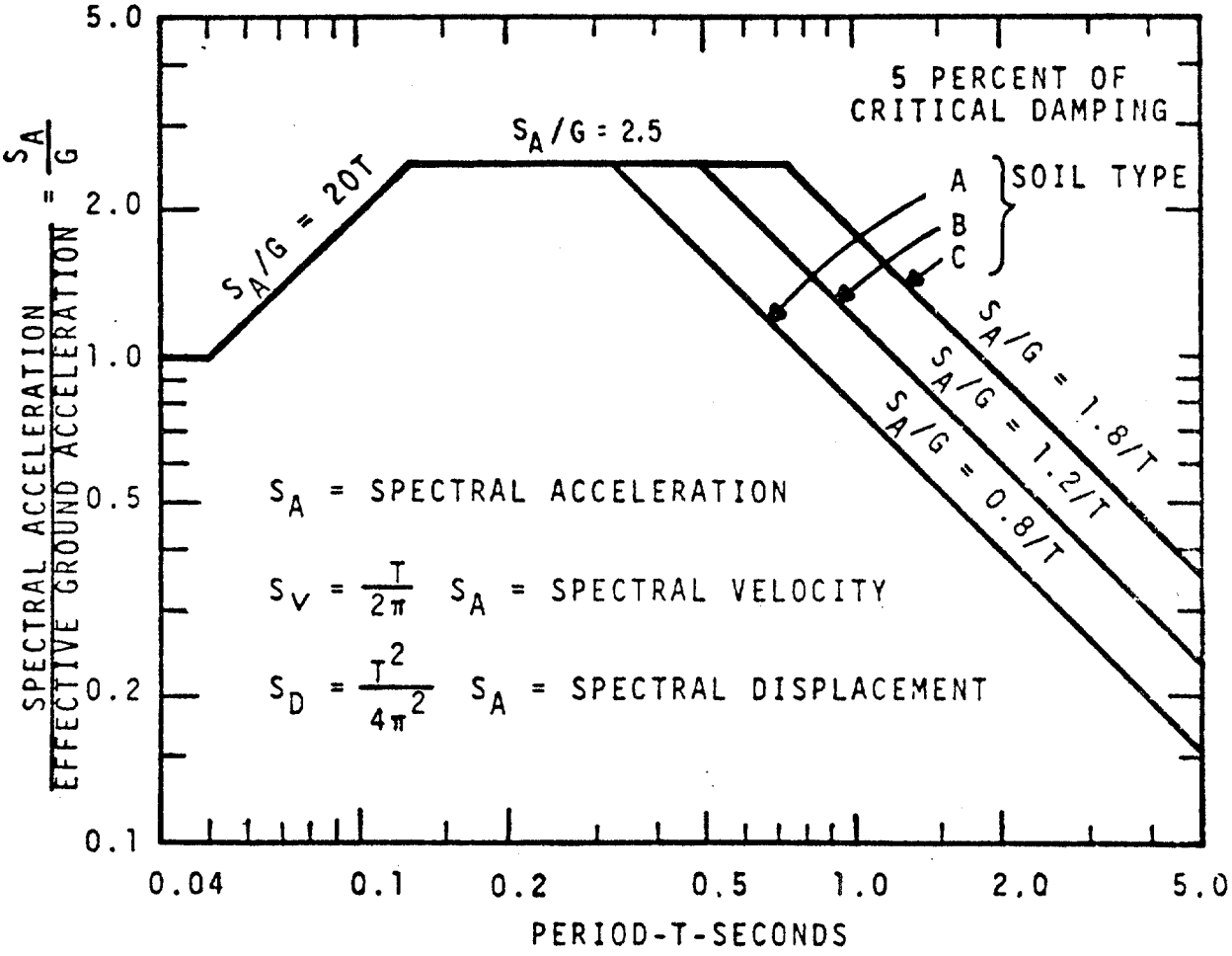

SOIL TYPE

A ROCK - CRYSTALLINE, CONGLOMERATE, OR SHALE LIKE MATERIAL GENERALLY HAVING SHEAR WAVE VELOCITIES IN EXCESS OF 3000 FT/SEC (914 M/SEC)

B SHALLOW STRONG ALLUVIUM - COMPETENT SANDS, SILTS AND STIFF CLAYS WITH SHEAR STRENGTHS IN EXCESS OF ABOUT 1500 PSF (72 kPa), LIMITED TO DEPTHS OF LESS THAN ABOUT 200 FEET (61 M), AND OVERLYING ROCK-LIKE MATERIALS

C DEEP STRONG ALLUVIUM — COMPETENT SANDS, SILTS AND STIFF CLAYS WITH THICKNESSES IN EXCESS OF ABOUT 200 FEET (61 M) AND OVERLYING ROCK-LIKE MATERIALS.

Fig. 1 — Response Spectra, Spectra Normalized to 1.0 Gravity (API RP2A-79)

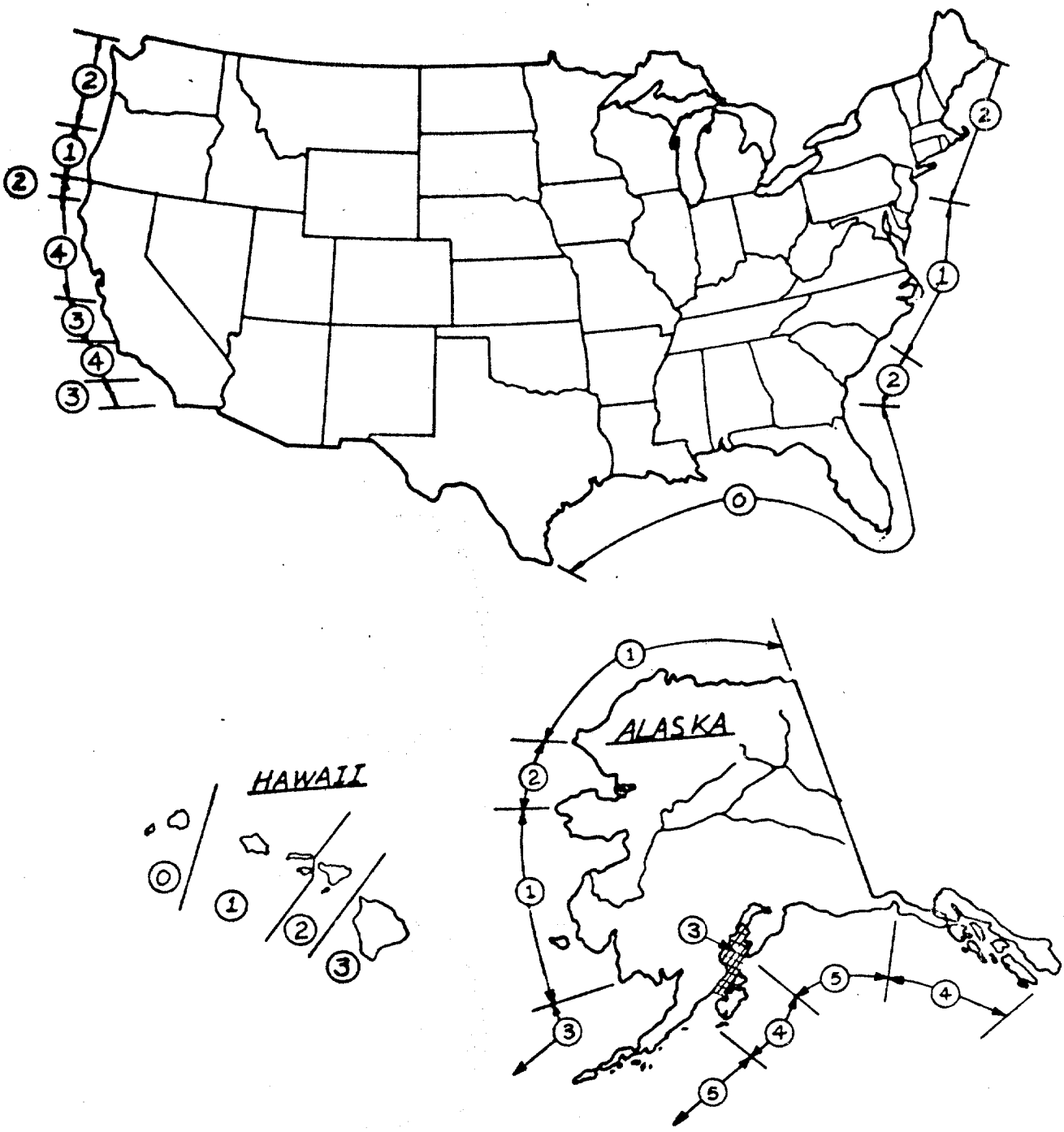

Fig. 2 – Seismic Risk Map of United States Costal Water
(API RP2A-79)

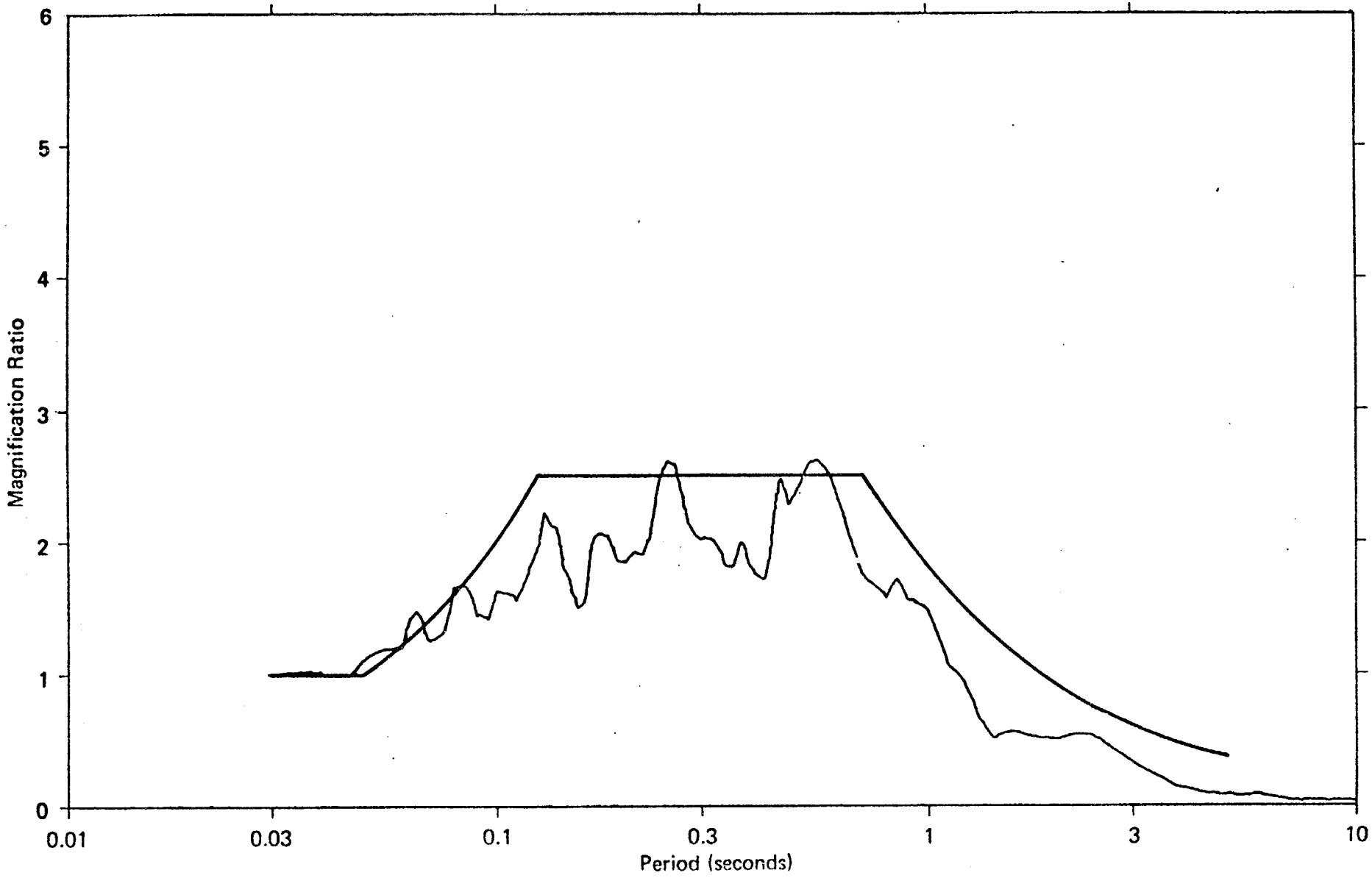

Fig. 3 – Normalized Response Spectra – Component A001/S00E

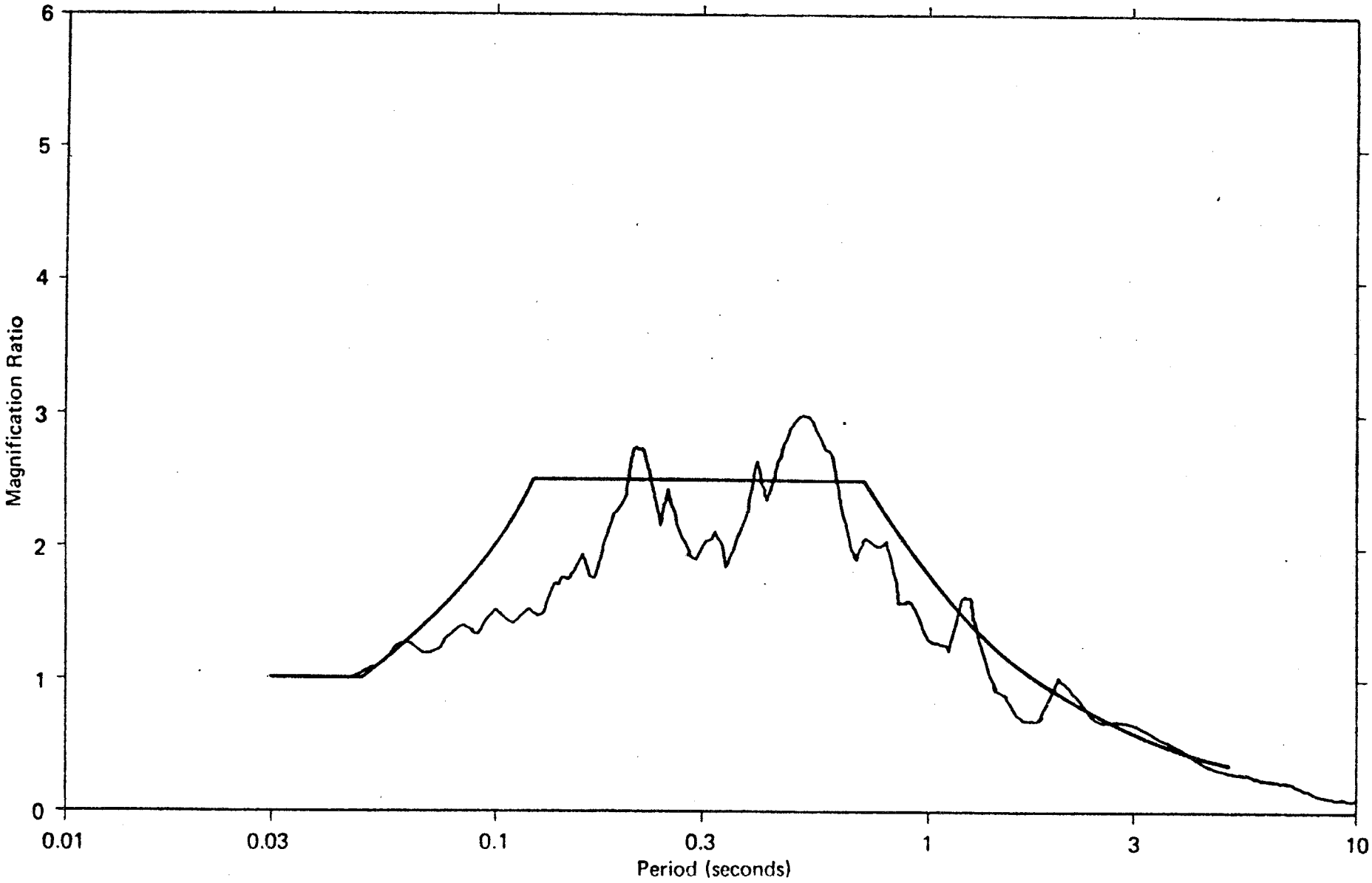

Fig. 4 — Normalized Response Spectra — Component A001/S90W

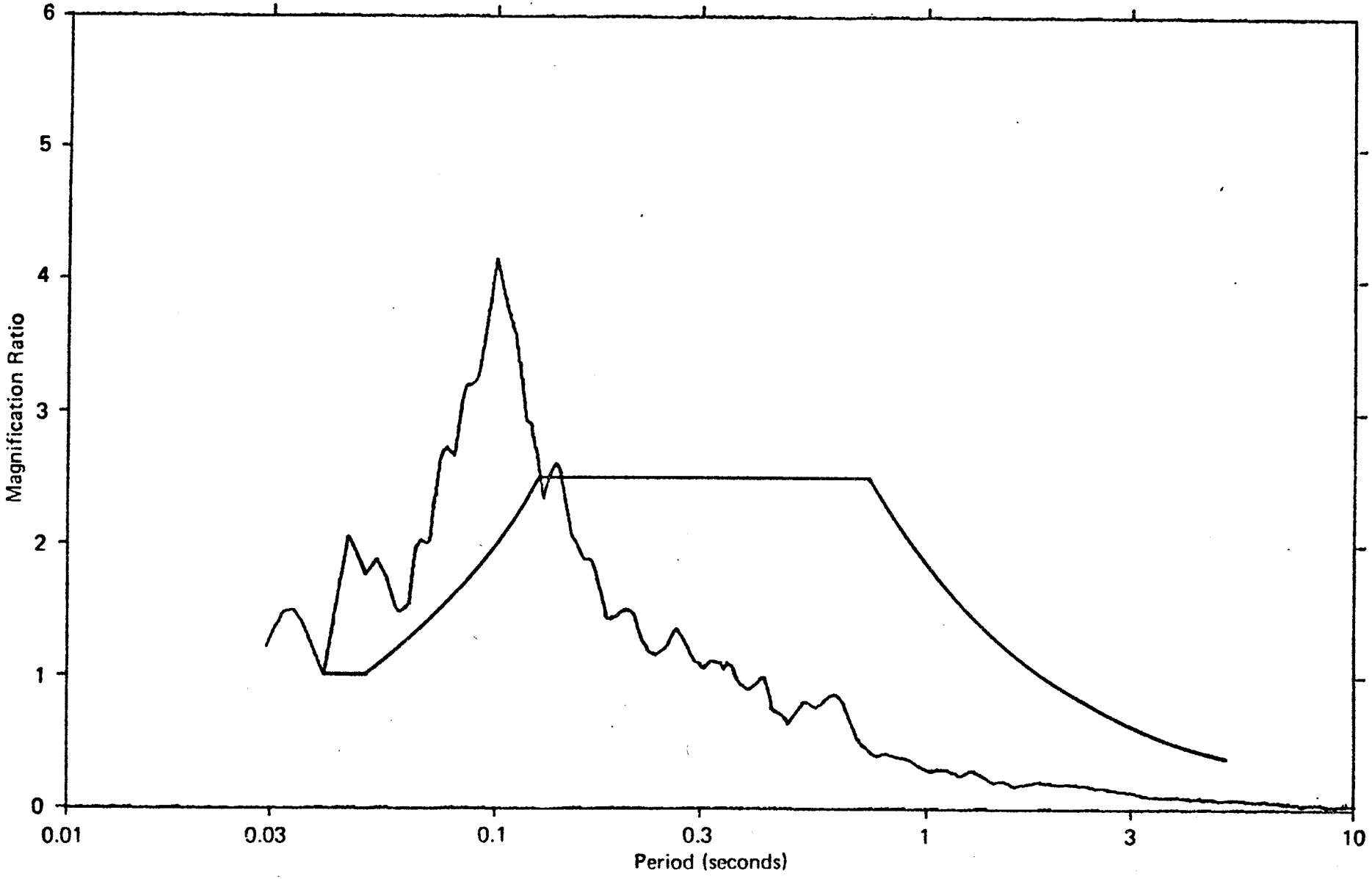

Fig. 5 – Normalized Response Spectra – Component A001/Vertical

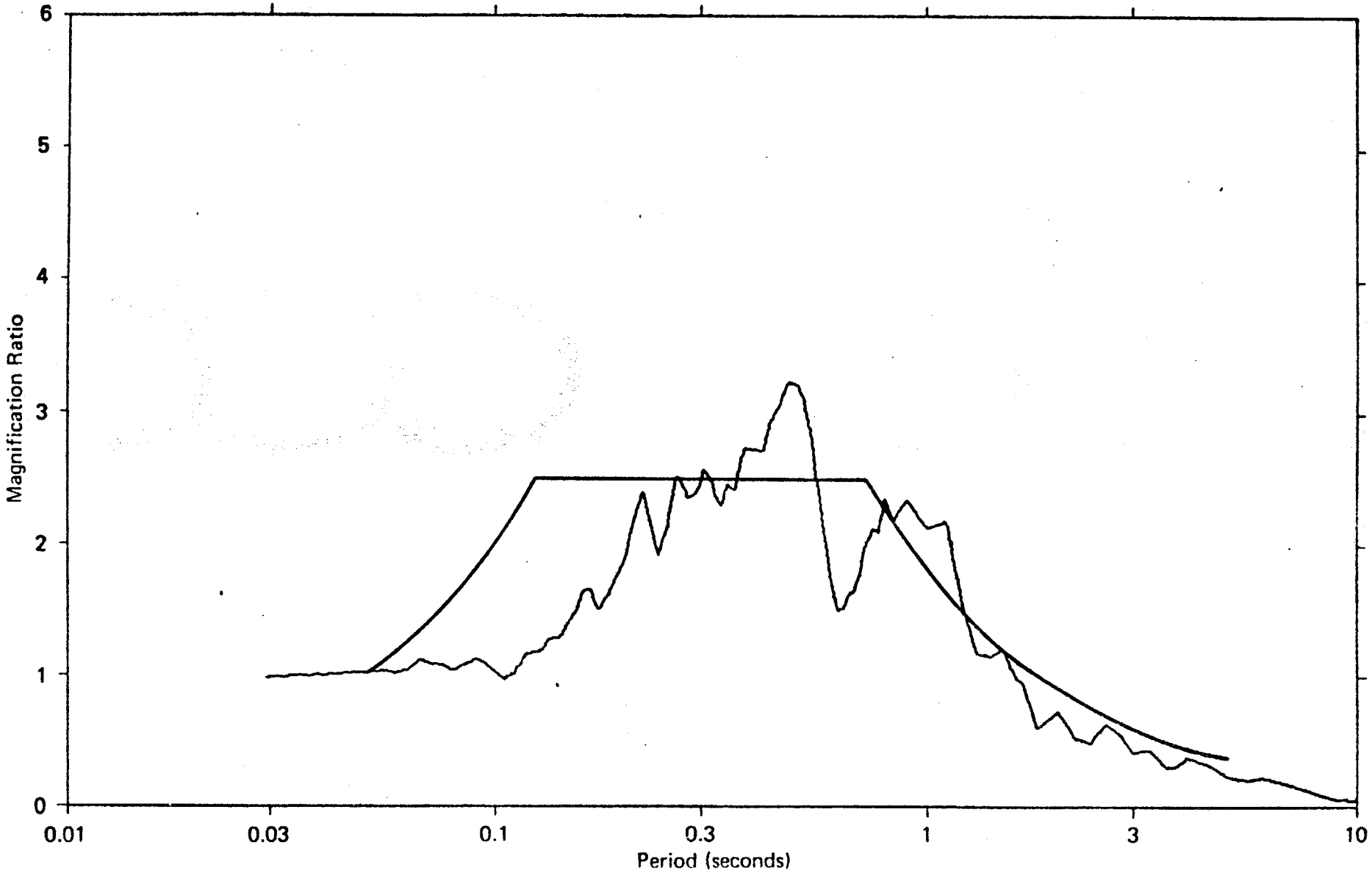

Fig. 6 — Normalized Response Spectra — Component A006/S00W

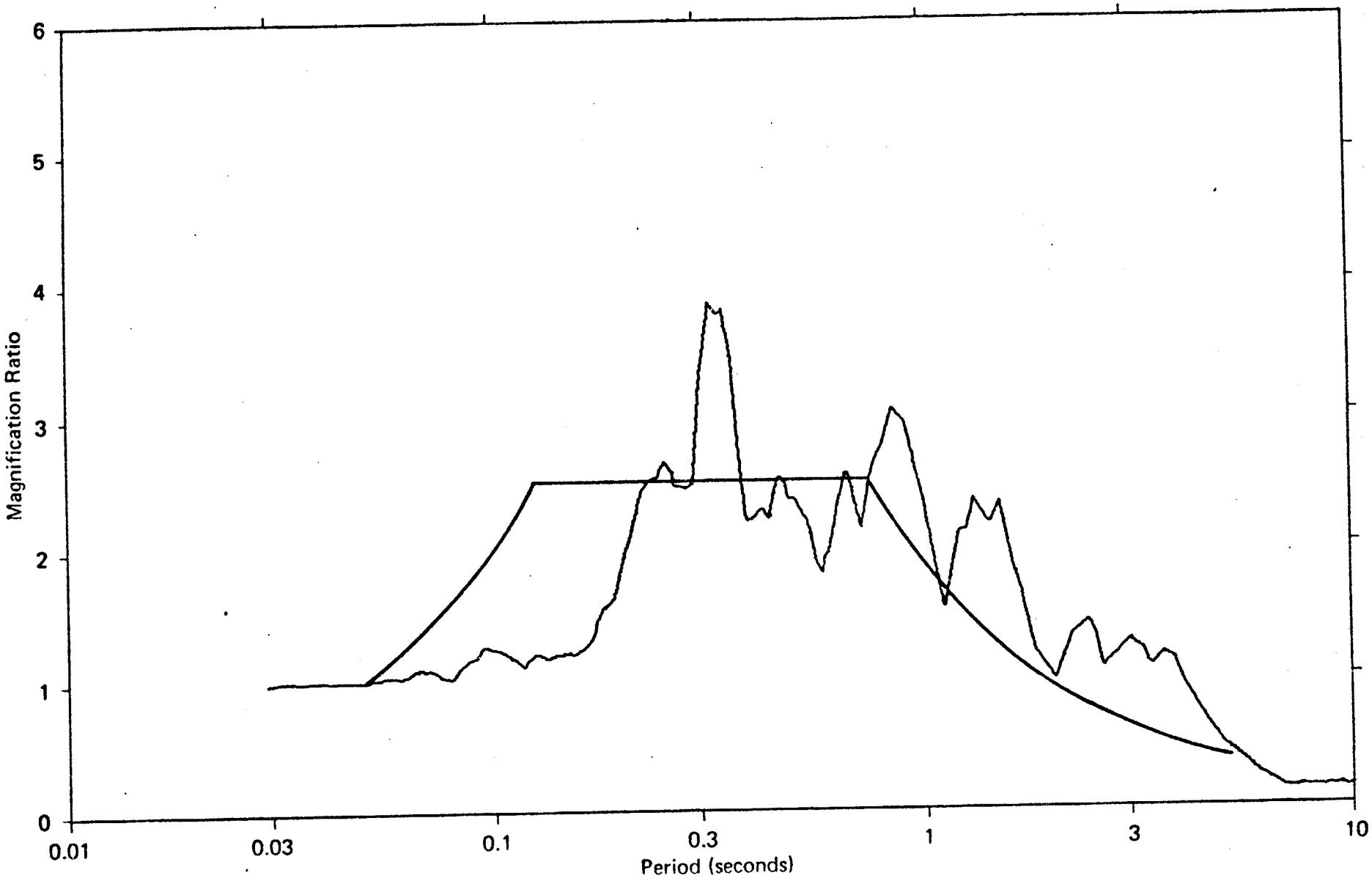

Fig. 7 – Normalized Response Spectra – Component A006/N90E

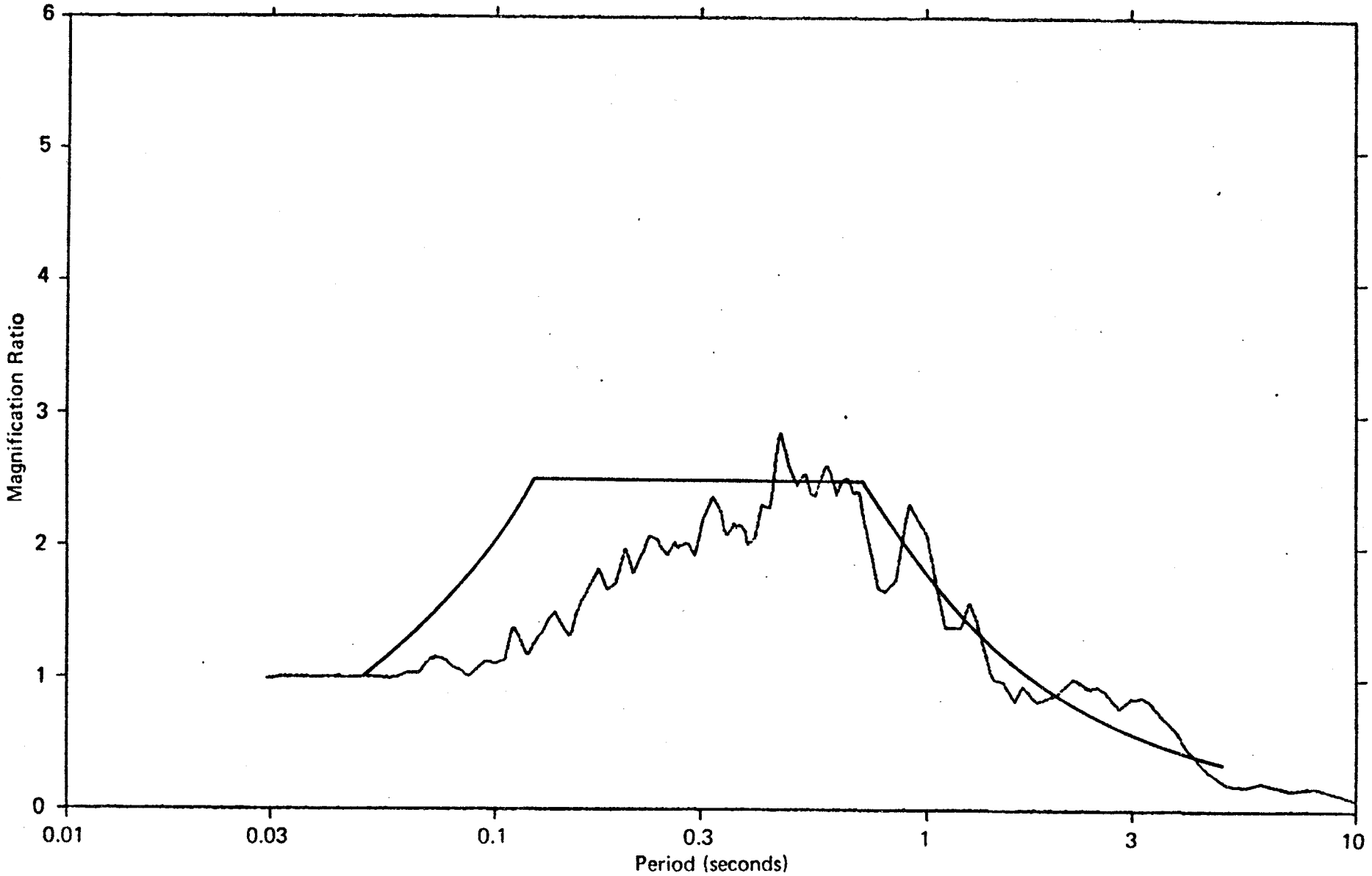

Fig. 8 – Normalized Response Spectra – Component A006/Vertical

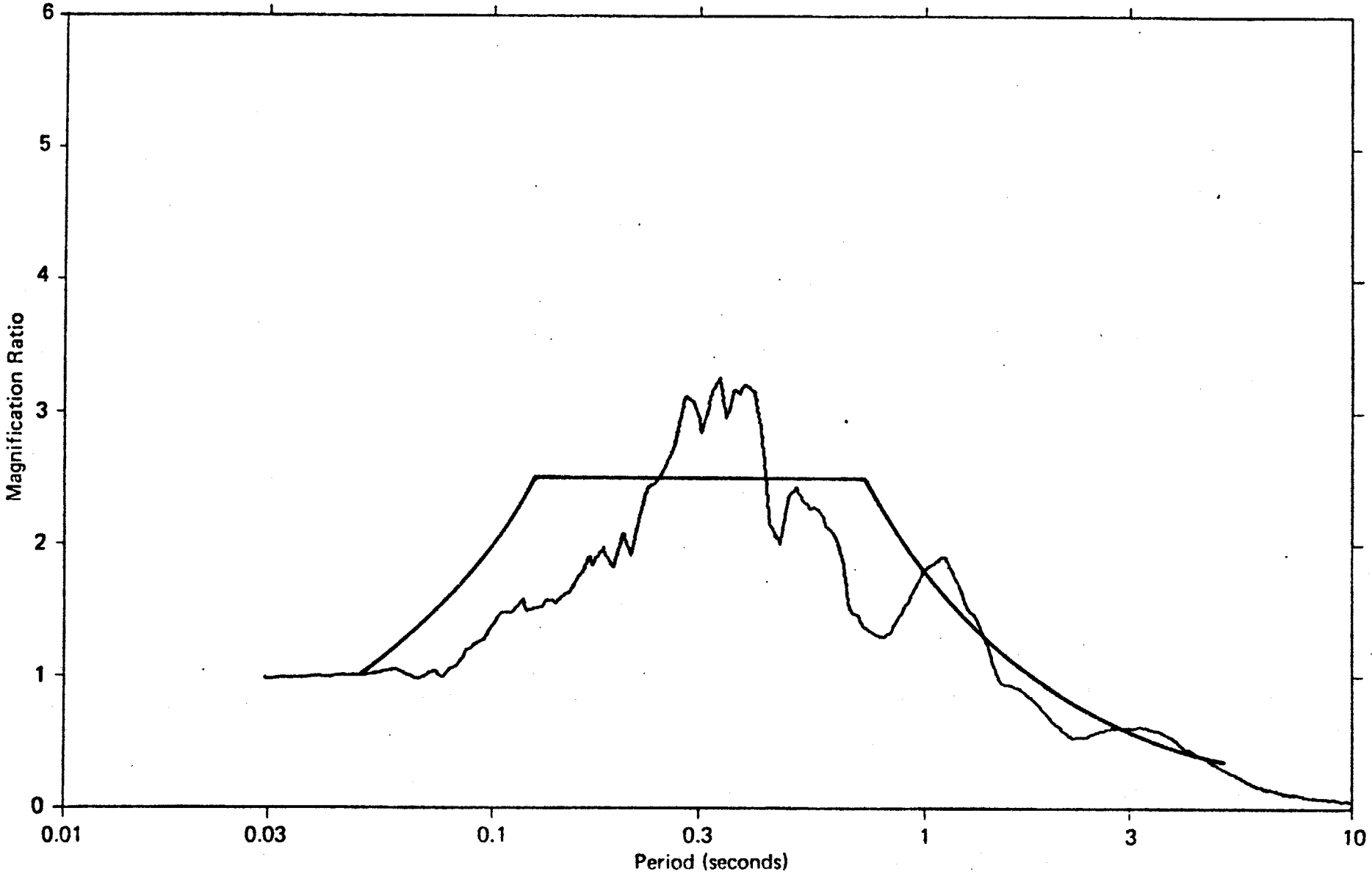

Fig. 9 – Normalized Response Spectra – Component A008/N11W

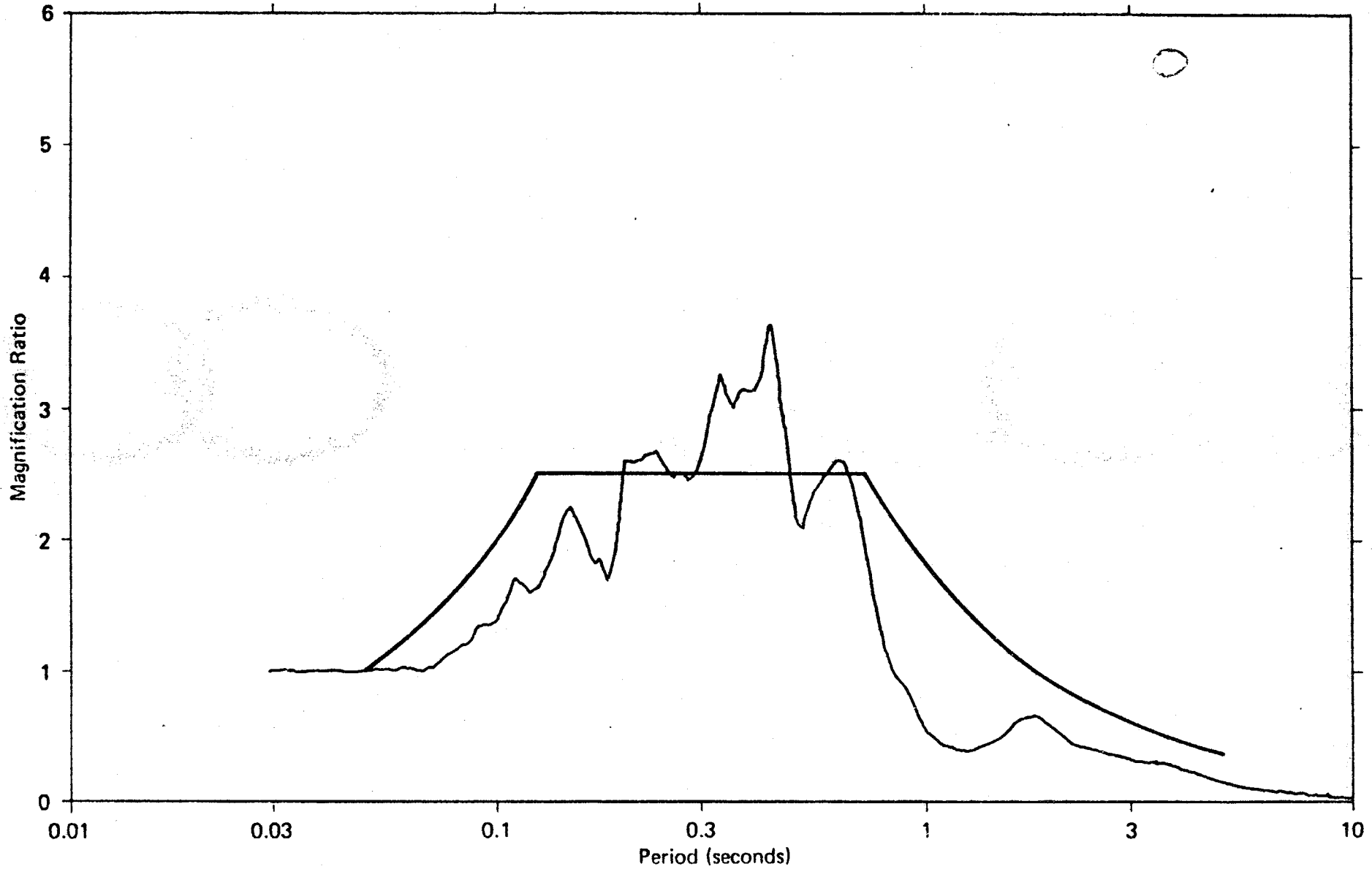

Fig. 10 — Normalized Response Spectra — Component A008/N79E

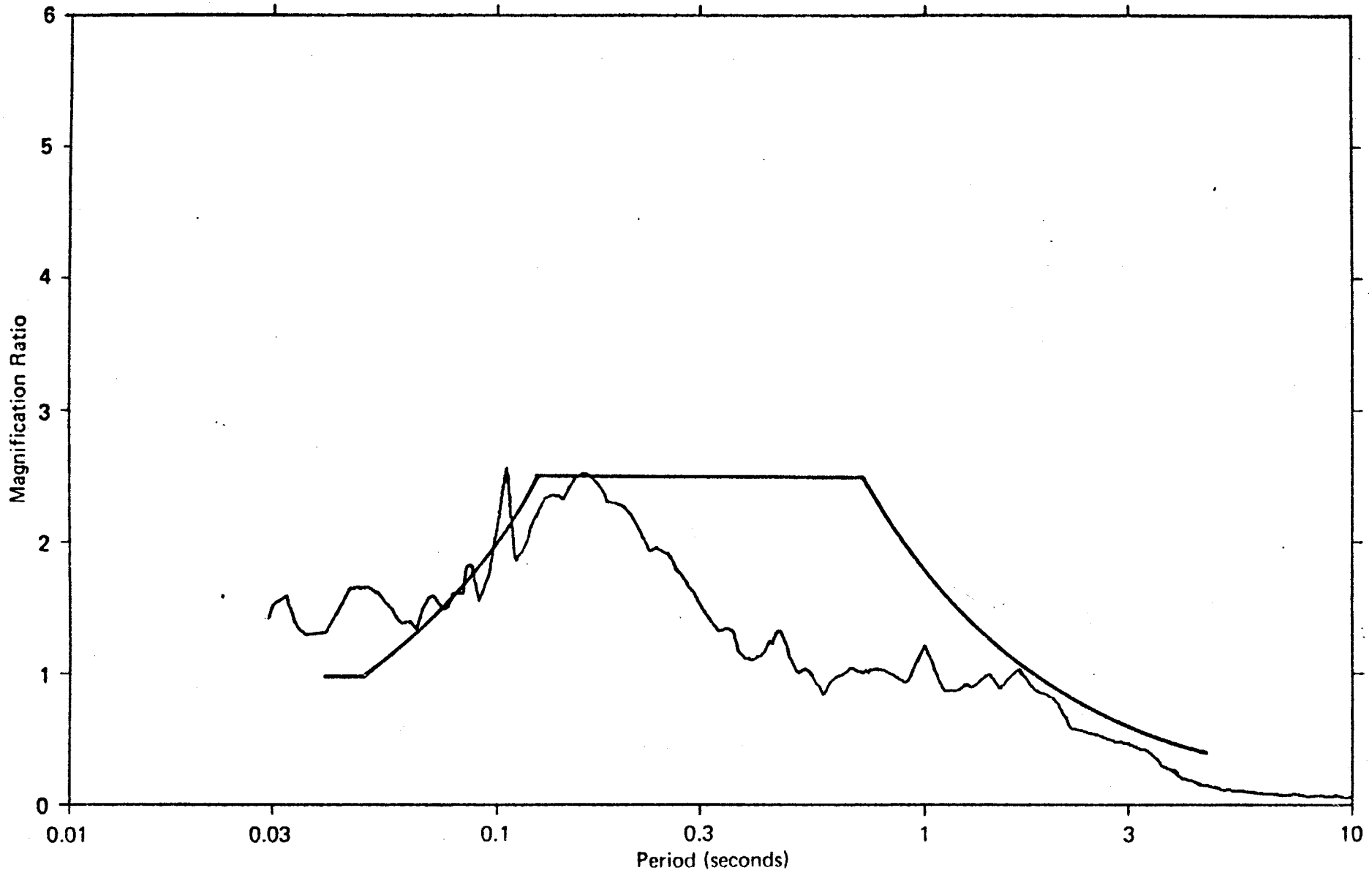

Fig. 11 – Normalized Response Spectra – Component A008/Vertical

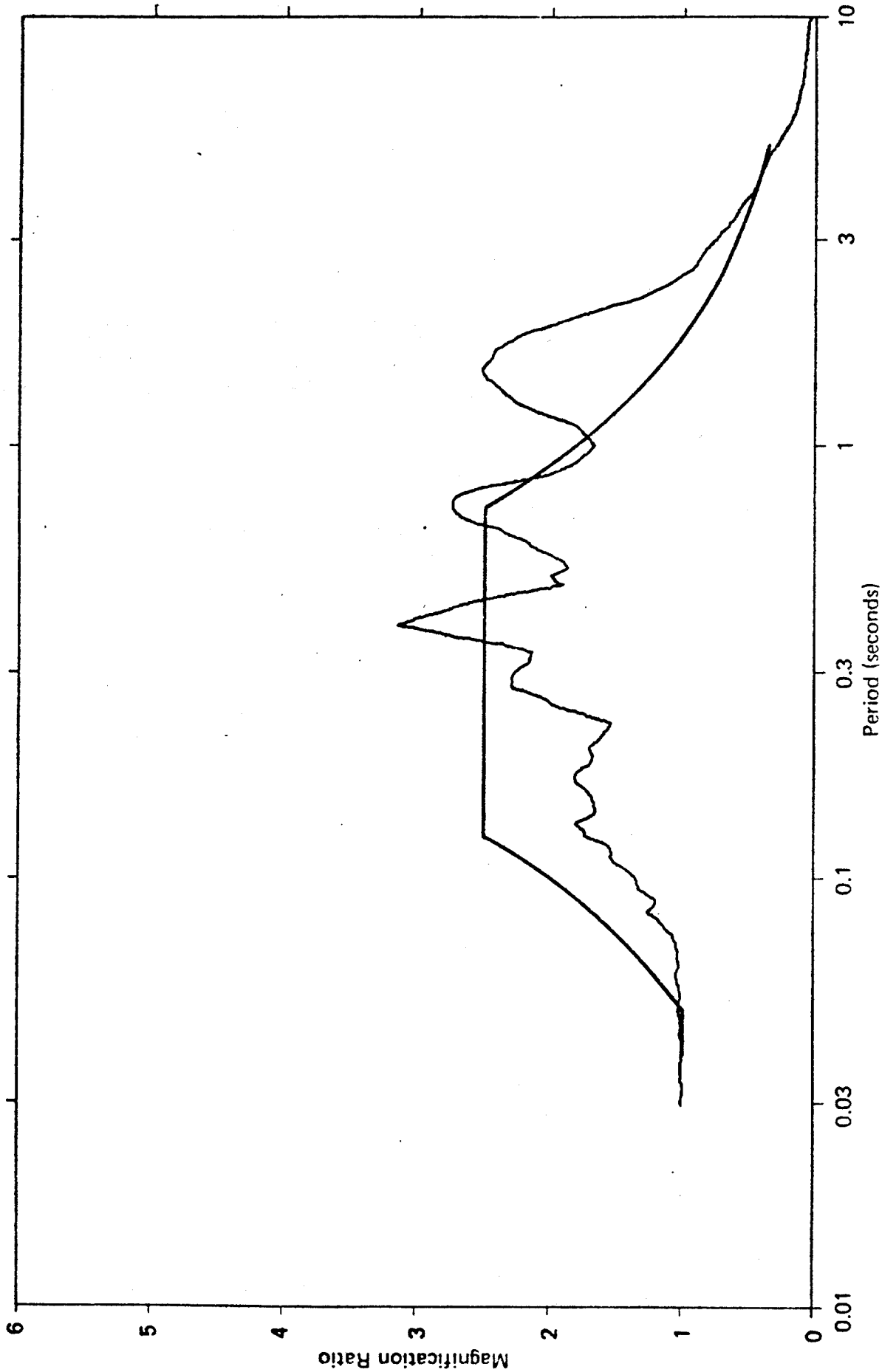

Fig. 12 -- Normalized Response Spectra -- Component A009/N44E

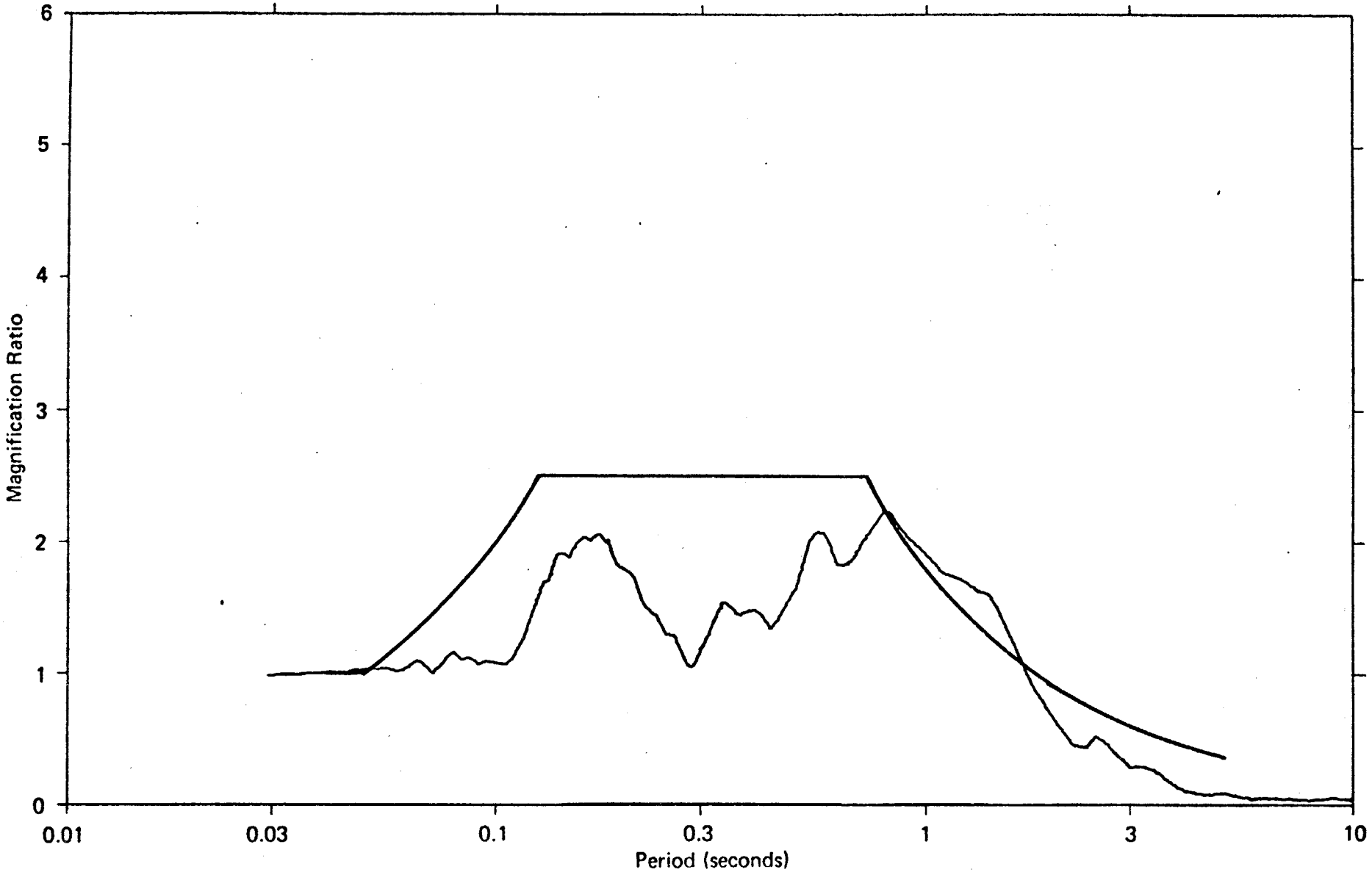

Fig.13 – Normalized Response Spectra – Component A009/N46W

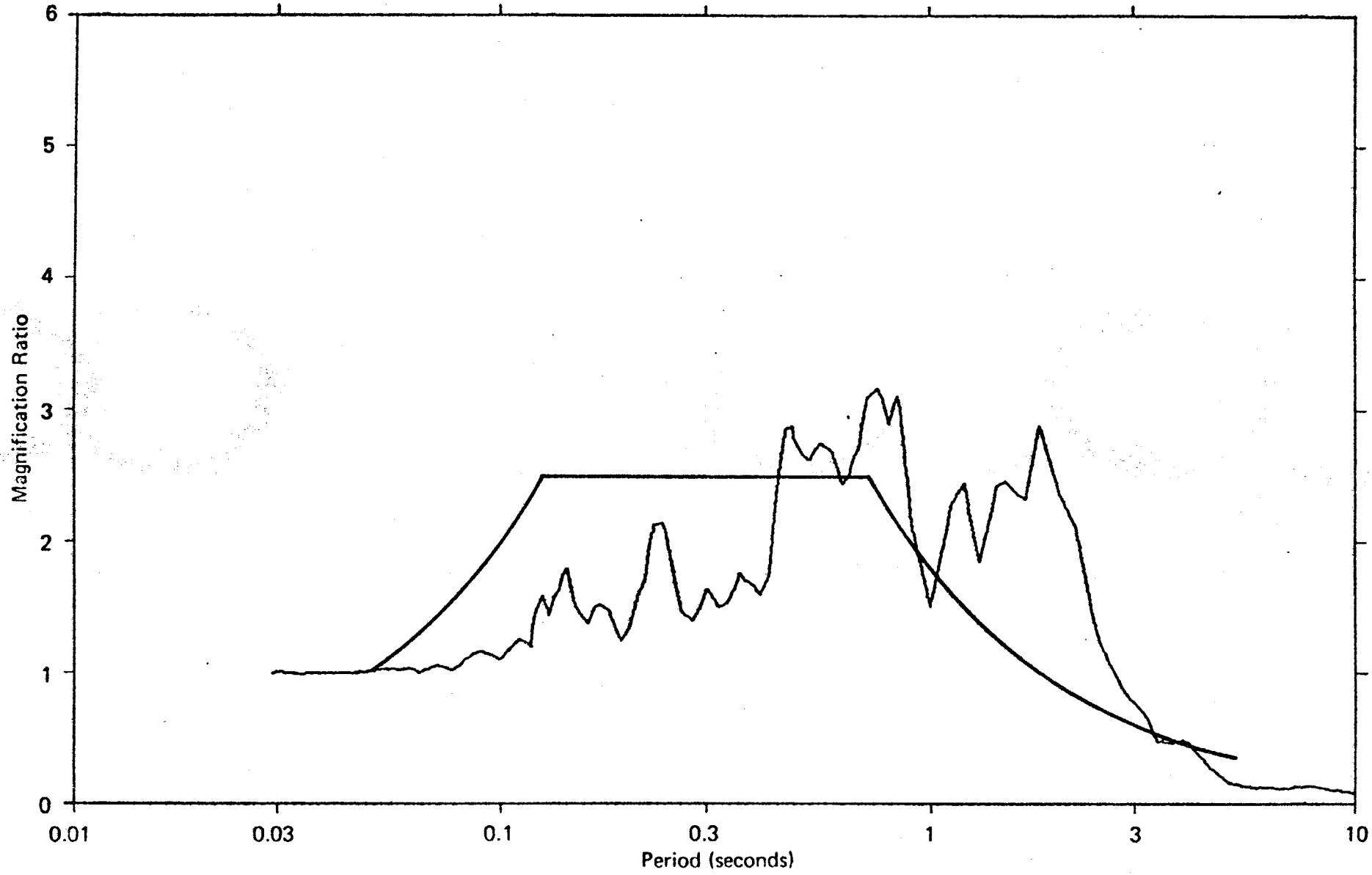

Fig. 14 – Normalized Response Spectra – Component A009/Vertical

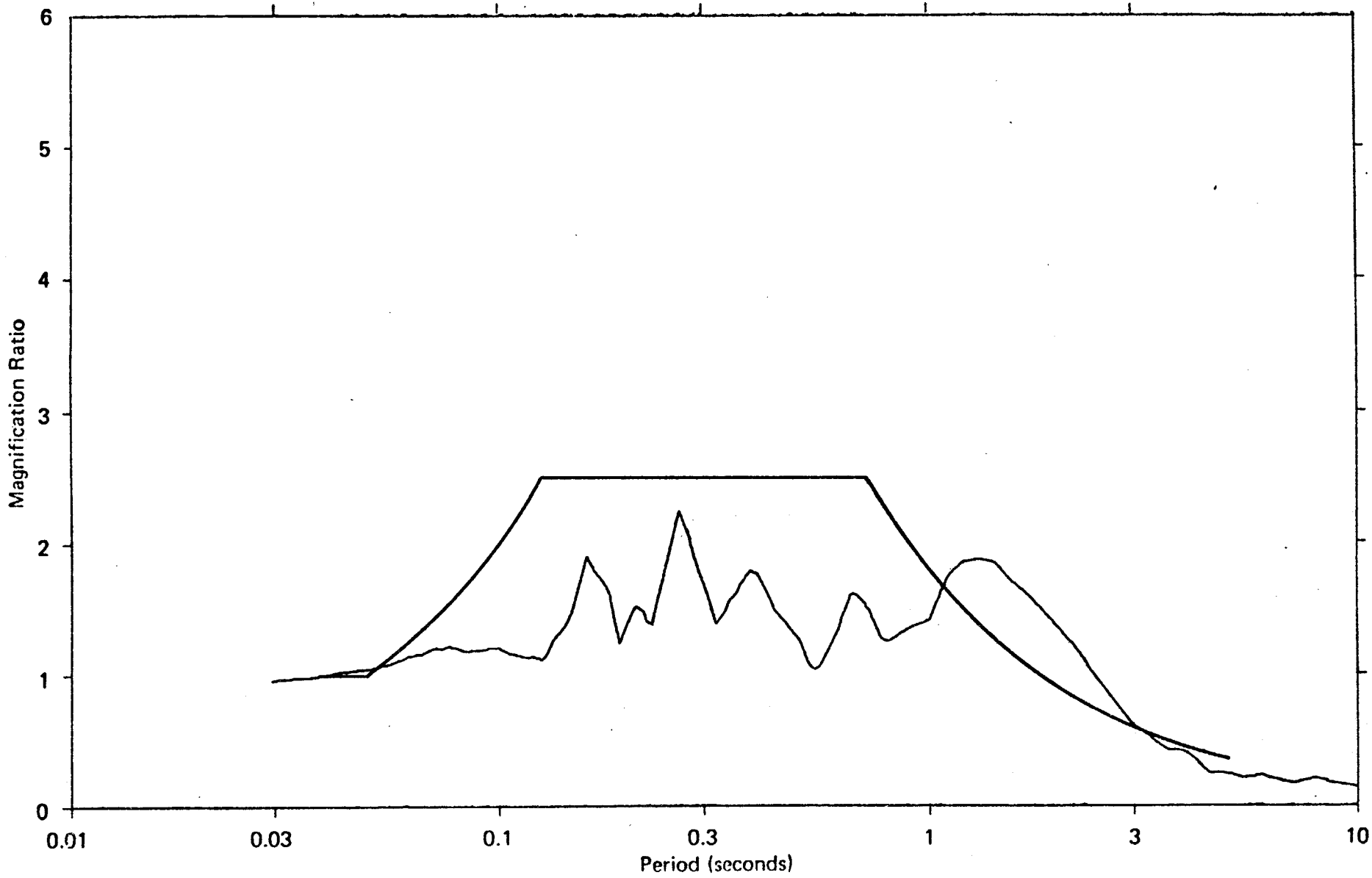

Fig. 15 – Normalized Response Spectra – Component A019/S00W

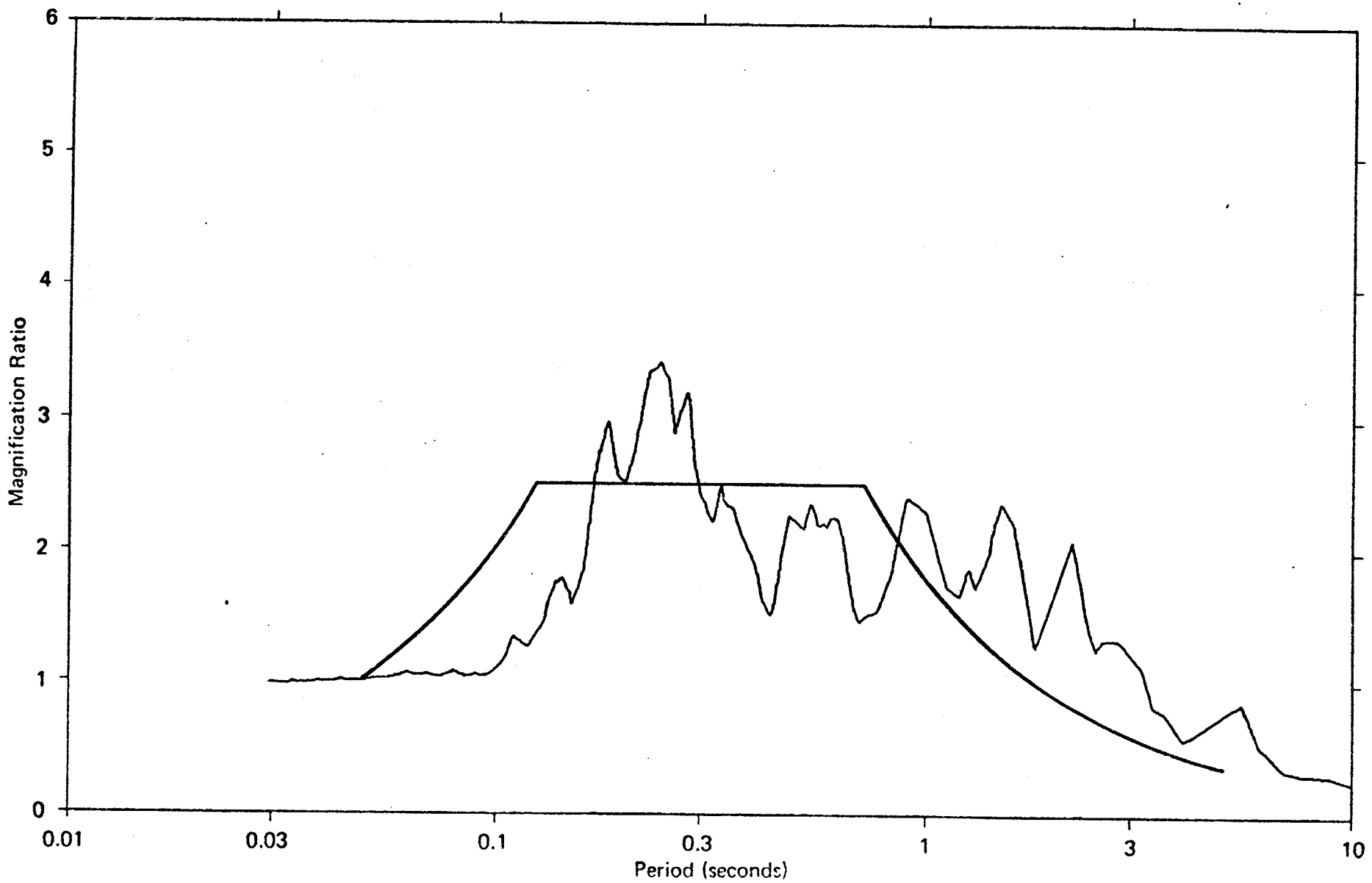

Fig. 16 — Normalized Response Spectra — Component A019/S90W

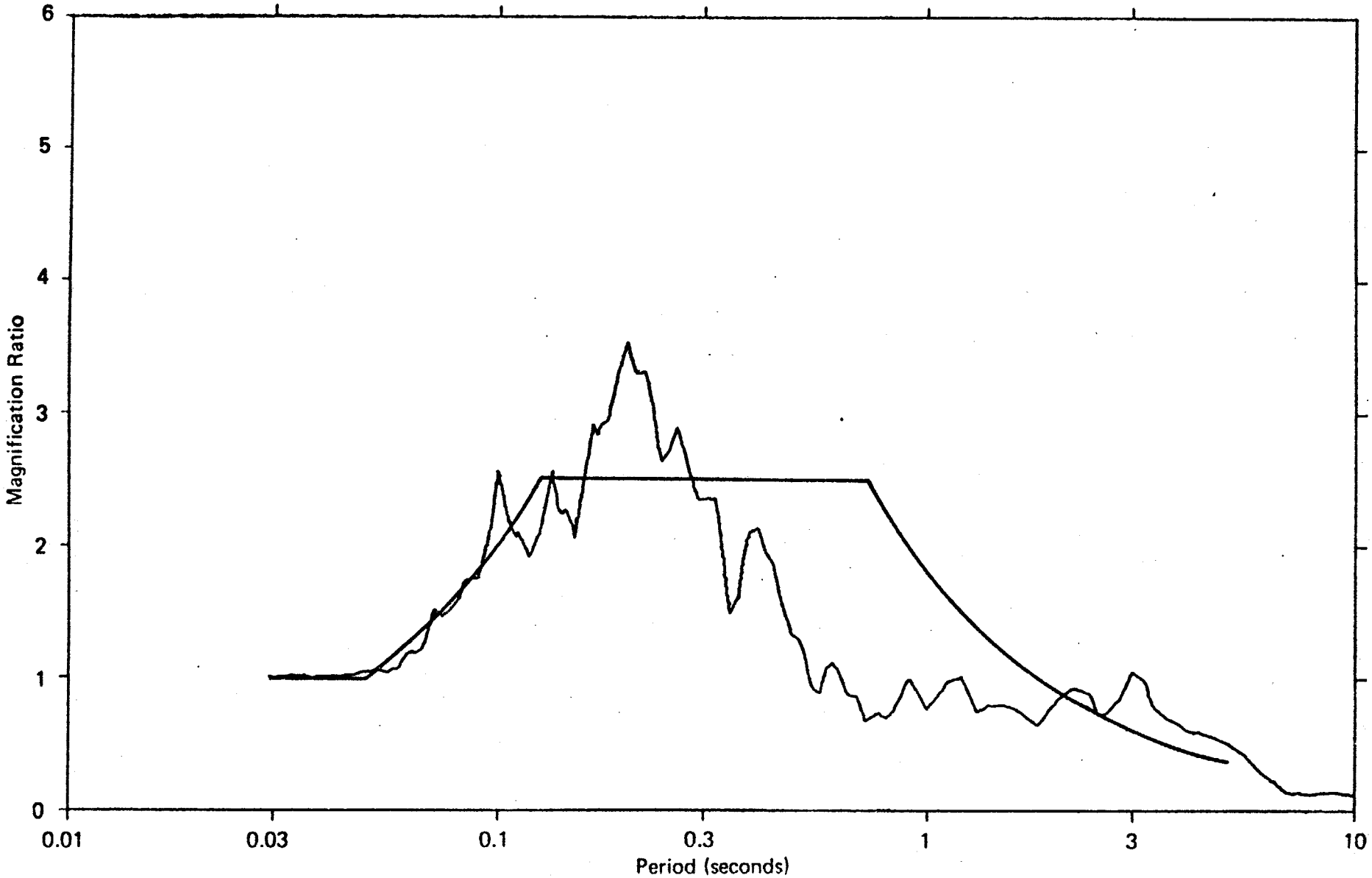

Fig. 17 – Normalized Response Spectra – Component A019/Vertical

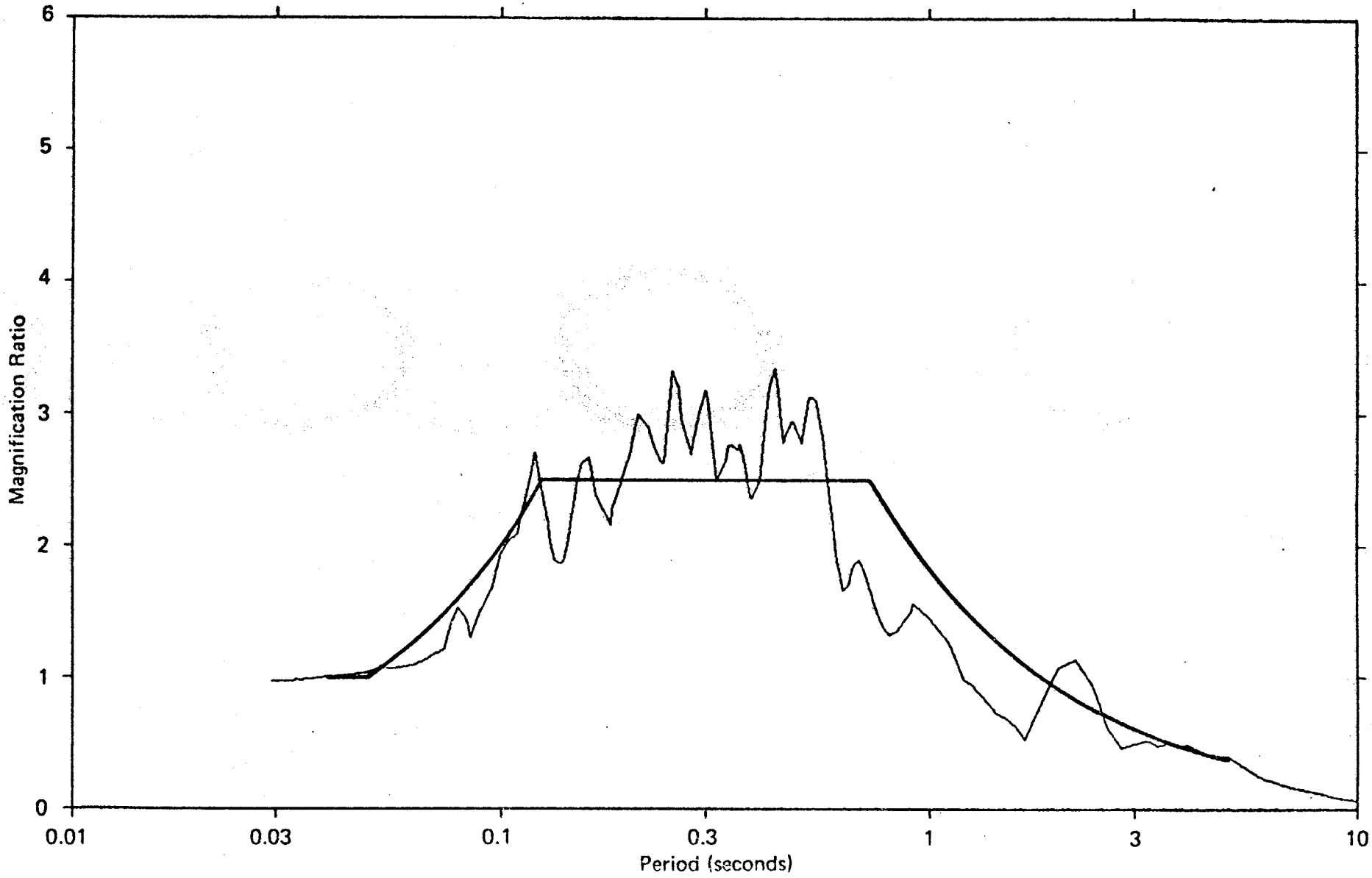

Fig. 18 – Normalized Response Spectra – Component D057/S00W

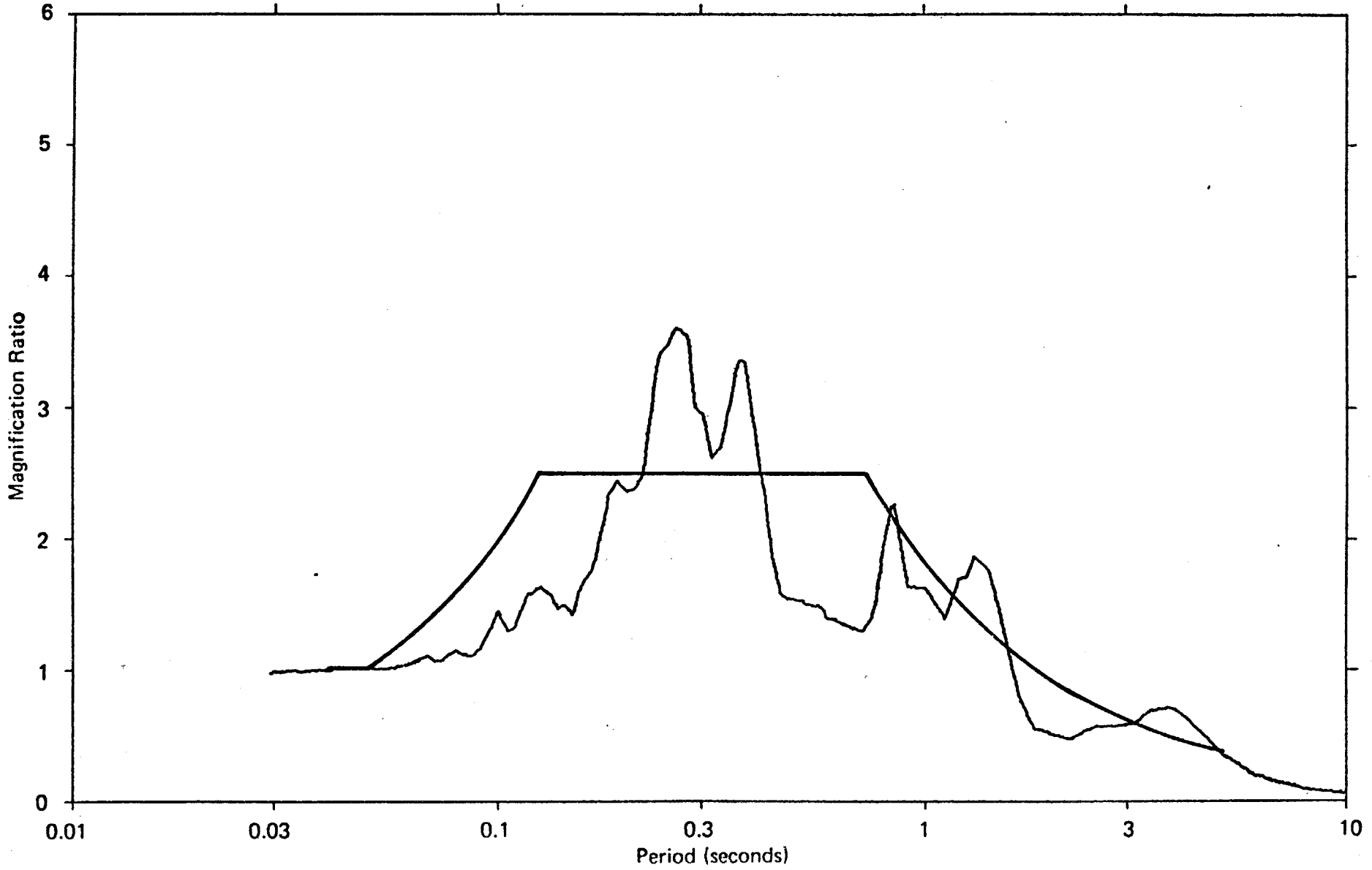

Fig. 19 – Normalized Response Spectra – Component DO57/N90E

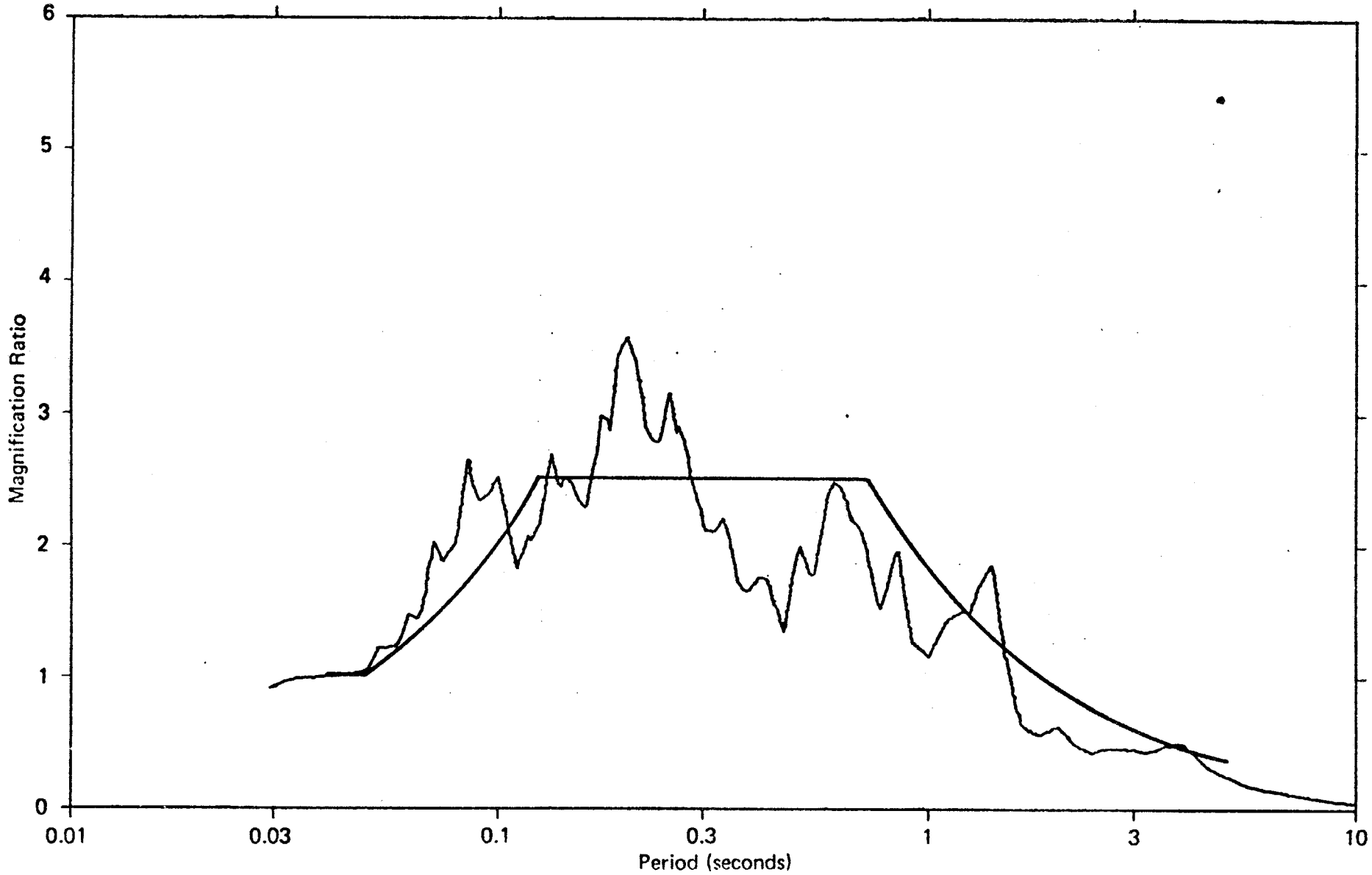

Fig. 20 – Normalized Response Spectra – Component D057/Vertical

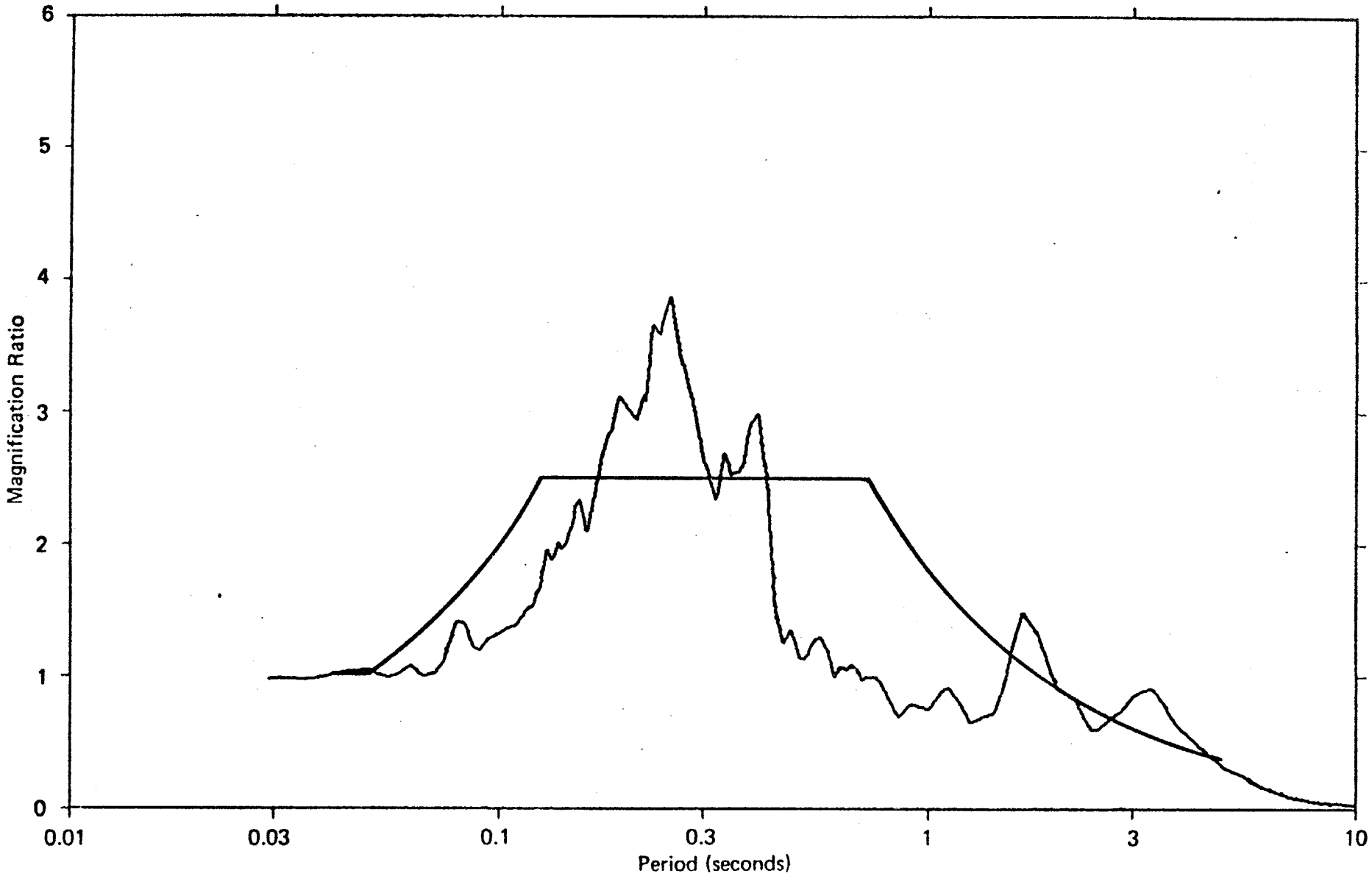

Fig. 21 – Normalized Response Spectra – Component H115/N11E

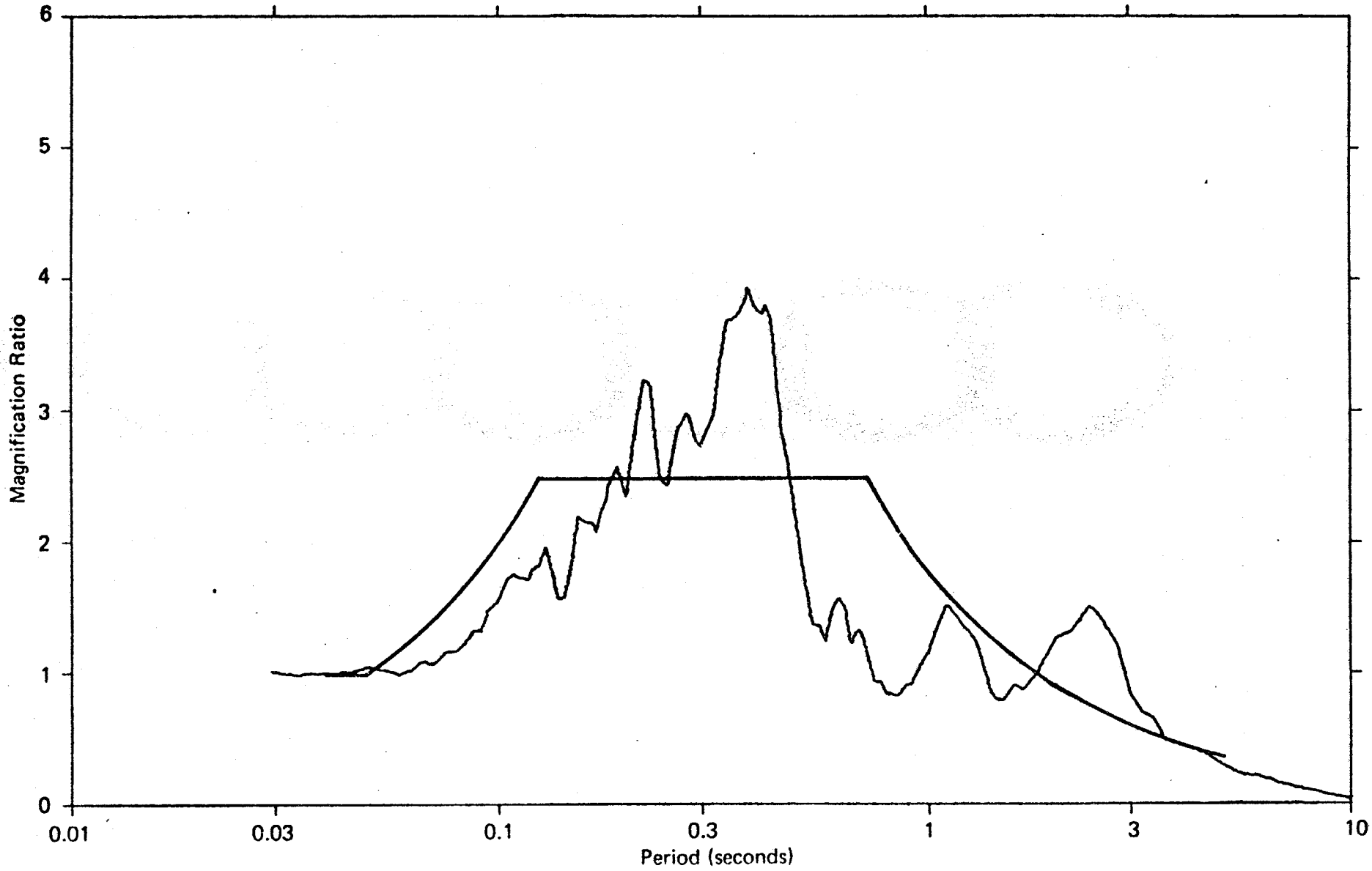

Fig. 22 – Normalized Response Spectra – Component H115/N79W

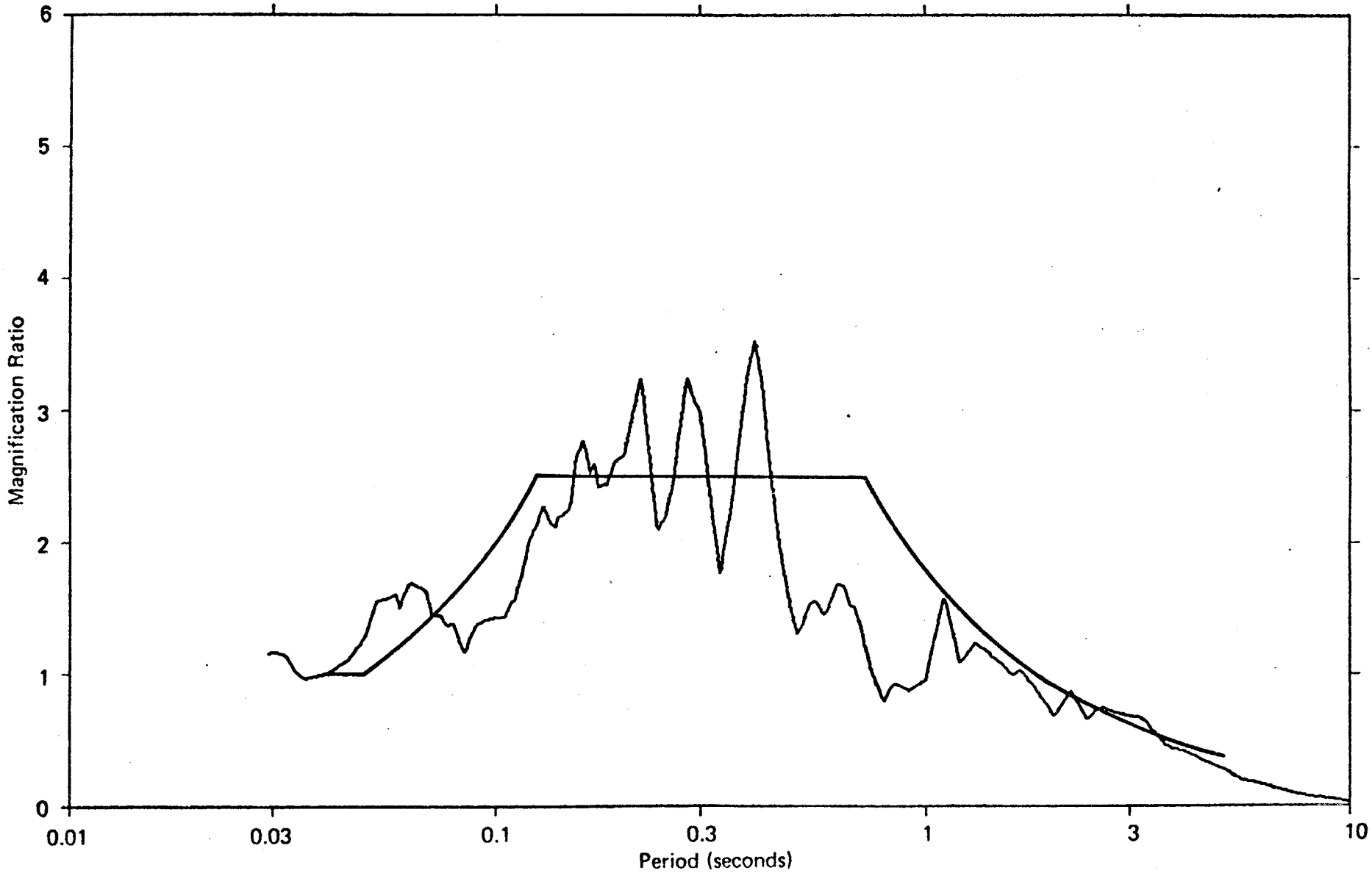

Fig. 23 – Normalized Response Spectra – Component H115/Vertical

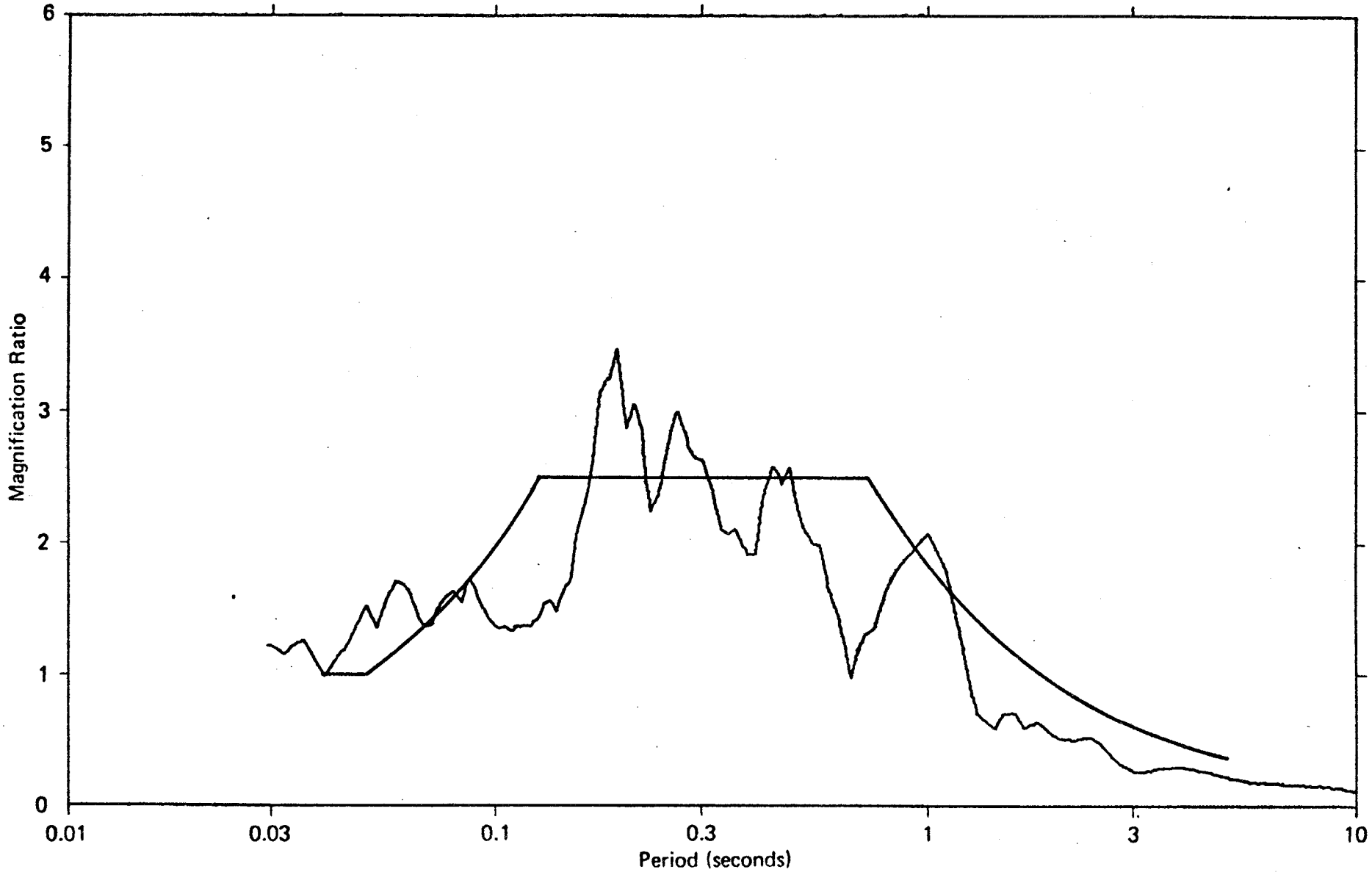

Fig. 24 – Normalized Response Spectra – Component V315/South

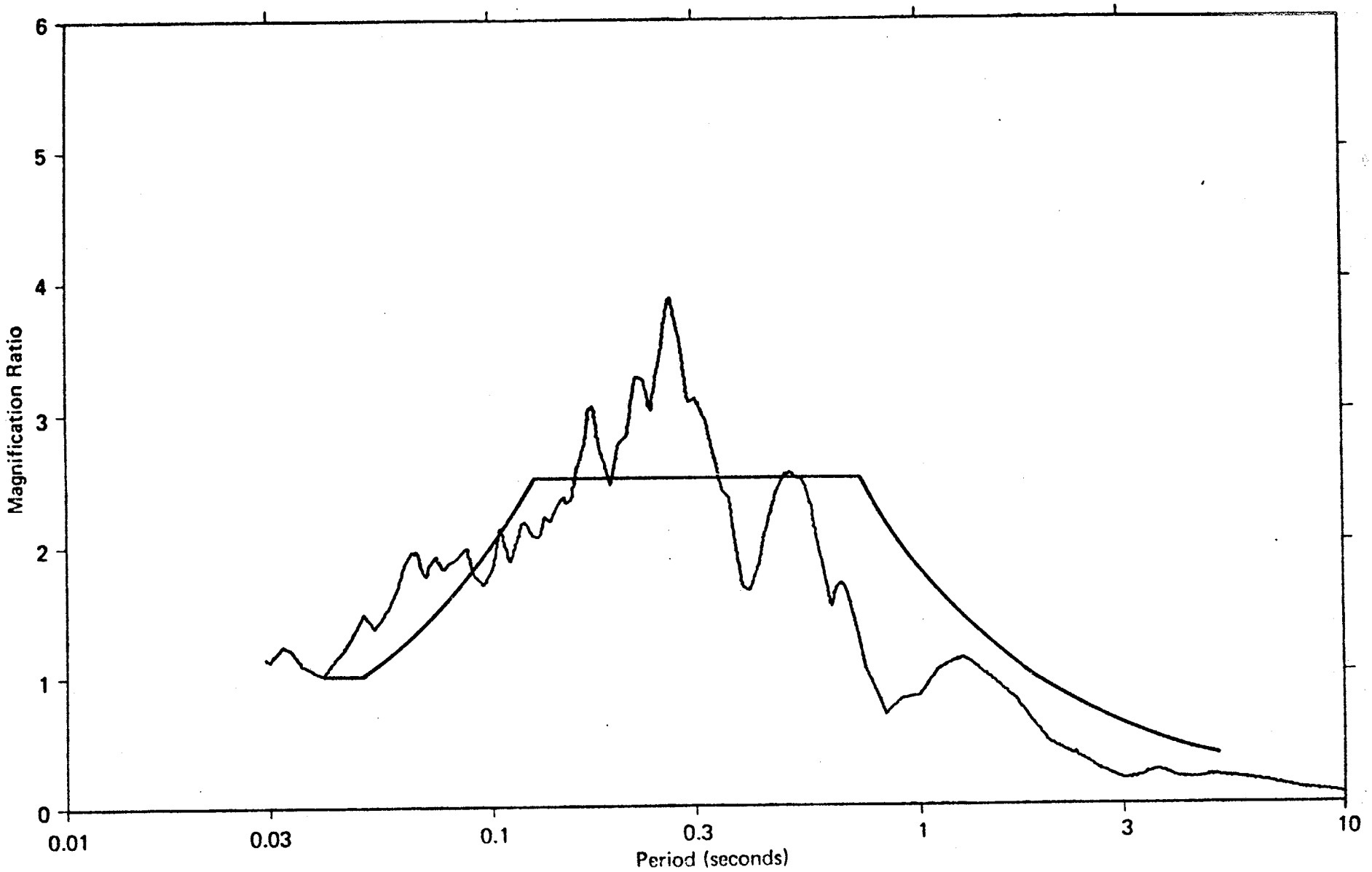

Fig. 25 – Normalized Response Spectra – Component V315/West

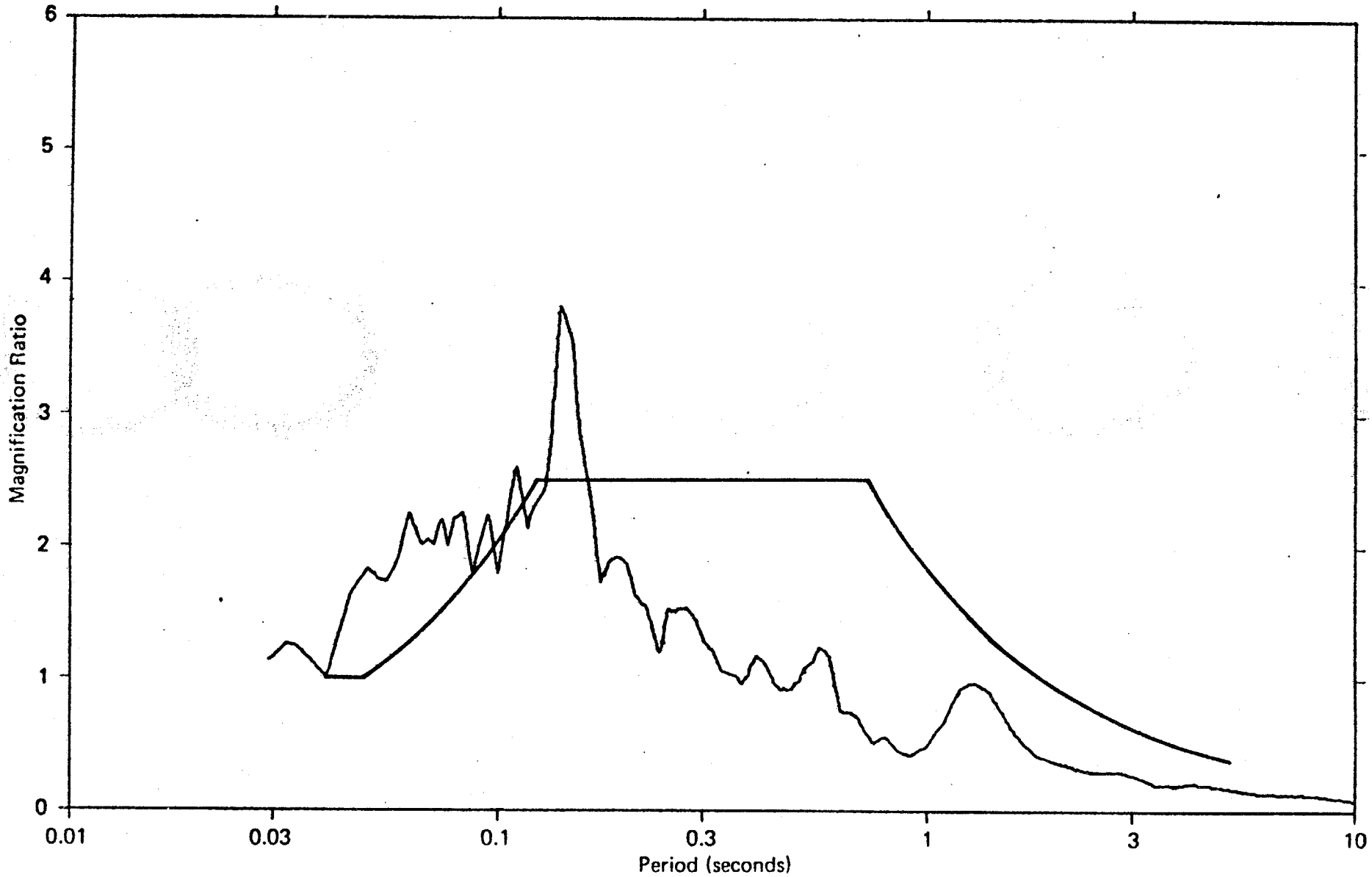

Fig. 26 – Normalized Response Spectra – Component V315/Vertical

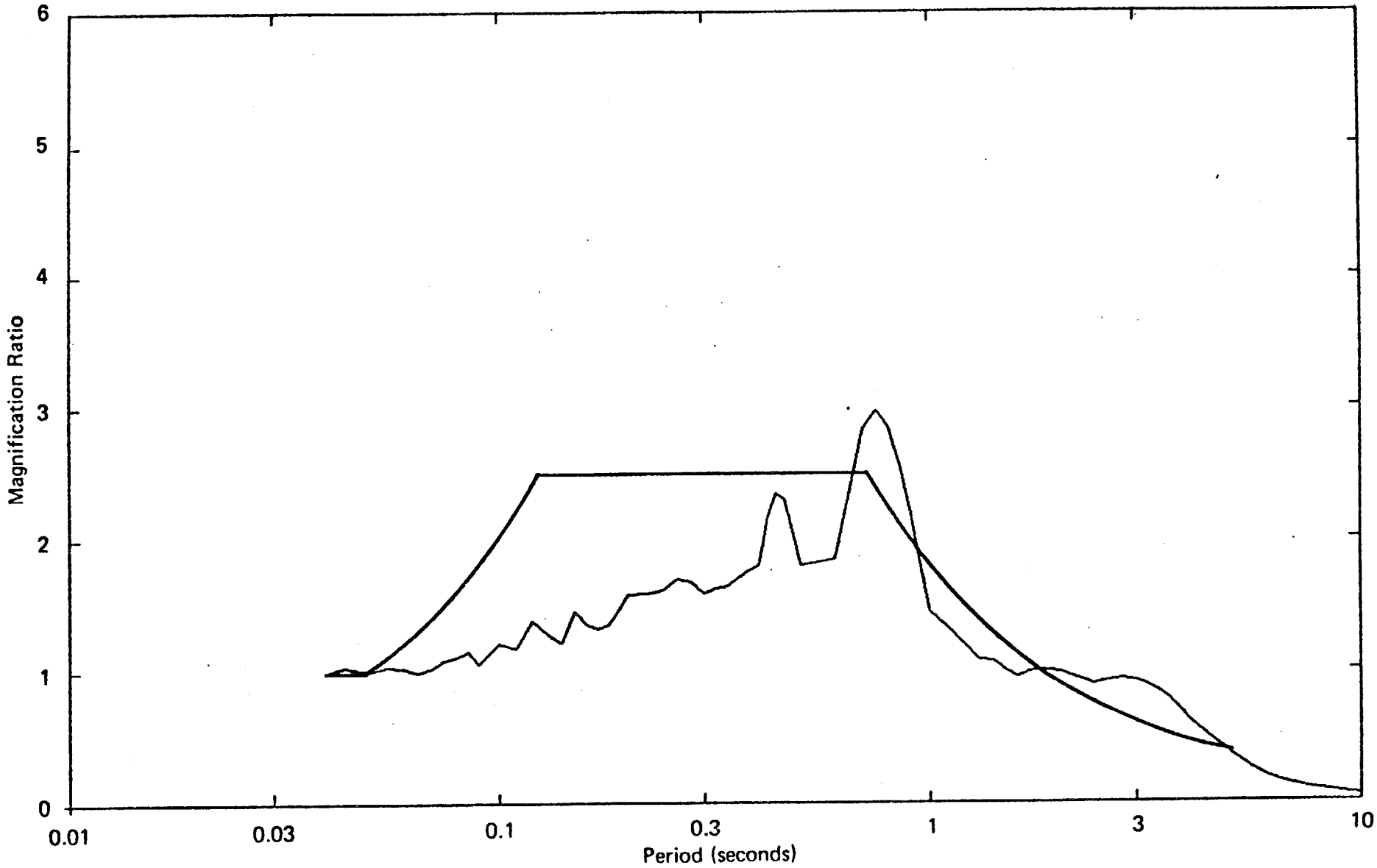

Fig. 27 – Normalized Response Spectra – 1979 Imperial Valley, El Centro Array 7, Component 230

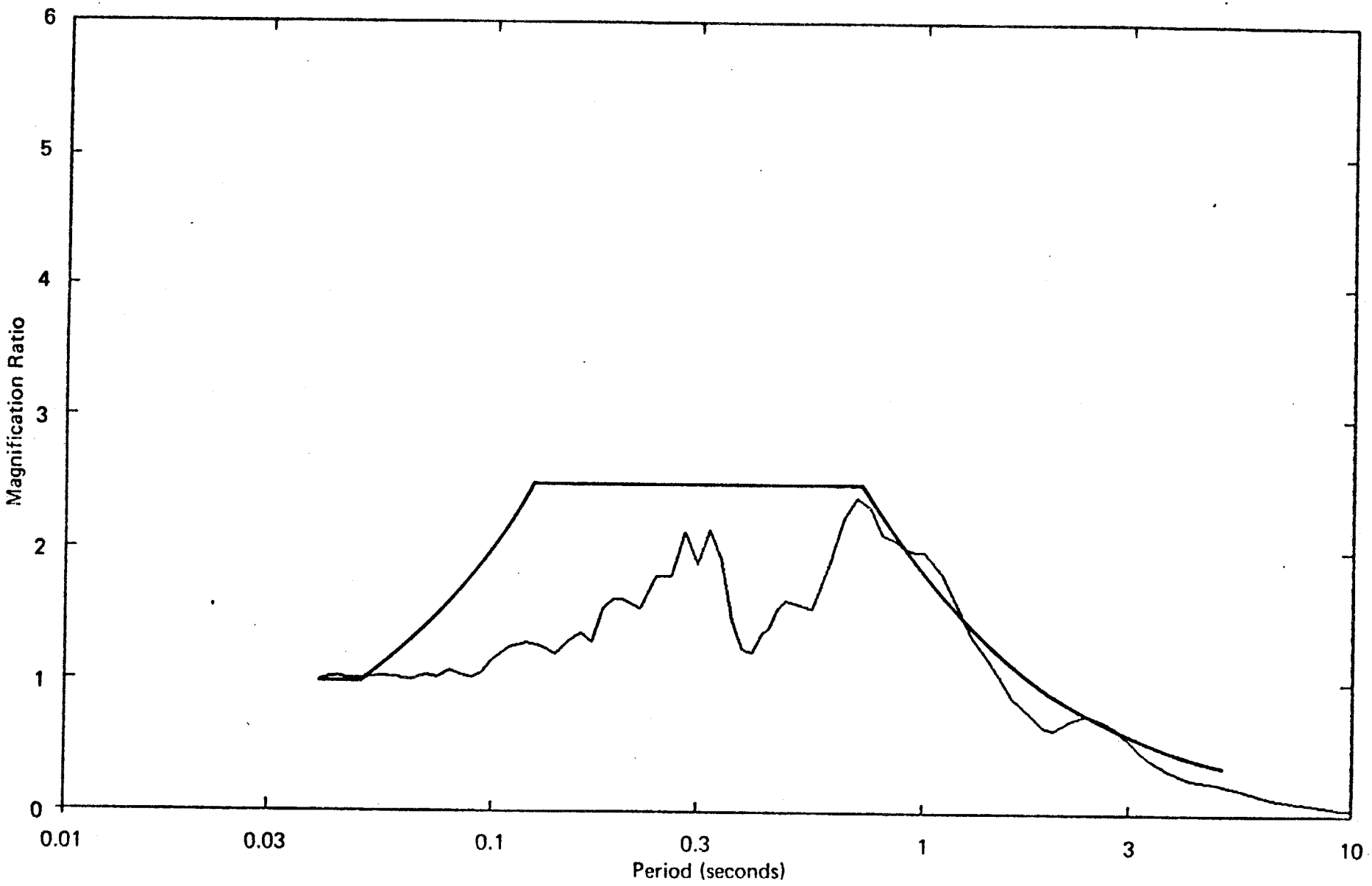

Fig. 28 – Normalized Response Spectra – 1979 Imperial Valley, El Centro Array 7, Component 140

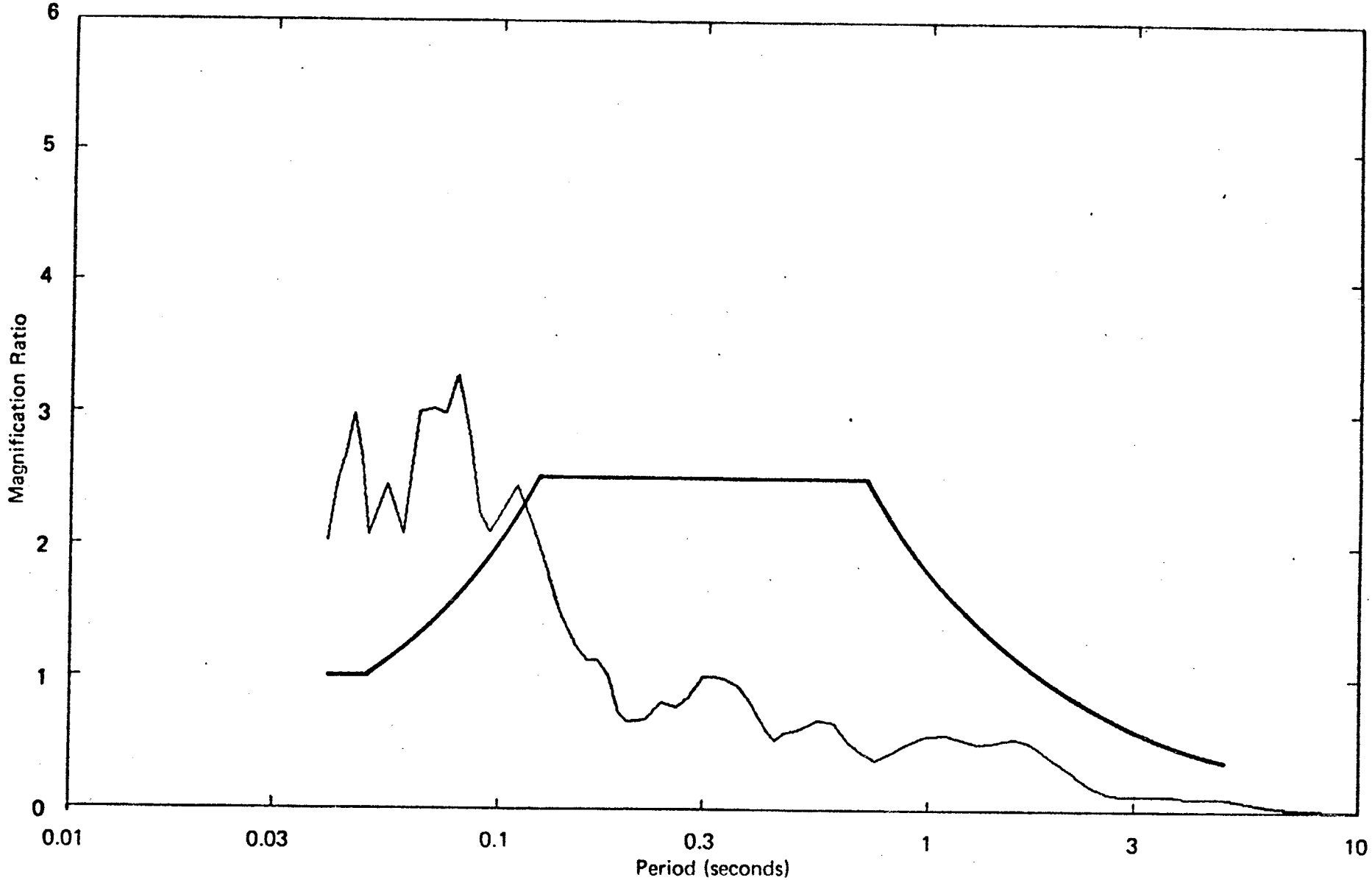

Fig. 29 – Normalized Response Spectra – 1979 Imperial Valley, El Centro Array 7, Component Vertical

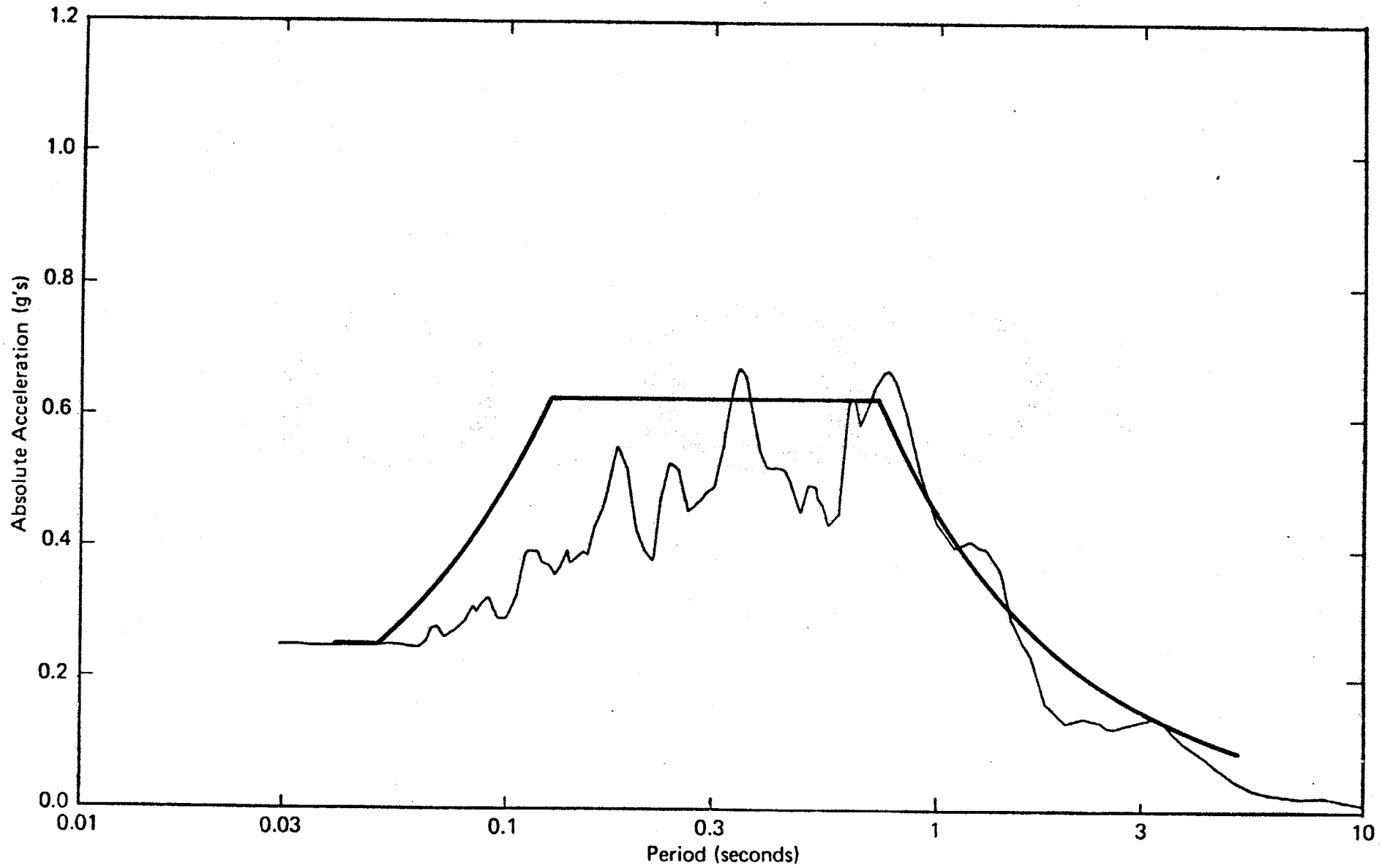

Fig. 30 – Acceleration Response Spectra – Earthquake I – Major Component

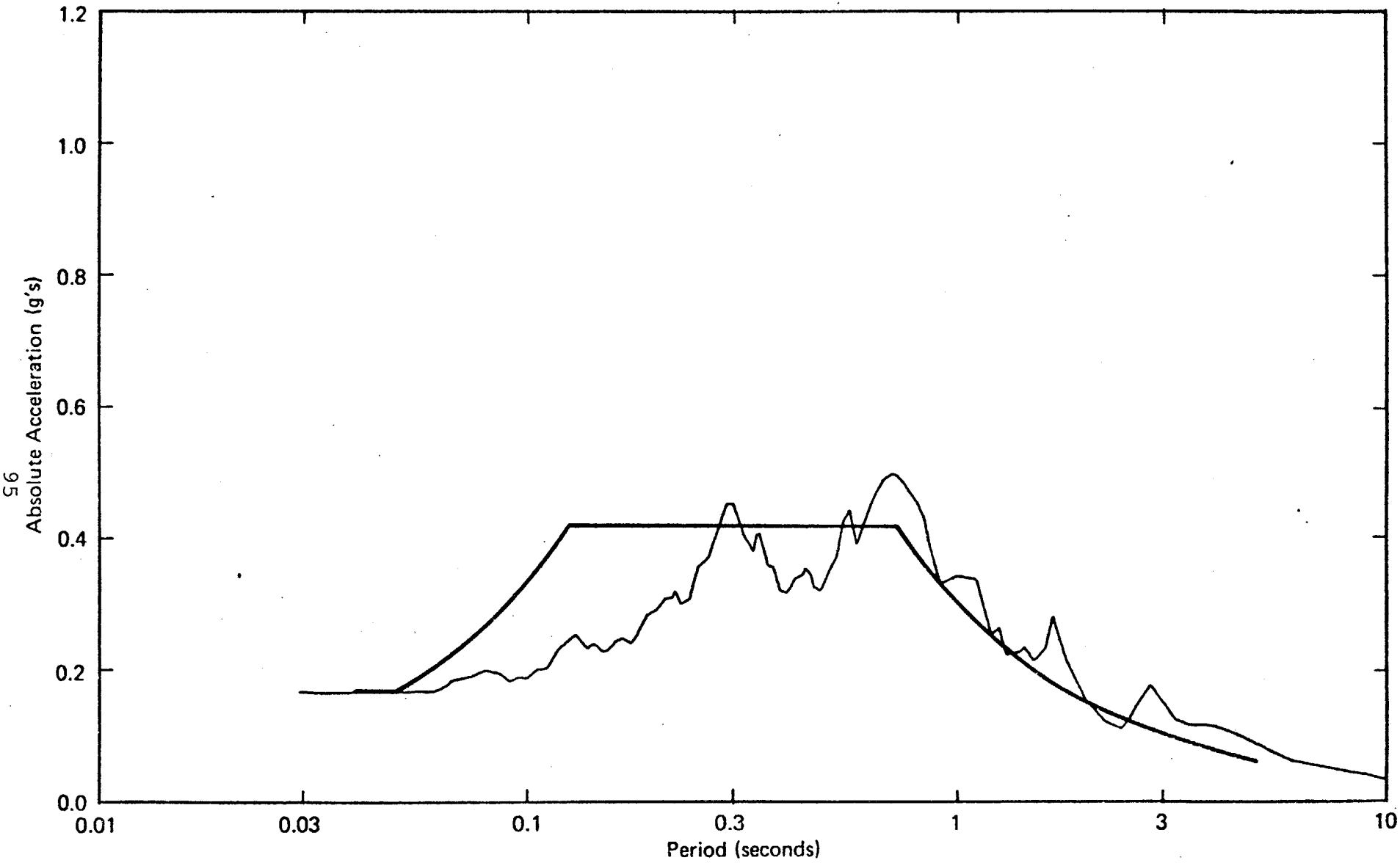

Fig. 31 – Acceleration Response Spectra – Earthquake I – Minor Component

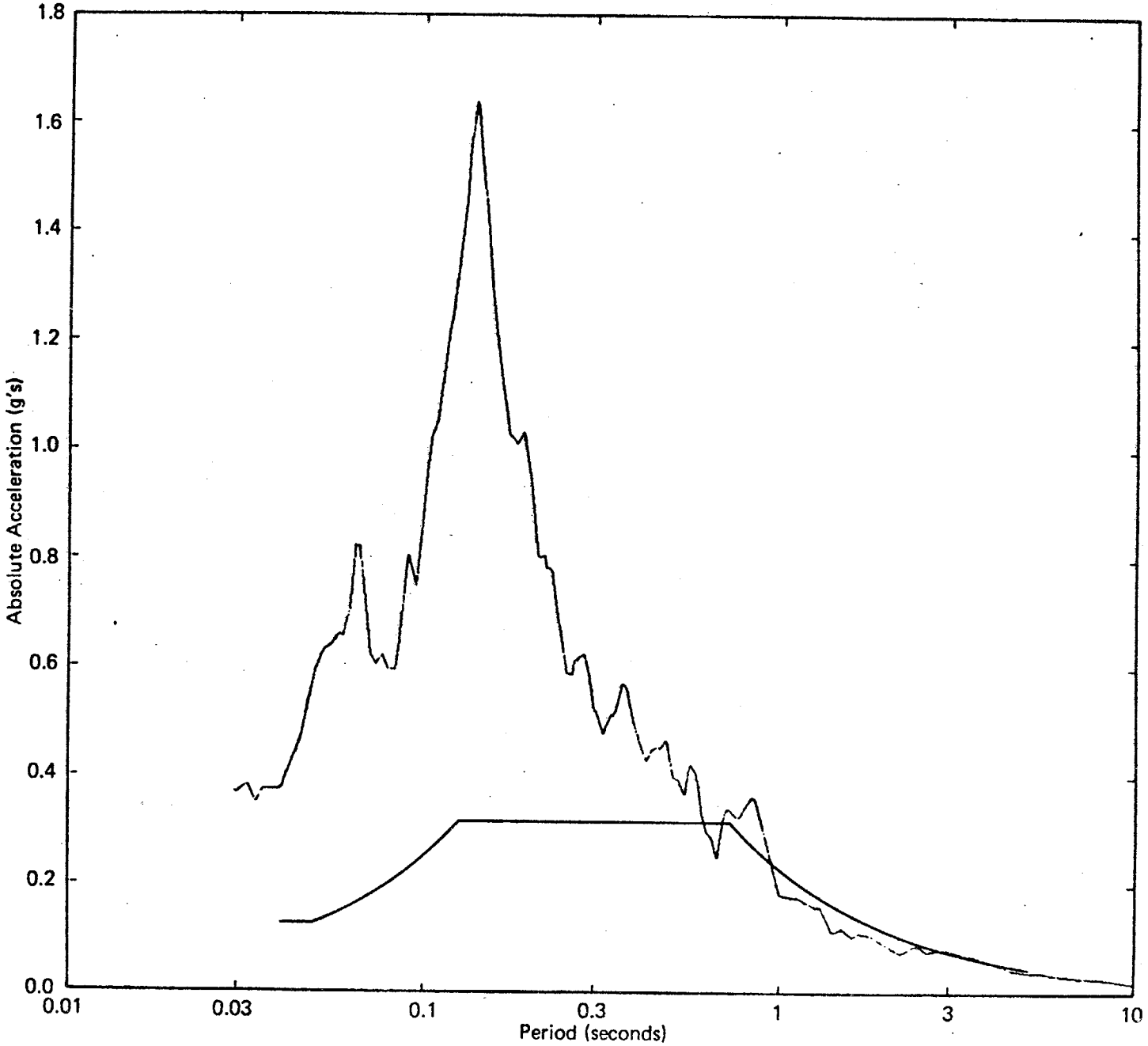

Fig. 32 – Acceleration Response Spectra – Earthquake I – Vertical

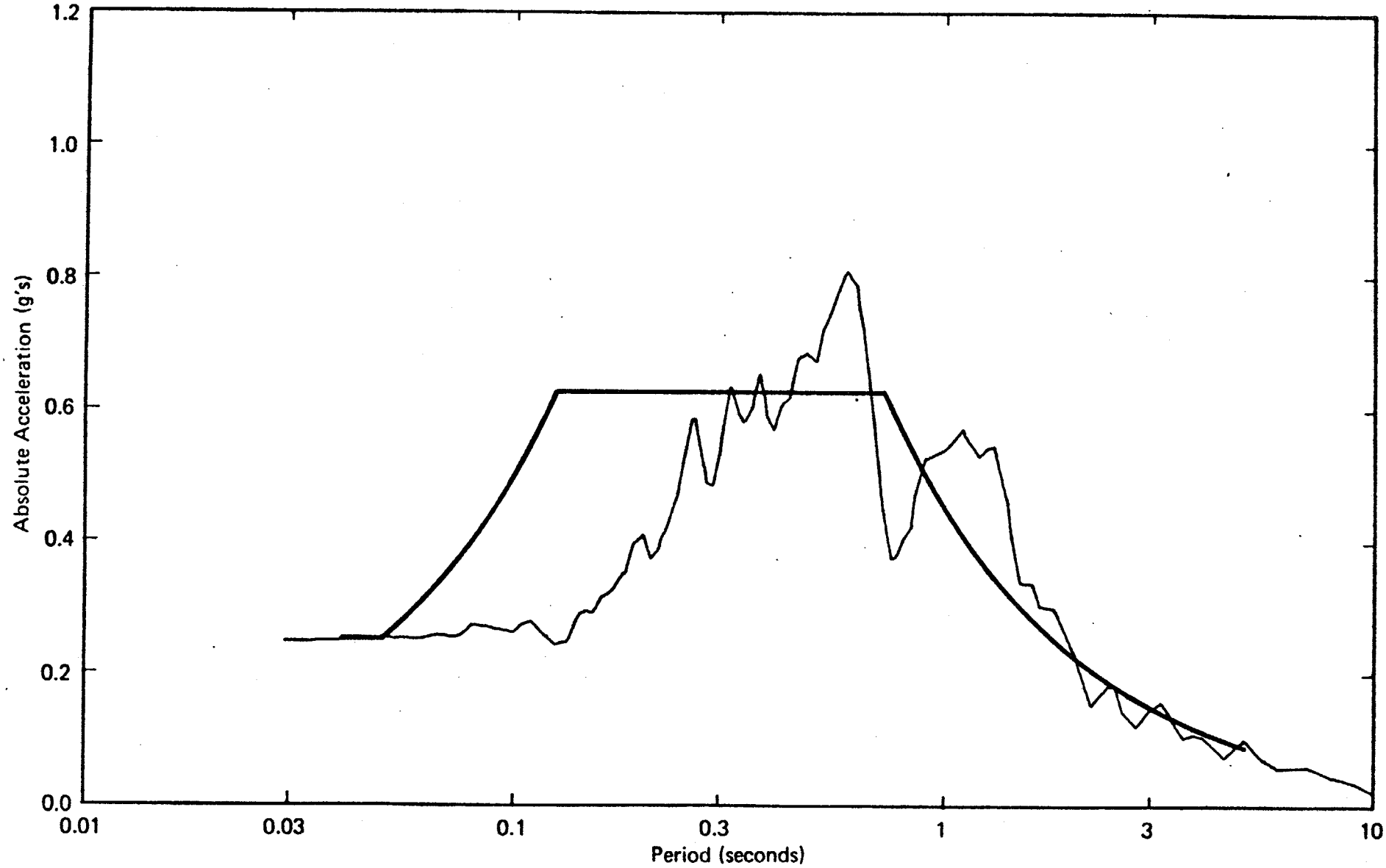

Fig. 33 – Acceleration Response Spectra – Earthquake II – Major Component

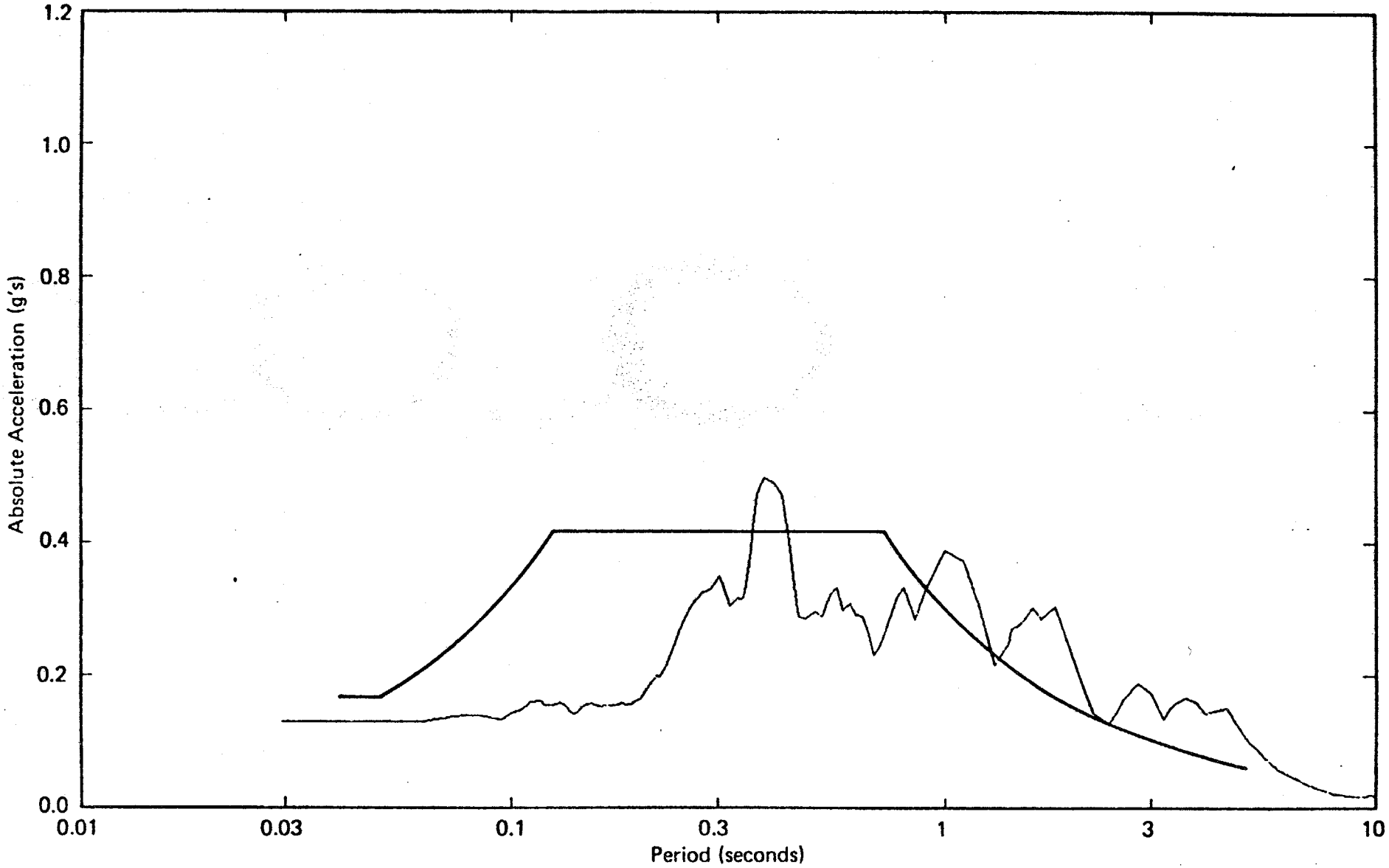

Fig. 34 — Acceleration Response Spectra — Earthquake II — Minor Component

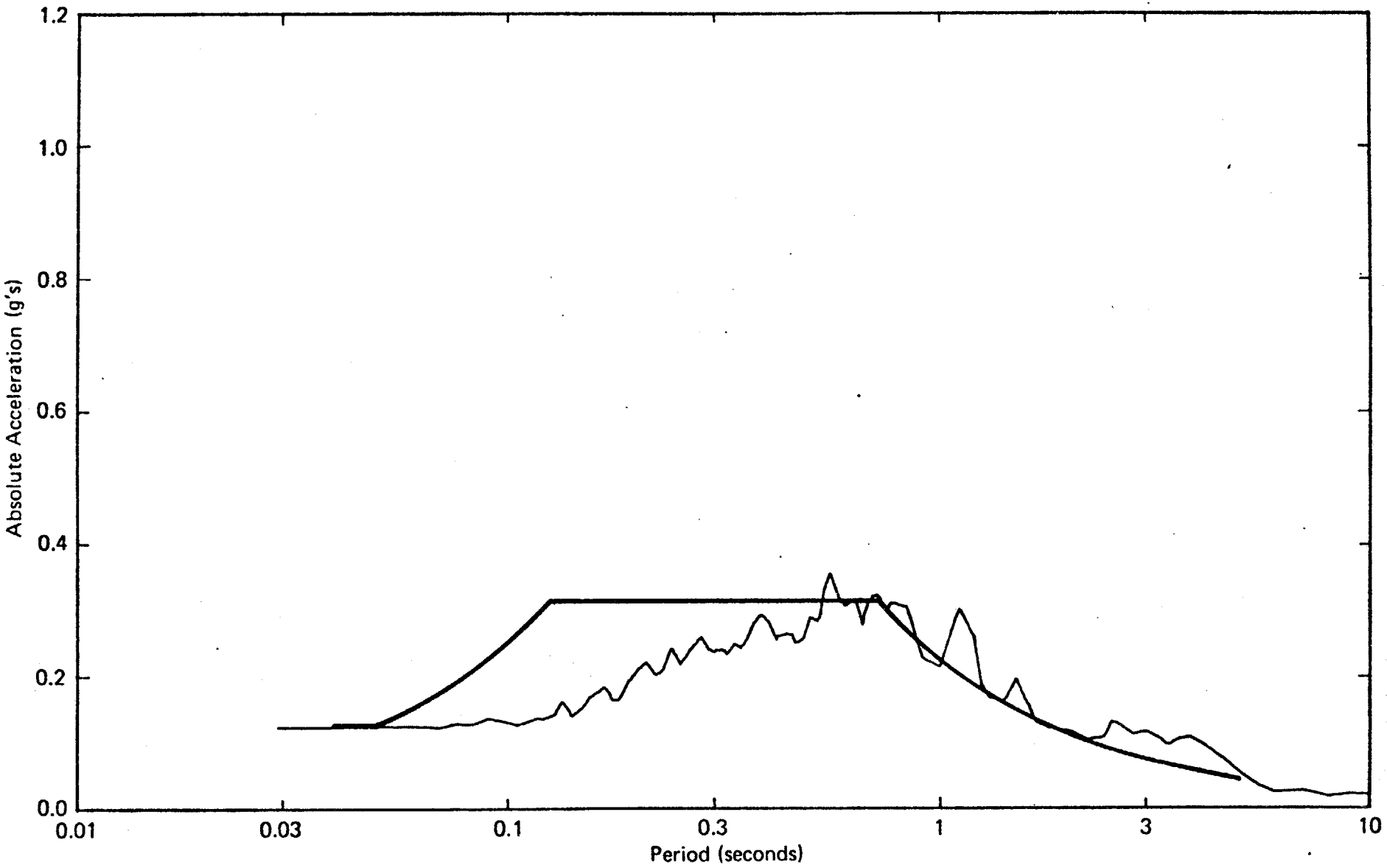

Fig. 35 – Acceleration Response Spectra – Earthquake II – Vertical

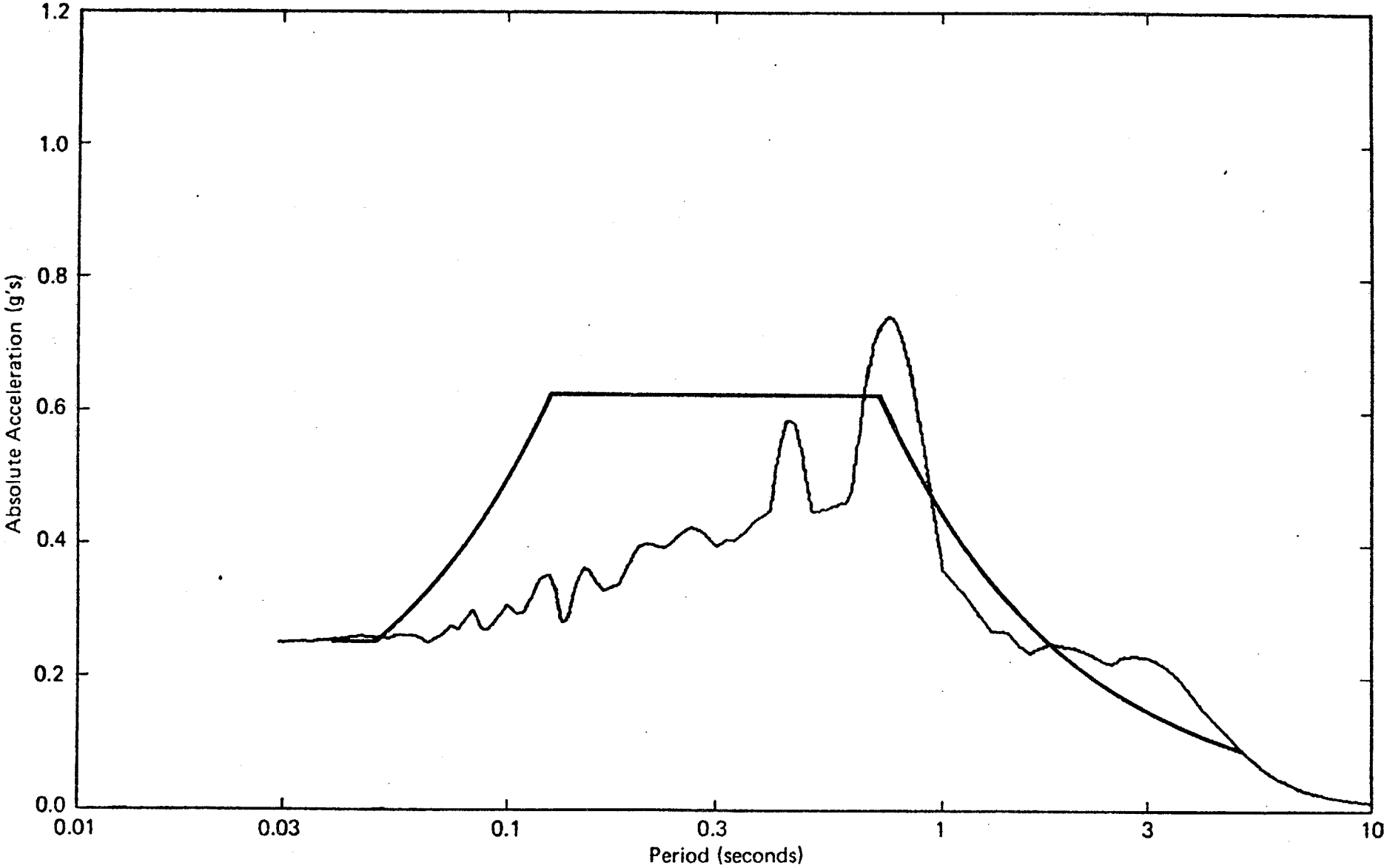

Fig. 36 – Acceleration Response Spectra – Earthquake III – Major Component

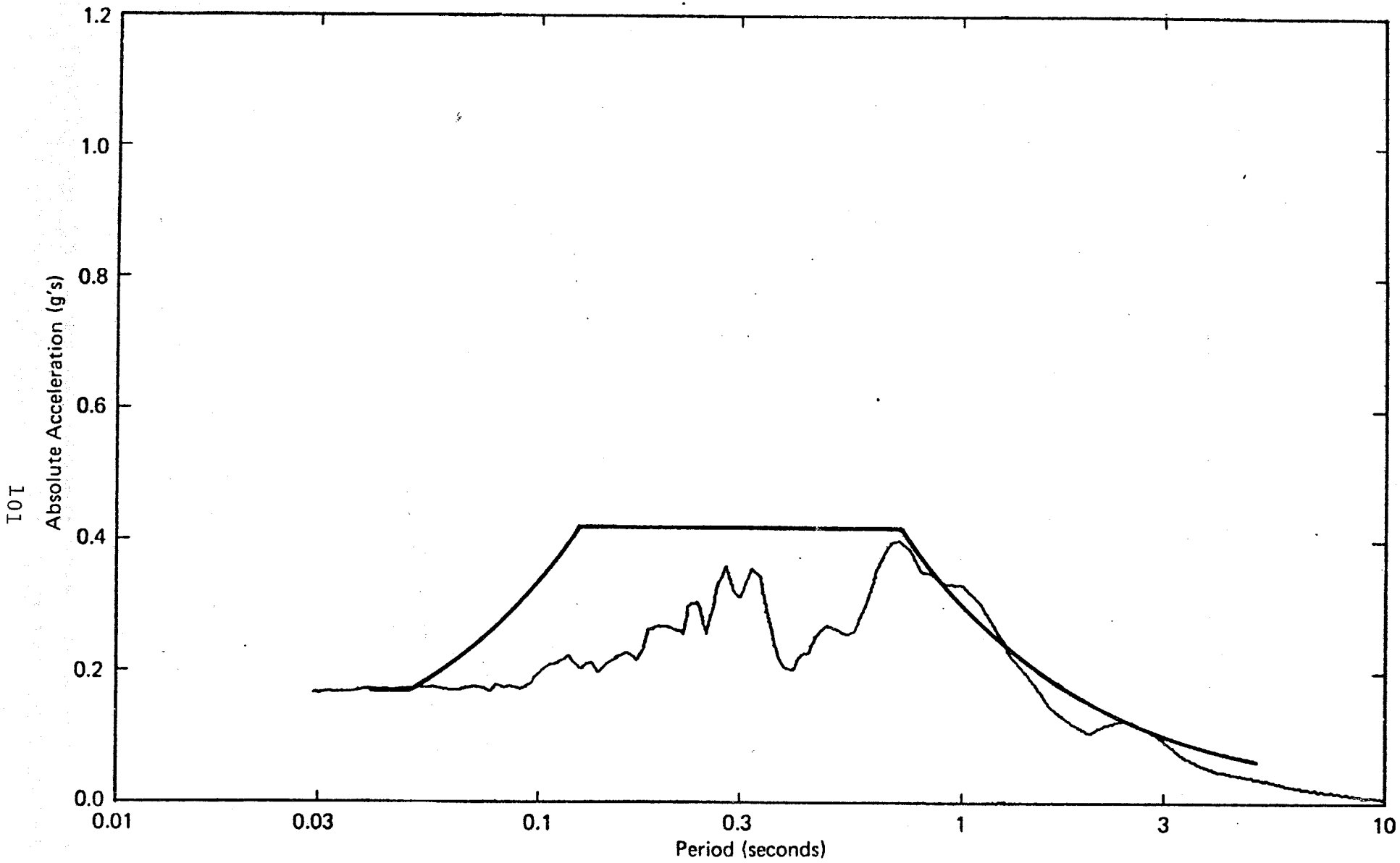

Fig. 37 – Acceleration Response Spectra – Earthquake III – Minor Component

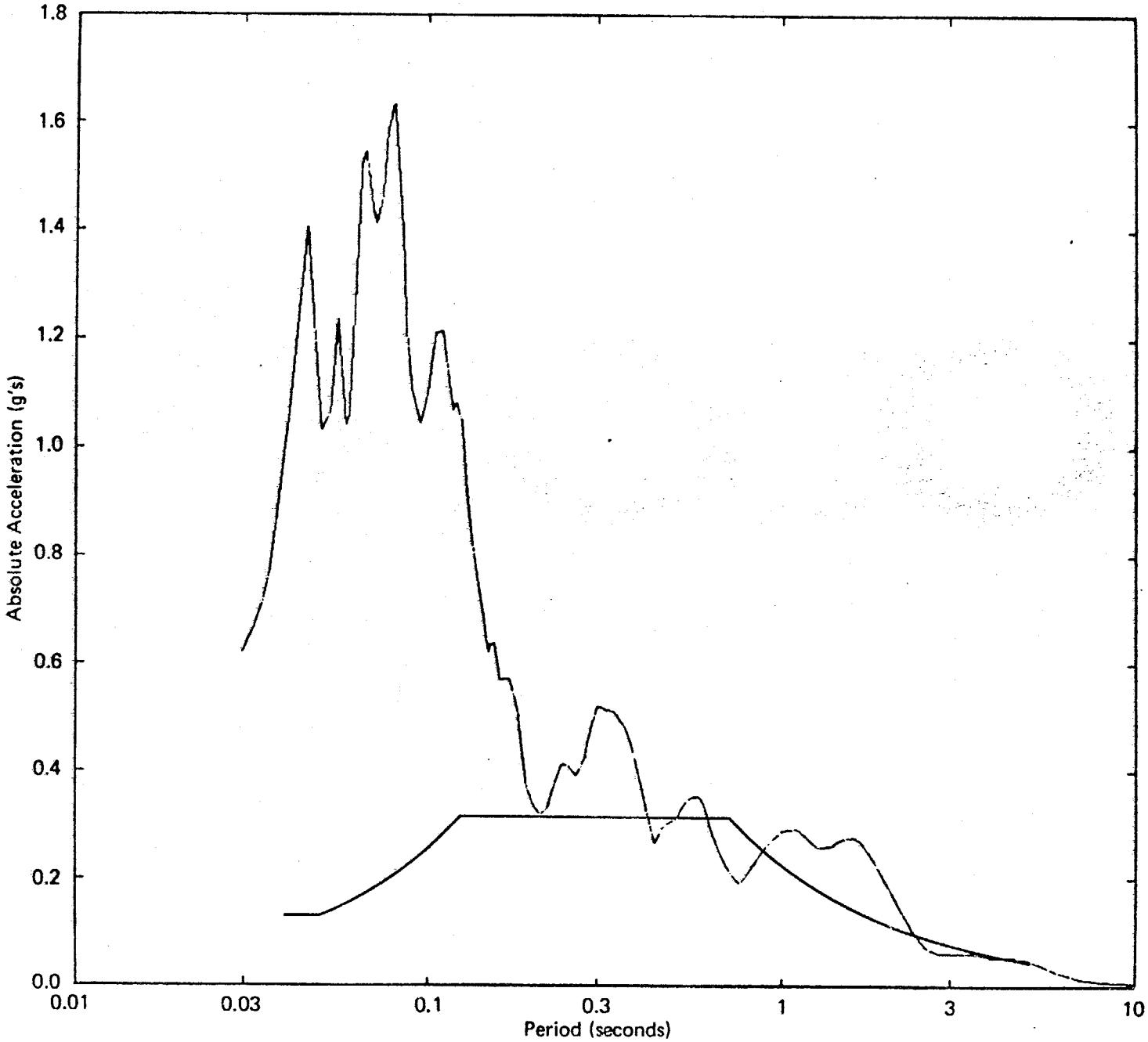

Fig. 38 – Acceleration Response Spectra – Earthquake III – Vertical

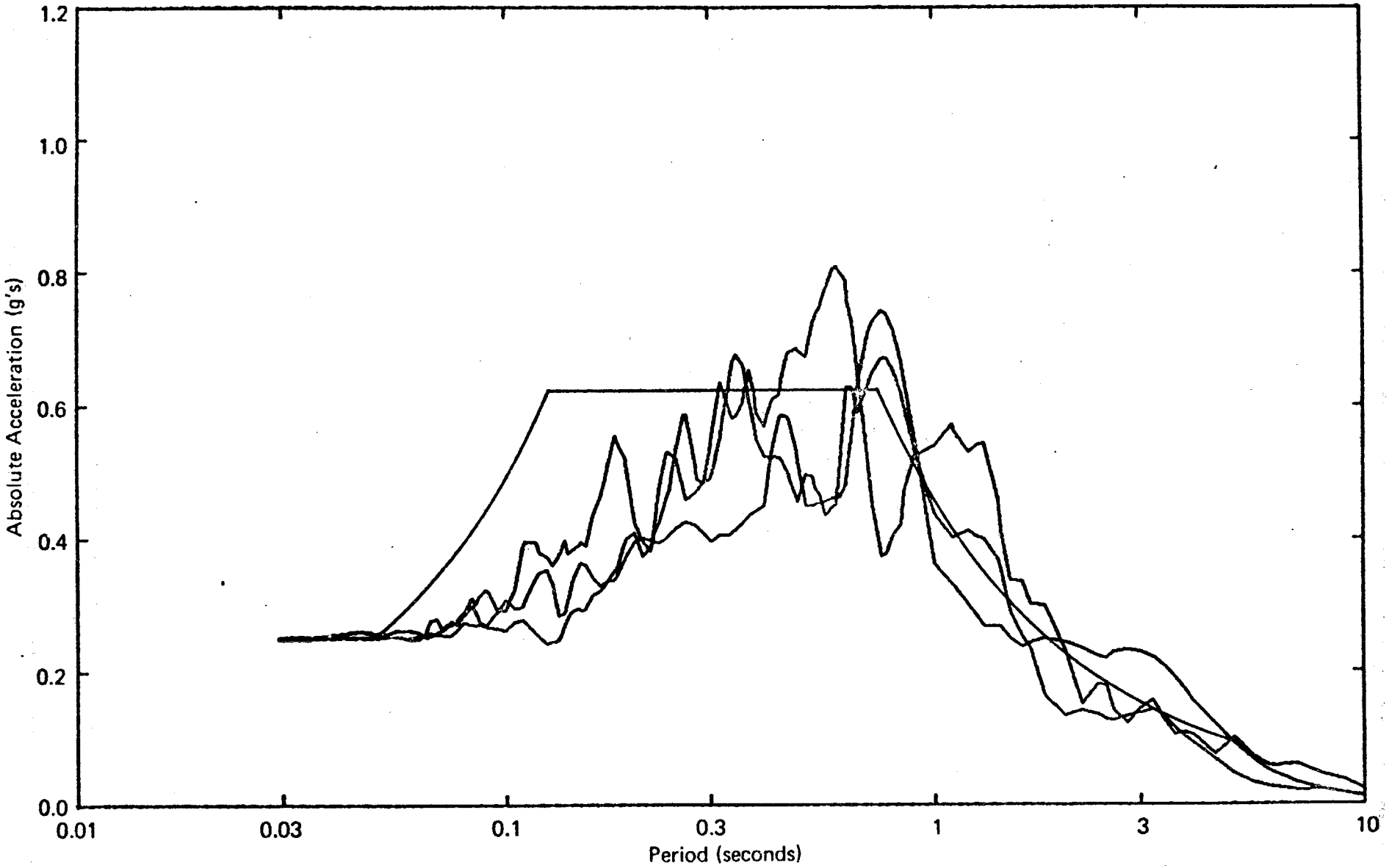

Fig. 39 – Acceleration Response Spectra – Major Components

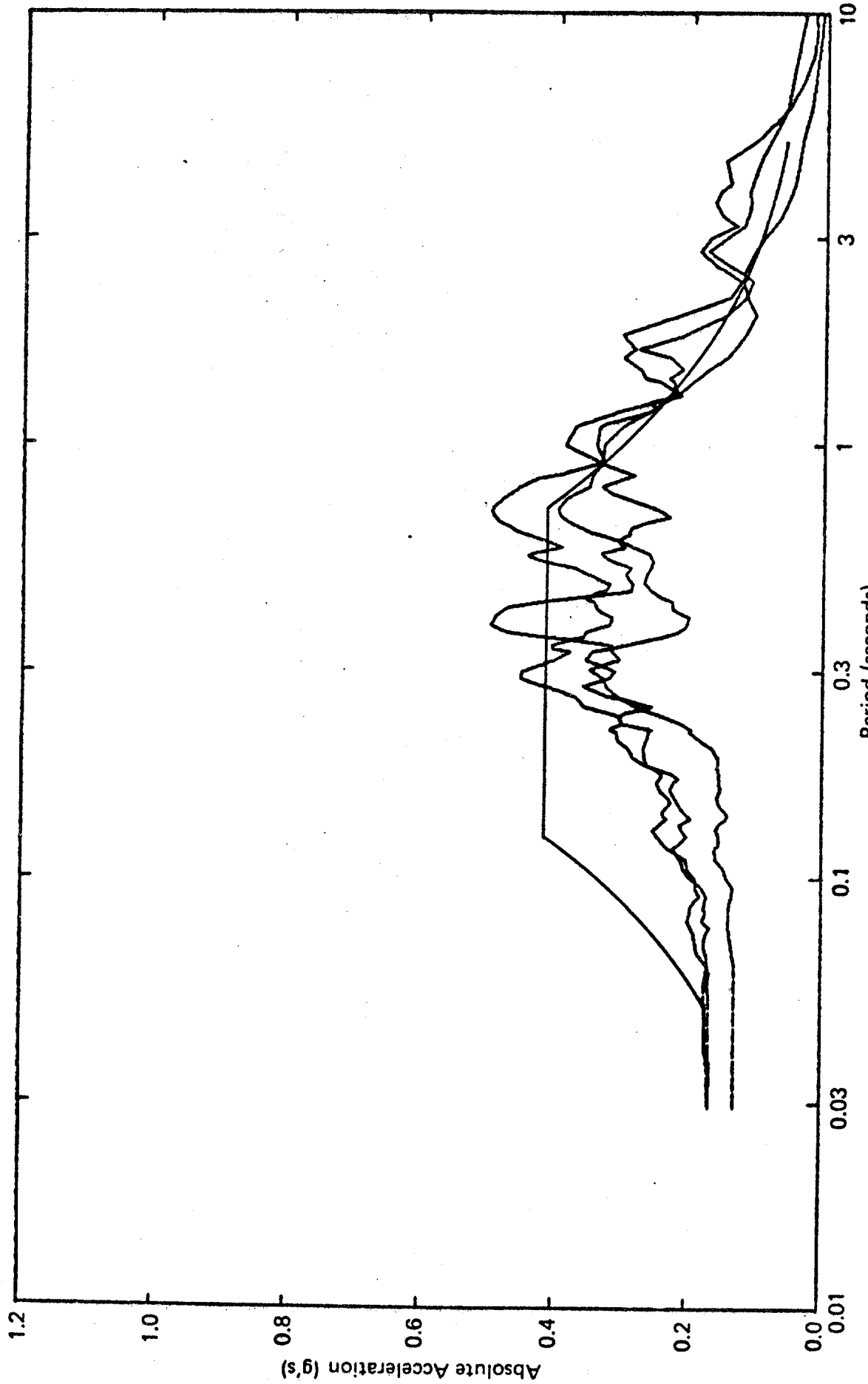

Fig. 40 – Acceleration Response Spectra – Minor Components

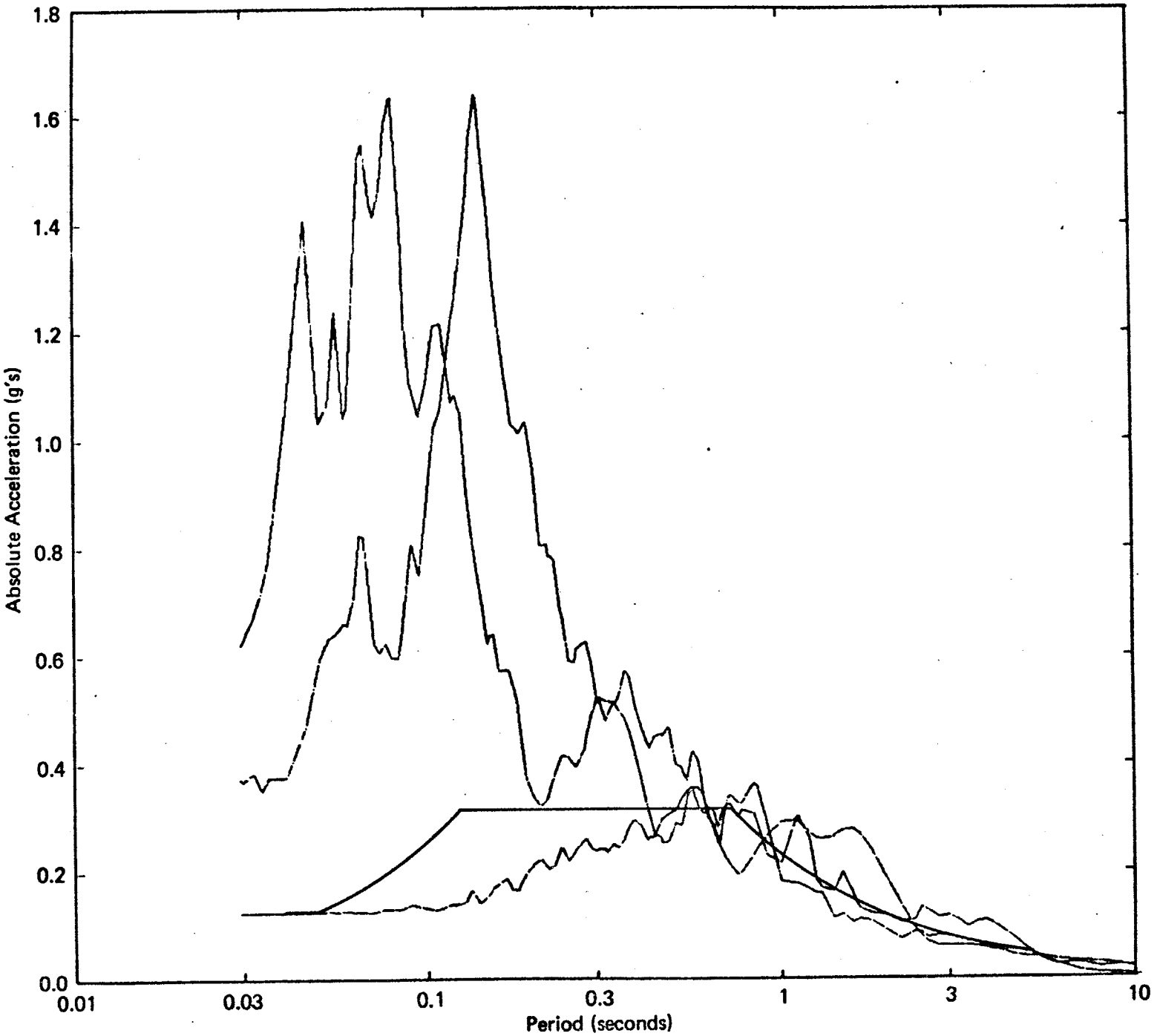

Fig. 41 – Acceleration Response Spectra – Vertical

DISTRIBUTION:

Charles Smith (50)
U. S. Dept. of Interior
Minerals Management Service
EMM - Mail Stop 647
Reston, VA 22091

DOE/ALO (2)
Albuquerque, NM 87115
Attn: Jim Coffey
Capt. John Hanson

R. L. McNeill (12)
3936 Garcia NE
Albuquerque, NM 87111

Iraj Noorany, Professor (12)
San Diego State University
San Diego, CA 92182

1620 M. M. Newsome
1621 C. E. Dalton
1621 K. K. Grube
1627 T. S. Edrington
6200 V. L. Dugan
6250 B. W. Marshall
6252 H. M. Dodd (10)
6252 R. W. Prindle (10)
8214 M. A. Pound
3141 L. J. Erickson (5)
3151 W. J. Garner (3)
3154-3 C. H. Dalin
(DOE/TIC - 25 Unlimited Release)